Validation of Top of the Line Corrosion Prediction Model Using Laboratory and Field Measurements

A thesis presented to

the faculty of

the Russ College of Engineering and Technology of Ohio University

In partial fulfillment

of the requirements for the degree

Master of Science

Ussama Kaewpradap

December 2012

This thesis titled

Validation of Top of the Line Corrosion Prediction Model Using Laboratory and Field Measurements

by

USSAMA KAEWPRADAP

has been approved for

the Department of Chemical and Biomolecular Engineering

and the Russ College of Engineering and Technology by

Srdjan Nešić

Professor of Chemical and Biomolecular Engineering

Dennis Irwin

Dean, Russ College of Engineering and Technology

ABSTRACT

KAEWPRADAP USSAMA, M.S., December 2012, Chemical Engineering

Validation of Top of the Line Corrosion Prediction Model Using Laboratory and Field Measurements

Director ofThesis: Srdjan Nešić

Top of the Line Corrosion (TLC) is a major issue in the oil and gas industry. Extensive research in both the laboratory and field has been conducted to understand its mechanism and to develop methods to mitigate TLC in pipelines. TLC models have been developed to predict the degree of corrosiveness in pipelines; however, the models are mostly based on laboratory results. Therefore, it is necessary to validate the models with the real field data to fill the gap in the understanding of the TLC mechanism.

In this thesis, a methodology for comparing TLC model prediction with real field data has been proposed. The methodology involves the analysis of complex field operating conditions and in-line inspection (ILI) data.

The performance of the developed methodology using selected TLC model shows good agreement between the model predictions and the data provided from the field. Nevertheless, there are still some discrepancies particularly at the beginning of the pipelines.

ACKNOWLEDGMENTS

First and foremost I would like to express my sincerest appreciation to my advisor, Dr. Srdjan Nešić, who has supported me with his guidance, knowledge and advice throughout my thesis while exploring the most beneficial research areas of corrosion engineering.

I would like to convey my deepest appreciation to Dr. David Young, the academic progress advisor for providing me with knowledgeable recommendations. I would like to thank Marc Singer, the project leader, for his guidance, patience, advice, leadership and assistance in the technical work. In addition, I am very thankful to all staff members, the fellow graduate lab-mates and campus friends for their assistance, companionship, and for providing a friendly working environment at the laboratory on campus.

I am extremely grateful to all sponsor companies; British Petroleum, Chevron, ConocoPhillips, ENI, Occidental Petroleum Corporation, PTT Exploration and Production, TOTAL and Saudi Aramco, on Top-Of-The Line Corrosion Project (TLC-JIP) for their financial support and field experience assistance. I would also like to acknowledge and give special thanks to PTT Exploration and Production for the useful field data and internship opportunity to collect very useful field data for my thesis.

Lastly, to the most important people in my life, I would like to express my gratitude to my parents and sister for their greatest affection that they have given to me.

TABLE OF CONTENTS

Page

LIST OF TABLES

Page

LIST OF FIGURES

Page

CHAPTER 1: INTRODUCTION

Corrosion is a natural phenomenon wherein a substance (usually metal) is deteriorated by an aggressive species in its environment [1]. In 2002, Koch *et al*. reported the high value of direct corrosion cost in the U.S., which is approximately $276 billion or 3.1% of the nation's Gross Domestic Production (GDP) [2]. The report states that the cost of corrosion within the oil and gas industry is very high.

Corrosion is a main cause for the failures in the oil and gas production process, especially in the transportation system. For economic reasons, carbon steel is the most commonly selected material used for the pipeline networks, even though it rapidly deteriorates in a corrosive environment. Over the past decades those corrosion failures have led to energy security concerns, decreases in production rate, financial loss and environmental contamination. In order to better understand the root causes of the corrosion and prevent future failures, many research projects have been conducted to study its mechanism.

In oil and gas production, a mixture of oil, solids, acid gases and water are produced. The presence of water from the production process causes corrosion problems inside the pipe. Internal corrosion in the oil and gas transportation system can be classified into two general categories: *Bottom of the line corrosion (BLC)* typical for all lines and *Top of the line corrosion (TLC)* typical for wet gas lines. Many research projects have been conducted over the last few decades leading to a clearer understanding of the mechanisms at work in BLC [3-12]. However, TLC mechanisms are not fully understood. Moreover, the injection of a conventional corrosion inhibitor is effective at

protecting the bottom of the wet gas pipelines but it cannot protect the topside of the pipelines. Therefore, efforts to understand TLC mechanisms and develop mitigation techniques have increased over the past few years.

Top of the line corrosion (TLC) is a phenomenon encountered in aqueous environments containing corrosive agents. Water condenses on the top of the wet gas pipeline surface due to the difference between external and internal pipeline temperatures. Corrosive agents, such as carbon dioxide (CO_2), hydrogen sulfide (H_2S) and volatile organic acids, will rapidly dissolve into this condensed water. General cases of the corrosion occur under dewing conditions in wet gas pipelines, which are operated in stratified flow regimes at low gas velocity. TLC in dewing conditions has been identified as the cause of numerous pipeline failures [13-18]. Consequently, TLC has become a growing concern for the oil and gas industry. Corrosion prediction models are often used to provide an overall assessment of the severity of corrosive conditions. However, the corrosion mechanisms implemented in the models are mostly based on laboratory data [24][34-36]. Therefore, it is necessary to evaluate the models capabilities when applied to real field conditions with actual pipe failures. Extensive researches have been conducted in both field and laboratory settings. However, these studies did not compare the prediction results with the real field data. As a result, there is a need that the TLC model predictions be tested against the field data. In the present research, an attempt has been made to develop the methodology for comparing the predicted TLC corrosion rates to the recorded field corrosion cases.

In the following chapter, the current understanding of the TLC mechanism, the published TLC laboratory studies, and the published TLC field experiences are reviewed.

It should be noted this part of the thesis was published at the NACE (National Association of Corrosion Engineers) International conference in 2012 [19].

1.1 TLC mechanism

Top of the line corrosion (TLC) occurs in a wet gas transportation pipeline when the temperature gradient between a cold environment and a hot fluid is high enough leading to the condensation of water vapor on the upper part of the pipe. The corrosion process usually takes place between the 10-2 o'clock positions in the pipe where it is poorly insulated. The inhibitor injection method, which is one of the most popular and commercial mitigation techniques used, cannot protect the TLC due to the gravity force accumulating protective liquid on the bottom of the pipeline.

TLC functions very differently depending on whether the environment is carbon dioxide (CO_2) dominated, referred to as the sweet environment, or hydrogen sulfide (H_2S) dominated, referred to as the sour environment. In 1983, Dunlop *et al*. suggested the value of 500 for the CO_2/H_2S partial pressure ratio as the transition point from sweet to sour corrosion [20]. However, the criterion used to define the transition between each regime is not clear. The ratio commonly used in the industry is based on inaccurate assumptions and should not be used as an engineering criterion. No other criterion to date has been widely accepted. The composition of the corrosion product layer (either $FeCO_3$

or Fe_xS_y) should be a good indicator of the corrosion mechanism's dominance but this criterion can only be used in failure analysis when such information is readily available.

1.1.1 Sweet environment

The presence of CO_2 (without H_2S) in the system leads to a corrosive environment called sweet corrosion. General chemical reactions involved in the corrosive mechanism are shown below [1],[21]:

Aqueous CO_2 is formed when the gas dissolves in water and is then hydrated to form carbonic acid (H_2CO_3):

$$CO_{2(g)} \rightleftharpoons CO_{2(aq)} \quad (1)$$

$$CO_{2(aq)} + H_2O_{(liq)} \rightleftharpoons H_2CO_{3(aq)} \quad (2)$$

Hydrogen ions (H^+) and bicarbonate (HCO_3^-) are then released into the solution from H_2CO_3 dissociation:

$$H_2CO_{3(aq)} \rightleftharpoons H^+_{(aq)} + HCO^-_{3(aq)} \quad (3)$$

Another H^+ and a carbonate ion (CO_3^{2-}) are then formed by HCO_3^- dissociation:

$$HCO^-_{3(aq)} \rightleftharpoons H^+_{(aq)} + CO^{2-}_{3(aq)} \quad (4)$$

In CO_2 corrosion for carbon steel, additional electrochemical reactions should be considered. The anodic reaction is the oxidative dissolution of iron in an aqueous solution:

$$Fe_{(s)} \rightarrow Fe^{2+}_{(aq)} + 2e^- \quad (5)$$

The cathodic reactions cover the reduction of H^+, H_2CO_3, HCO_3^- and/or H_2O:

$$2H^+_{(aq)} + 2e^- \rightleftharpoons H_{2(g)} \quad (6)$$

$$2H_2CO_{3(aq)} + 2e^- \rightleftharpoons H_{2(g)} + 2HCO^-_{3(aq)} \quad (7)$$

$$2HCO^-_{3(aq)} + 2e^- \rightleftharpoons H_{2(g)} + 2CO^{2-}_{3(aq)} \quad (8)$$

$$2H_2O_{(l)} + 2e^- \rightleftharpoons H_{2(g)} + 2OH^-_{3(aq)} \quad (9)$$

Consequently, the overall reaction of steel in an aqueous in sweet environment can be written below:

$$Fe_{(s)} + CO_{2(aq)} + H_2O_{(l)} \leftrightarrows FeCO_{3(s)} + H_{2(g)} \quad (10)$$

1.1.2 Sour environment

Sour environments are defined by the presence of a significant amount of H_2S being present, typically with CO_2 present as well. The presence of H_2S in the gas leads to dissolution: [12],[22]

$$H_2S_{(g)} \rightleftharpoons H_2S_{(aq)} \quad (11)$$

Aqueous H_2S can directly dissociate after dissolving in the solution. Bisulfide (HS^-) and sulfide (S^{2-}) species can form in the dissociation processes, as shown in the reactions below:

$$H_2S_{(aq)} \rightleftharpoons H^+_{(aq)} + HS^-_{(aq)} \quad (12)$$

$$HS^-_{(aq)} \rightleftharpoons H^+_{(aq)} + S^{2-}_{(aq)} \quad (13)$$

Similar to the sweet environment, acidic H_2S can behave as an additional source of hydrogen ions. The possibility of reduction of H_2S also exists:

$$2H_2S_{(aq)} + 2e^- \rightleftharpoons H_{2(g)} + 2HS^-_{(aq)} \quad (14)$$

Finally, the overall reaction of steel in sour environment can be written below:

$$Fe_{(s)} + H_2S_{(aq)} \leftrightarrows FeS_{(s)} + H_{2(g)} \quad (15)$$

1.2 Top of the line corrosion research results review

1.2.1 Top of the line corrosion experimental setup

To study the TLC mechanism and to investigate the influence of key parameters on TLC such as temperature, partial pressure, water condensation rate (WCR) etc., extensive researches have been conducted in the laboratory. TLC studies at the laboratory scale can be separated into sweet and sour environments based on the conditions as described above.

Laboratory protocols for TLC tests have been developed and proved for studying the mechanism of corrosion occurring on the upper parts of pipelines. With particular emphasis on TLC, the experimental configuration is quite different from the bottom of the line corrosion studies. The following sections describe experimental setups that have been used in the laboratory, which can be categorized into two main setups: the *Small-scale laboratory TLC studies* and the *Large-scale laboratory TLC studies.*

1.2.1.1 Small-scale laboratory TLC studies

Depending on the different project objectives, small-scale laboratories have been set up to study the effects of TLC. TLC studies have not only focused on the corrosion itself, but also looked at the effects of condensation on the corrosion processes. The following describes several experiments conducted in a small-scale laboratory for TLC studies.

In 1991, Olsen and Dugstad studied the temperature effect on protective film formation in small-scale laboratory experiments [23]. The study was performed in a

special designed autoclave, which is illustrated in Figure 1. It was found that the steel is well protected by an iron carbonate film when the temperature was higher than 70^{o}C and the condensation rate was low.

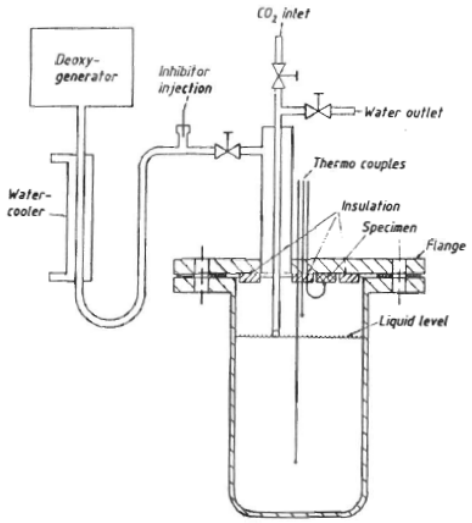

Figure 1: Experimental setup in autoclave originally proposed by Olsen and Dugstad (Reproduced with a permission from ©NACE International [23])

In 2000, Pots and Hendriksen conducted an experiment in a special facility shown in Figure 2, specifically designed for TLC studies [24]. The objective of this work was to validate their iron-super saturation model by testing the effects of major TLC parameters, namely gas temperature, condensation rate and gas velocity. Even though the equipment was designed to mimic TLC on a laboratory scale, the flow pattern across the specimen is questionable as being representative of real field conditions.

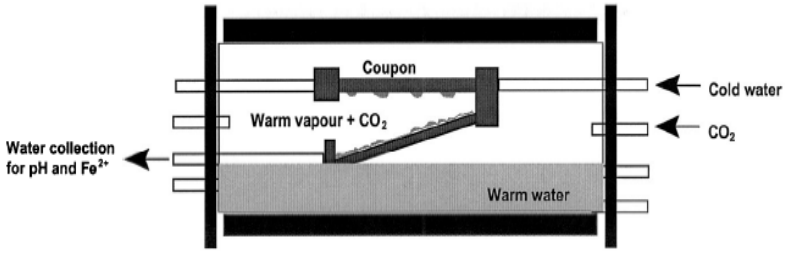

Figure 2: Special TLC facility designed by Pots and Hendriksen (Reproduced with a permission from ©NACE International [24])

In 2008, Hinkson studied the effect of acetic acid concentration on TLC by conducting experiments in a small-scale laboratory setup as shown in Figure 3 [25]. The experiments were performed in both non-corroding and corroding systems. This small-scale setup performed well in conducting the vapor/liquid studies in condensing conditions. The experimental results showed that the concentration of total acetic acid decreased as the water condensation rate increased.

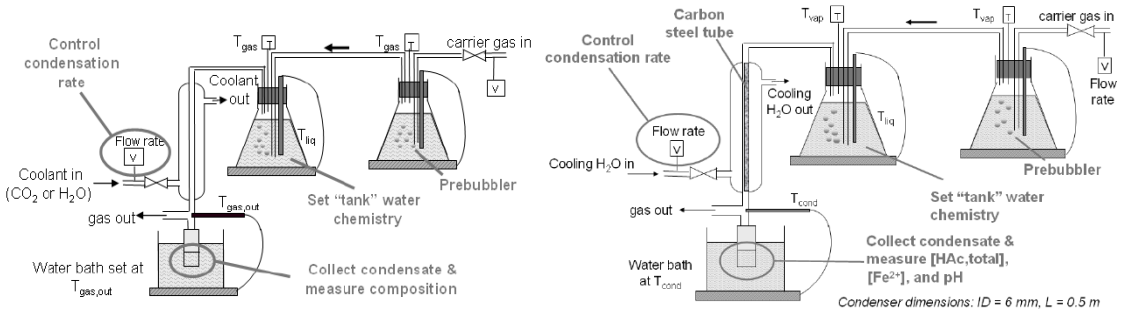

(a)Non-corroded test (b) Corroded test

Figure 3: Small scale experimental setup for effects of acetic acid concentration study proposed by Hinkson (Reproduced with a permission from ©NACE International [25])

In 2011, several TLC studies in small-scale laboratory systems were published. Chen *et al.* conducted a TLC experiment in a high temperature and pressure autoclave in order to study the effects of temperatures between 40-80^{o}C on TLC in CO_2 environments [26]. A threshold was given for the wall temperature which stated if the temperature is less than 34^{o}C, the corrosion rate will be smaller than 0.5 mm/yr.

Qin *et al.* conducted TLC experiments in an autoclave to study the effect of temperature [27]. Specifically, TLC on highly chilled surfaces with a high water condensation rate (WCR) was investigated. The gas temperature was varied and the surface temperature was fixed at 5^{o}C. The experimental result showed that the corrosion rate increased with gas temperature as water condensation rate increased.

Pojtanabuntoeng investigated the influence of light hydrocarbon on the condensation rate [28]. The experiments were conducted focusing on wetting, condensation processes and corrosion. For the wetting test, when a water-in-oil system was employed, water had a stronger attraction to the steel surface and this was accentuated by increased surface roughness. In the oil-in-water system, roughness had no effect on wettability. For the condensation process, n-heptane condensed as a film which filled space between water droplets. For the corrosion process, in the absence of n-heptane, corrosion increased with the water condensation rate. In the presence of n-heptane, corrosion was less influenced by an increase of co-condensation rate.

1.2.1.2 *Large- scale laboratory TLC studies*

Large-scale TLC experiments are conducted in flow loops designed to simulate field conditions more realistically. The influence of parameters including gas temperature, gas velocity, condensation rate, CO_2 partial pressure, H_2S partial pressure and acetic acid concentration have been studied and their effect on TLC elucidated in both short and long term experiments [29-32].

A flow loop for corrosion tests both in sweet and sour environments was previously designed and built for TLC experiments at the Institute for Corrosion and Multiphase Technology (ICMT), Ohio University. It is a 4-inch diameter horizontal flow loop 30 m eters long. The flow loop schematic for the CO_2 environment is shown in Figure 4. Several sweet TLC experiments have been conducted in the flow loop.

In 2004, Singer investigated the effect of free acetic acid (CH_3CO_2H, free HAc) in a CO_2 condition in the flow loop test [29]. The test was conducted at a constant inlet gas temperature (70^oC) and gas velocity (5 m/s). The concentration of free HAc was varied between 0-1000 ppm. The experimental results showed that the condensation rate is the main factor affecting TLC. On the other hand, it has naturally no effect on bottom of the line corrosion. The presence of acetic acid did increase the corrosion at both the top and bottom of the line and the test duration was too short (2 days) to make any definitive conclusion as to the extent of localized corrosion.

In 2005, M endez also used the flow loop to study the effect of other TLC parameters such as H Ac, and monoethylene glycol (MEG) hydrate inhibitor [30]. The flow loop test results showed that the MEG does not significantly influence TLC rate.

Both studies were conducted as short-term experiments leading to non-steady state corrosion rates, observance of onset localized corrosion was inconclusive in these tests.

In 2008, Zhang conducted TLC experiments in the large-scale flow loop to verify his developed TLC model, which will be discussed in the next section [31]. TLC parameters such as partial pressure of CO_2, temperature, water condensation rate, gas velocity and HAc concentration were investigated. A good agreement between the model predictions and test results was obtained.

At the Institute for Energy Technology, Norway, another large flow loop for TLC studies has been constructed. The schematic of the flow loop is presented in Figure 5. In 2009, Nyborg investigated the effect of a small amount of H_2S by carrying-out experiments in the flow loop [32]. The results showed that even a small amount of H_2S (2 mbar H_2S partial pressure) could seriously affect TLC in CO_2 environments due to the formation of a porous iron sulfide film, which is not protective to the steel surface.

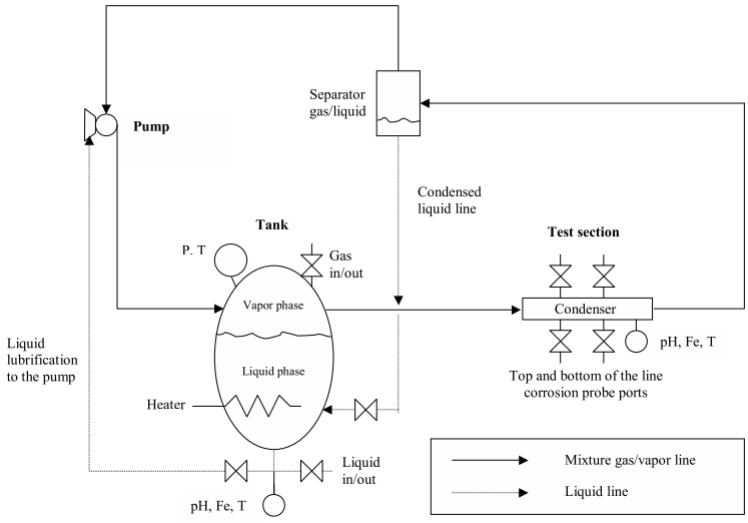

Figure 4: Schematic of CO_2 flow loop at ICMT, reproduced with a permission from ©NACE International [29]

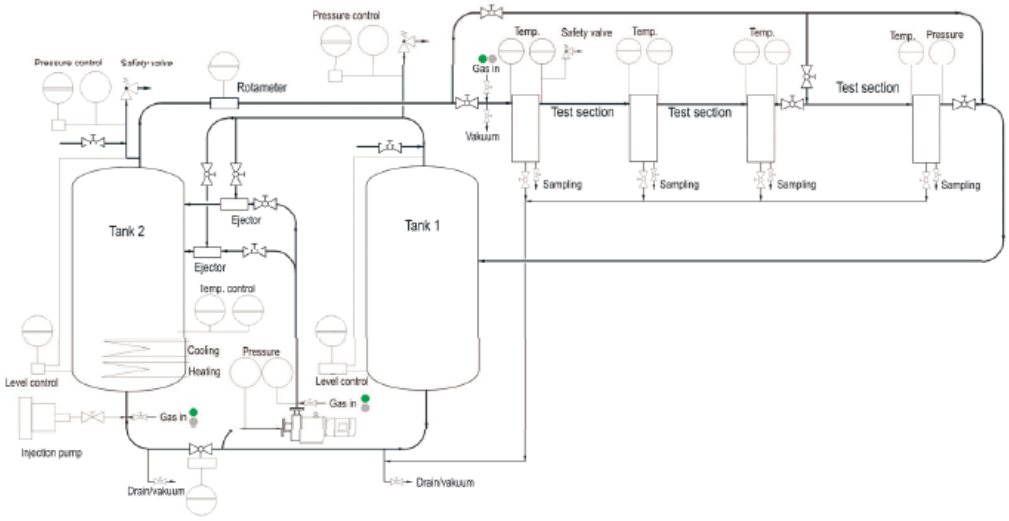

Figure 5: Schematic of flow loop at IFE reproduced with a permission from ©NACE International [32]

1.2.2 Top of the line corrosion prediction models

The extensive research presented in the previous sections helps to better explain the TLC mechanism and the influence of key parameters. Models predicting the corrosiveness of TLC have also been developed. Initially, the deWaard correlation, a well known corrosivity calculation, derived from empirical data, was proposed [33]. With increased improvements through experimentation, semi-empirical and fully mechanistic models have been subsequently proposed [24][34-36].

In 1991, deWaard *et al*. proposed an extension of his correlation [33] to include the effect of water condensation in TLC. The empirical factor in the correlation was based on a specific set of experiments. The empirical factor for TLC calculation is shown below:

$$\log(CR_{TLC}) = \log(F_{cond}) \times 5.8 - \frac{1710}{273+T} + 0.67 \times log(P_{CO_2}) \qquad (16)$$

Where:

CR_{TLC} is TLC corrosion rate (mm/y)

WCR is water condensation rate (mL/m^2/s)

F_{cond} is empirical factor and equals 0.1when WCR less than 0.25 mL/m^2/s

and equals 1 when WCR higher than 0.25 mL/m^2/s

P_{CO_2} is partial pressure of CO_2 (bar)

In 2000, an iron super-saturation model, developed by Pots and Hendriksen was proposed [24]. The following equation shows that the corrosion rate is a function of the water condensation rate and iron concentration:

$$CR = 2.26 \times 10^8 [Fe^{2+}]_{supersaturation} \times \frac{WCR}{\rho_w} \quad (17)$$

Where:

CR is corrosion rate, mm/y

$[Fe^{2+}]_{supersaturation}$ is iron concentration in the condensed water, ppm

WCR is condensation rate, mL/m^2/s

ρ_w is water density, kg/mL

Subsequently, for a more accurate TLC prediction model, a mechanistic model has been in development.

In 2002, Vitse *et al*. proposed a semi-empirical model to explain TLC [34]. Heat and mass transfer fundamental were considered to model the water condensation process in filmwise phenomenon. The corrosivity calculation was calculated based on the kinetics of electrochemical reactions and the change in the water chemistry was predicted by thermodynamic theory and chemical equilibria.

In 2008, Zhang *et al*. proposed the first fully mechanistic model for TLC [31][36]. Fundamental principles of thermodynamics and chemical equilibria are used to calculate the change in chemistry in condensed water. Corrosion models for the TLC rate are predicted based on the kinetics of the electrochemical reaction. Zhang's intensive study clarified that the water condensation on the steel surface is a dropwise phenomenon, which is used for the condensation rate calculation and is based on heat and mass transfer theory.

For more information concerning the model, readers may wish to consult Zhang's thesis for a full description [36].

1.3 Top of the line corrosion in real fields

Failures due to TLC will not only lead to production and economic problems, but may also directly affect human health and lead to environmental contamination. In this section, several published TLC cases are reviewed. In addition, common techniques used in TLC detection in the field are described.

1.3.1 Historic cases

In 1963, Paillassa *et al*. reported the first TLC failure in a sour gas field in France [13]. The cause of the failure was clearly explained as water condensation at the top side of the pipeline operating in stratified flow regime and low gas velocity.

In 1999, Gunaltun *et al*. published another case history of TLC [14]. The TLC was detected in a multiphase pipeline located in the delta of Mahakam River, Indonesia.

The in-line inspection (ILI) tool discovered high wall thickness loss in the area where the pipeline was not buried. Therefore, there were high differences between internal and external temperatures of the pipeline leading to a high water condensation rate at the top of the pipeline.

In 2010, a *cold spot corrosion*, a special case of TLC, was presented [18]. Cold spot corrosion refers to the corrosion that occurs on small pipe surfaces where the water condensation rates are locally very high compared to the surrounding pipe sections. This is the case when the thermal insulation is defective or not applied uniformly. Cold spot corrosion is considered to be *the worst case of TLC* due to the very localized and penetrating corrosive features. The authors presented two cases of cold spot corrosion on offshore pipelines that had been in operation for 16 years before leaks occurred. The visual inspection showed that one leak was at the riser/dogleg connection where there was no external coating (Figure 6). On another line, the leak appeared underneath an anode pad where there was no external coating (Figure 7).

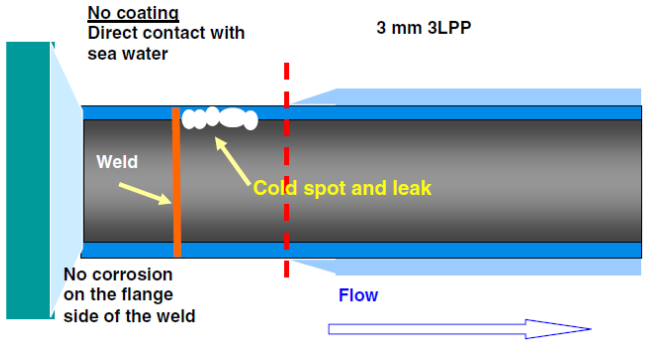

Figure 6: Cold spot corrosion at the uncoated area of the dogleg flange connected to the riser (Reproduced with a permission from ©NACE International [18])

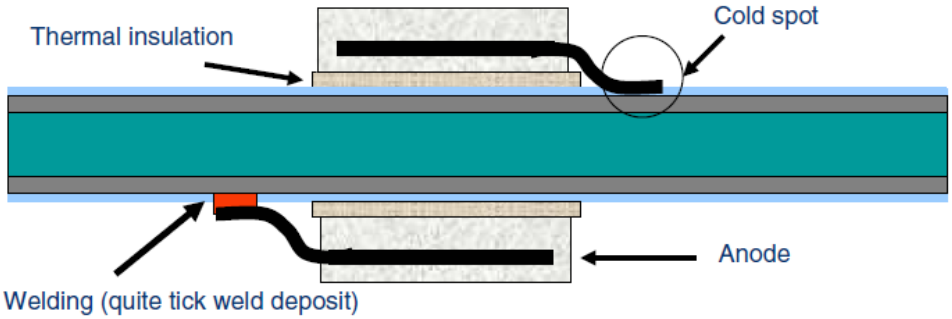

Figure 7: Cold spot corrosion at the anode pad connection (reproduced with a permission from ©NACE International [18])

1.3.2 Field measurements

Measurement techniques have been developed to help mitigate TLC risk in the oil and gas industry. Generally, TLC measurement techniques are separated into two major categories: *monitoring* and *inspections methods*. In this section, common techniques widely applied in TLC measurement are reviewed, with particularly focus on the advantages and disadvantages of the various techniques.

1.3.2.1 Monitoring methods

1.3.2.1.1 Weight loss coupons

The weight loss coupon technique, which is an in-line corrosion monitoring method, is the simplest and most basic way to measure corrosion. Typically a steel coupon is inserted into a pipeline at a convenient location and removed after a given amount time and analyzed. This technique provides reliable corrosion information for a given test environment. In addition, corroded coupons can be characterized by various analytical techniques, such as scanning electron microscopy (SEM), energy dispersive X-

ray spectroscopy (EDS), X-ray diffraction (XRD) and Raman spectroscopy, in order to obtain information on the identity of corrosion products. Coupon mass loss for a given surface area will give information on the corrosion rate. In general, pre-weighed metal specimens have a designated metallurgy and geometry when they are exposed to a corrosive environment. After certain exposure times, corroded coupons are removed and inspected. Corrosion products are then dissolved by Clarke solution treatment [37] and the coupons reweighed. The weight difference of the coupons before and after the corrosion process is calculated and converted to a corrosion rate (*CR*) by the equation below:

$$CR = \frac{m_b - m_a}{S_c \rho_{Fe} t_e} \times 365 \times 24 \times 3600 \times 1000 \quad (18)$$

Where:

CR is corrosion rate (mm/y)

m_b is mass of specimen before mounting to the test section (kg)

m_a is mass of specimen after Clarke's solution treatment (kg)

S_c is surface area of the specimen (m^2)

ρ_{Fe} is iron density (kg/m^3)

t_e is exposure time (s)

Corrosion information provided by weight loss of a coupon corresponds to cumulative (time-averaged) corrosion after the designated exposure time. The technique is also an effective method to detect localized corrosion; however, it's success depends on the choice of location of installation. Corrosion information for a specific point in time within the exposure interval cannot be determined by this technique. Corrosion damage

along a pipeline might occur at different location and at a different time which might not be detected by using weight loss coupon monitoring.

1.3.2.1.2 Electrical resistance (ER) probe

The electrical resistance (ER) probe is another in-line corrosion monitoring technique used to measure the rate of corrosion. The fundamental concept that underpins the ER probe technique is the measurement of the electrical resistance of a thin metal test wire (sensor element) inserted into the line in a similar way as the weight loss oupon [38]. The electrical resistance is a function of wire thickness which is decreased by corrosion. In other words, resistance increases with decreasing wire thickness.

ER is considered to be an "intelligent" weight loss technique. The change of electrical resistance is detected and transmitted to an instrument analyzing corrosion information "on-line". The method does not require sample removal to determine the corrosion rate.

A drawback is that the ER probe shares with the weight loss technique in the inability to detect localized corrosion. In addition, (semi)conductive deposits, such as iron sulfide produced in sour (H_2S) environments, are likely to deposit on the sensor element and lead to inaccuracies in electrical resistance measurements. Temperature is another factor affecting the effectiveness of ER probe measurements. Therefore, ER probes should not be used in high temperature environments and give erroneous results when used in environments with large temperature fluctuations.

1.3.2.2 Inspection methods

These techniques are able to determine pipeline geometry, as well measure and locating pipeline defects along the line. In oil and gas industry, inspection techniques encompass a number of techniques used to measure the wall thickness loss along a pipeline. Following are the most common monitoring techniques for TLC monitoring.

1.3.2.2.1 Magnetic flux leakage testing (MFL)

Magnetic flux leakage testing (MFL) is probably the most widely used in-line inspection (ILI) tool in the oil and gas industry for inspecting pipeline structures. The basic principle of the instrument is based on the idea that defects in the pipe's steel surface can be detected through the change of magnetization of the metal pipe wall [39]. Distortions in the magnetic flux signal are related to the presence of internal or external metal loss features. As previously mentioned, MFL does not directly measure wall thickness loss. Deviations in the magnetic fluxes are translated into defect "sizing" by proprietary algorithms. These algorithms are specific to vendors/clients, instruments and corrosion type and are regularly updated. The algorithm type can greatly affect the sizing of the detected corrosion features and can lead to important variations in wall loss calculations. MFL requires interruption of production for its employment making it very complex and expensive.

1.3.2.2.2 Ultrasonic testing (UT)

Ultrasonic testing (UT) is another typical tool applied for corrosion monitoring in oil and gas field. It can be deployed as an ILI tool or from the outside of the line requiring removal of insulation and clear access to the external pipeline surface. The basic principle of UT is founded on the reflection of ultrasonic waves [39]. The ultrasonic signal is propagated through the media and pipe wall. The difference of the reflection time arriving back to the transducer is related to the distance between the transducer and pipe wall surface (further – nearer). Therefore, the wall thickness can be estimated locally.

CHAPTER 2: RESEARCH OBJECTIVE

Based on the information presented in Chapter 1, extensive research and experiments have been conducted related to TLC. The TLC mechanisms and key parameters are now better understood and improved. TLC prediction models have been developed and improved. However, the TLC prediction model developments may be of little use if there is no validation with the real field data.

Oil and gas production and transportation are one of the most complex processes in the industry. Parameters collected from the fields are also complicated. The analysis of the complex operating data is necessary. Moreover, the accuracy of the corrosion inspection in the field is often questionable. It is necessary to analyze the data to identify the best representation of TLC in the pipeline before comparing it with the model prediction results.

In order to verify the TLC prediction model as a practical instrument used to predict and diagnose failures in oil and gas transportation, it is crucial to validate its capabilities. The procedure for analyzing complex field data should be developed first. Consequently, the main objectives of this thesis are:

- To develop the methodology for comparing the TLC model predictions with the corrosion data provided from the real field.
- To validate the TLC model by comparing its prediction results with the field data.
- To identify the gaps in understanding between the mechanistic model and reality in the field.

- To increase the levels of confidence in using TLC model prediction for design or failure analysis.

CHAPTER 3: METHODOLOGY FOR COMPARING TLC MODEL PREDICTION WITH FIELD DATA

3.1 Introduction

As indicated in previous chapters, it is difficult to directly compare TLC model predictions with the experimental data due to the variability of both laboratory data and complex field data. This chapter will present the criteria for developing the methodology for comparing TLC model predictions with MFL data.

As a part of the Top-Of-The Line Corrosion Project (TLC-JIP) at the Institute of Corrosion and Multiphase Technology (ICMT), Ohio University (OU), this thesis was conducted mainly to validate Zhang's TLC model [31]. Therefore, the performance of the developed methodology in this research will use his fully mechanistic model.

The details of the developed methodology were published at the NACE (National Association of Corrosion Engineers) International conference in 2012 [19].

3.2 Overall methodology

Figure 8 shows the outline of the procedure for comparison of the model prediction and MFL data. Since the accuracy of the field data is often questionable, the actual field parameters need to be initially, and carefully, analyzed to quantitatively and qualitatively determine the extent of TLC along the pipeline. Secondly, the analysis of MFL data has to be clearly performed to evaluate the accuracy of the data and to select the best representation of the TLC severity. Lastly, a meaningful comparison between both model predictions and measured corrosion is performed.

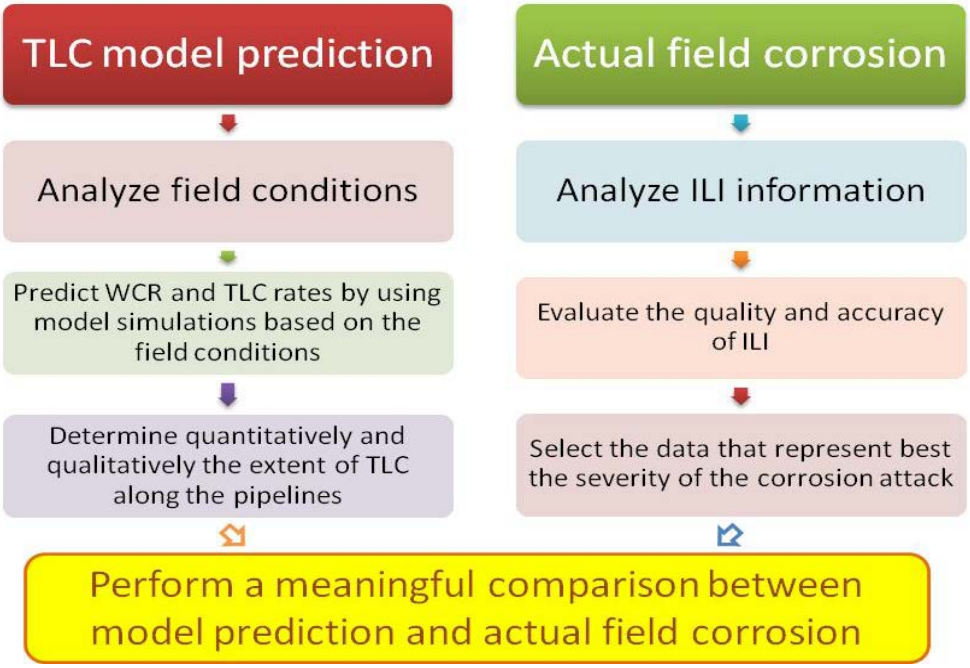

Figure 8: Procedure for comparison of model predictions with the field data.

3.3 Field data collection and analysis

Oil and gas production data acquisition, as p resented in Figure 9, is a very complex process. To be a practical methodology, which is useful for corrosion management, minimally required information is listed in this section. In addition, the challenges related to accuracy of the collected operating data are discussed. Finally, steps in analyzing complex operating data are also addressed.

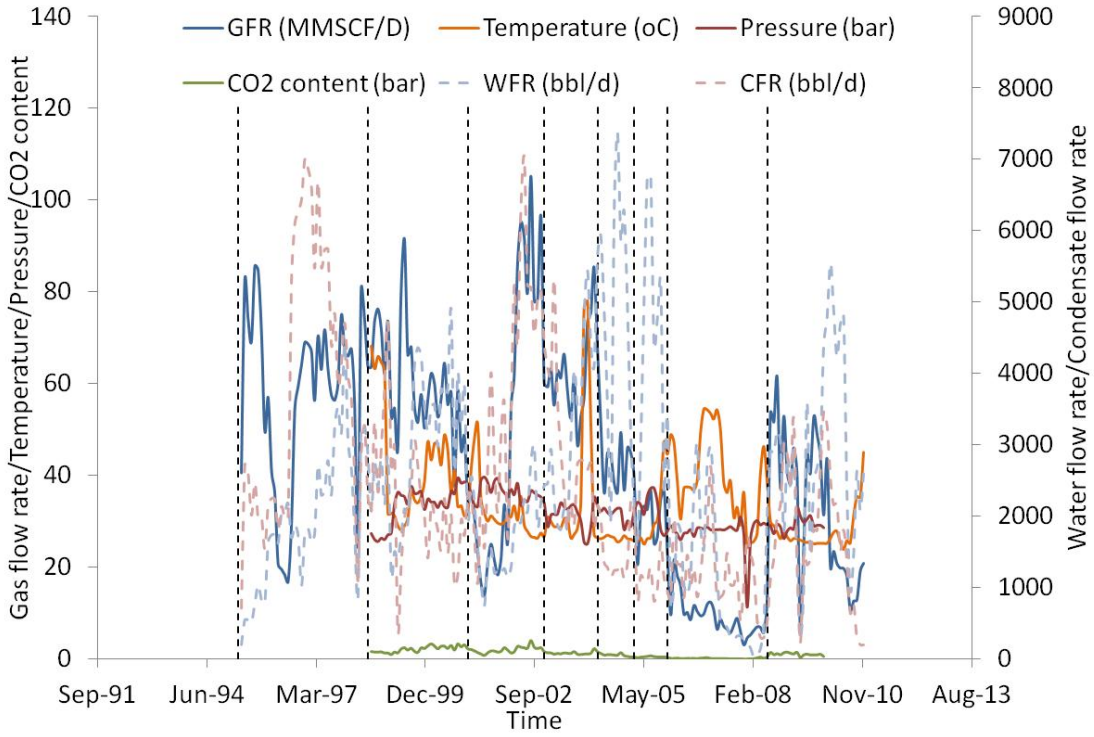

Figure 9: Example of complex collected operating data from the field

3.3.1 List of production data and field information needed for TLC assessment

The following presents a list of the main operating parameters needed to conduct a TLC assessment on a particular flow line:

- *Pipeline topography*

Topography is referred to as a change in elevation and/or inclination along the length of the pipeline due to the surface shape and features of the earth. The change in topography directly affects the change of the flow regime and velocity of the multiphase fluid flowing in the pipeline. In other words, occurrences of TLC are possible in different locations along the pipeline as the pipe topography changes. As a result, information

about the topography is crucial for the model input data to evaluate the probability and location of TLC.

- *Pipe burial depth*

In reality, parts of the pipeline, often only the bottom side, are buried under the soil or seabed. The soil provides some thermal insulation between the inner wall of the pipeline and the ambient environment. However, in many cases of TLC the pipelines are not fully covered or buried, which leads to significant temperature gradients and water condensation at the upper part of the pipeline surface. Therefore, the depth of the seabed or soil covering the pipeline is important information for determining the possibility of TLC.

- *Pipeline characteristics (pipe thickness, thermal conductivity)*

Physical properties and characteristics of the pipeline such as internal diameter, wall thickness and thermal conductivity are important values for predicting flow regime, calculating the water condensation rate and corrosion rate. Therefore, it is necessary to know these properties for the pipeline.

- *Thermal insulation and coating (thickness, thermal conductivity)*

Insulation and coating are applied to the surface of the pipe to structurally protect the steel both internally and externally. One of the main purposes of insulation and coating is to provide protection from external corrosion. However, in many cases the temperature gradient remains high. Consequently, to accurately predict the condensation rate information concerning both the thermal insulation and coating type must be known.

- *Flow rates profile with time (gas, water and condensate)*

One important key factor of TLC occurrence is the flow regime. As mentioned earlier, TLC occurs only in a stratified flow regime. The multiphase flow regime can be calculated from the fluid flow rates. Production flow rates such as gas flow rate, water, and oil/condensate flow rate are crucial in calculating the liquid velocity leading to the prediction of the flow regime in the pipeline. Since the flow rates vary continuously from the start-up of operations onwards, knowing a flow (production) rate history is crucial for analyzing the corrosion process.

- *Outside environment information (medium, average temperature, current velocity)*

Temperature gradient is a key factor in determining the amount of heat transfer and condensed water. The outside environment temperature is directly related to the temperature gradient. Therefore, information about environmental temperature, ocean current velocity (for cases of subsea pipelines), and wind speed (for cases of onshore pipelines) are critical for calculating TLC.

- *Temperature and pressure profiles*

In addition to production data, temperature and pressure information are not constant during the operating life of a pipeline. In some time intervals, those values are high and can lead to severe TLC, and in some they are not. Therefore, it is necessary to know the history of temperature and pressure changes in order to predict the severity of TLC in the pipeline.

3.3.2 The issue of accuracy of collected operating data

The main challenges encountered with the collection of operating data are listed below:

- Availability, completeness and accuracy of production data.
- Significant variations over time in production data.
- Availability of accurate topographic data.

The TLC model is rather sensitive to variations in input conditions, such as production rates, temperature, pressure, etc., which are common in a field situation. The level of uncertainty and inaccuracy related to these data can be significant and represents a definite challenge in the analysis. In addition, the topography, which includes pipeline burial information, is essential for calculation of the condensation rate and TLC corrosion evaluation.

All operating conditions such as carbon dioxide (CO_2) content, temperature, pressure, production rates and water analysis are essential in evaluating the severity of TLC and to validate the model capabilities. However, the main concern in collecting the data is the inaccuracy of the production parameters obtained during the pipeline field life. Figure 9 shows the complexity of the operating conditions and profiles one of the lines from the production startup. The chart also shows incomplete data related to CO_2 contents, temperature and pressure. It clearly indicates that the simple use of minimum and maximum values would not enable an accurate evaluation of the production characteristics. A possible approach to overcome these limitations is to divide the service life into time intervals and use the weighted average values from each time interval to

calculate the corrosion rates. The corrosion rates from each time interval can then be used to calculate wall thickness loss over the life time of the line. Therefore, the operating conditions should be carefully analyzed for the case histories. More details about the operating conditions analysis are addressed in the following chapters.

3.3.3 Analysis of production data for TLC assessment

The following procedure was implemented to effectively analyze the field data:

- The evolution of the operating parameters for a selected line from the start-up to the present time is divided into a number of time intervals during which these parameters had relatively stable values. For each of these time intervals, a time averaged value is calculated for each operating parameter.

- The values for these parameters are used to calculate water condensation rates and temperature profiles using a heat and mass transfer line model.

- The simulations are then run in order to obtain TLC rate predictions for a number of selected points along the pipeline. The simulations are executed until a steady state corrosion rate is obtained.

- Cumulative wall thickness (WT) loss is calculated for each time interval; they are then added and compared with provided MFL data.

3.4 Challenges related to the analysis of inspection data

One of the most common ILI inspection techniques widely used in the industry involves magnetic flux leakage (MFL). The basic principle of the MFL tool was explained in Chapter 1. However, it is necessary to emphasize that the MFL tool does not directly measure the wall thickness loss. The deviation in the magnetic fluxes is translated into defects sizing by using proprietary algorithms. Therefore, the analysis to determine the accurate value of wall thickness loss for TLC should be carefully considered. The following section presents the challenges related to the analysis of inspection data. Subsequently, the steps developed for analyzing complex MFL data are proposed.

3.4.1 The issue of accuracy of MFL inspection

Several issues need to be assessed in order to extract useful information from ILI/MFL data for TLC assessment:

- How to take into account the inherent inaccuracy of TLC feature sizing?
- Should the size or spatial distribution of the TLC features be considered in addition to the maximum depth of attack?
- What is the best approach to compare model predictions with the complex MFL data?

The performance of MFL technique is strongly affected by the velocity of the tool, magnetization values and presence of pipe joints. Consequently, the data obtained

by MFL needs to be filtered in order to identify those data, which are most accurate and would be best compared with the model predictions.

3.4.2 Analysis of ILI data for TLC assessment

Not all MFL data are of the same accuracy/quality. Consequently, caution is required when analyzing MFL data and only the most accurate and representative MFL data should be used for comparison with the model simulation. The following procedure is implemented with the current approach:

- Only the first few kilometers of a pipeline were considered in this study, since it is the section where the most severe TLC is typically encountered.
- Corrosion features in the vertical riser were not included in the analysis because they cannot be categorized as TLC due to the slug/churn flow regime.
- Only features in the upper section of the pipe (between 9 and 3 o'clock) were analyzed.
- MFL data obtained for features close to weld joints are known to be notoriously noisy and consequently unrepresentative. Joints were present every 12 meters along the line and therefore the features located ±0.5 meter around the weld joints were eliminated from the analysis.
- As the model has been developed to predict the most severe TLC rate, the set of data points along the line representing the maximum wall thickness

loss was retained for comparison with the simulations. This set is referred to as the "maximum penetration envelope".

- Another feature of the model is that it predicts uniform TLC (as opposed to a localized attack), therefore an effort has been made to separate out the MFL data representative of uniform attack. This was achieved by eliminating the small size isolated features, which did not appear in the so called "clusters". Clusters were defined as large corrosion features (where width and depth was at least 3 times the wall thickness) [40].

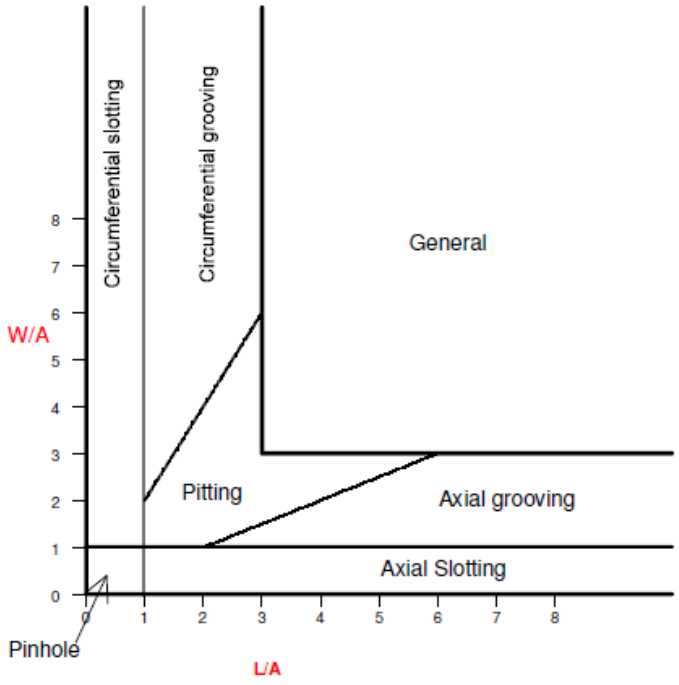

Figure 10: Feature classification originally from (Reproduced with permission from Pipeline Operator Forum (POF) [40])

CHAPTER 4: VALIDATION OF TLC MODEL WITH FIELD DATA

4.1 Introduction

The established TLC models and methodology may be of little practical use if they cannot be validated with field data. In this chapter, the selected TLC model is validated using the developed methodology. The validation uses real field data provided by a sponsoring company. The details and problems encountered with the field data are described below using a few examples. In addition, the analysis of both field operating conditions and MFL data are thoroughly explained for these cases. The comparison between model predictions and field data is performed. Finally, the limits of the validity of this type of analysis are proposed and can be used for future reference.

4.2 Analysis of a single pipeline

4.2.1 Field data presentation

Field X is an offshore gas field located in the Gulf of Thailand in operation since 1992. The pipelines in this field have been subjected to TLC since production start-up, due to a highly corrosive environment. The gas produced contains an average of 23% CO_2, which along with water, acts as a reservoir for the formation of corrosive carbonic acid (H_2CO_3). Fluid temperatures in the lines are typically higher than 80^{o}C. With the low external environmental temperature (26^{o}C on average), the temperature difference between the internal and external pipeline environment leads to a high condensation rate and consequently severe TLC.

Therefore the selected pipelines from Field A chosen for this analysis met three important criteria. Firstly, they had complete and accurate production data. Secondly, topography information was known for proper WCR and TLC rate calculation along the pipelines. Thirdly, MFL inspection results were given and could be analyzed for the validation of the mechanistic model.

4.2.2 Field conditions analysis

4.2.2.1 Line A

Production data and weight-averaged information from Line A are shown in Figure 11 and Figure 12, respectively. Due to the lack of temperature and pressure profiles in the first and second time intervals these were assumed to be equal to the averaged values in the third time interval because the temperature and pressure profiles did not significantly fluctuate. The characteristics of this line are presented in Table 1.

Table 1: Pipe characteristics of Line A

Pipe characteristics	Line A
Steel type	Seamless (API 5LX52)
Pipe length (km)	5.9
Internal diameter (m)	0.39
Steel thickness (mm)	15.9
Insulation type	3LPP
Insulation Conductivity (W/mK)	0.22
Insulation thickness (mm)	2

Note: 3LPP is three-layer polypropylene insulation

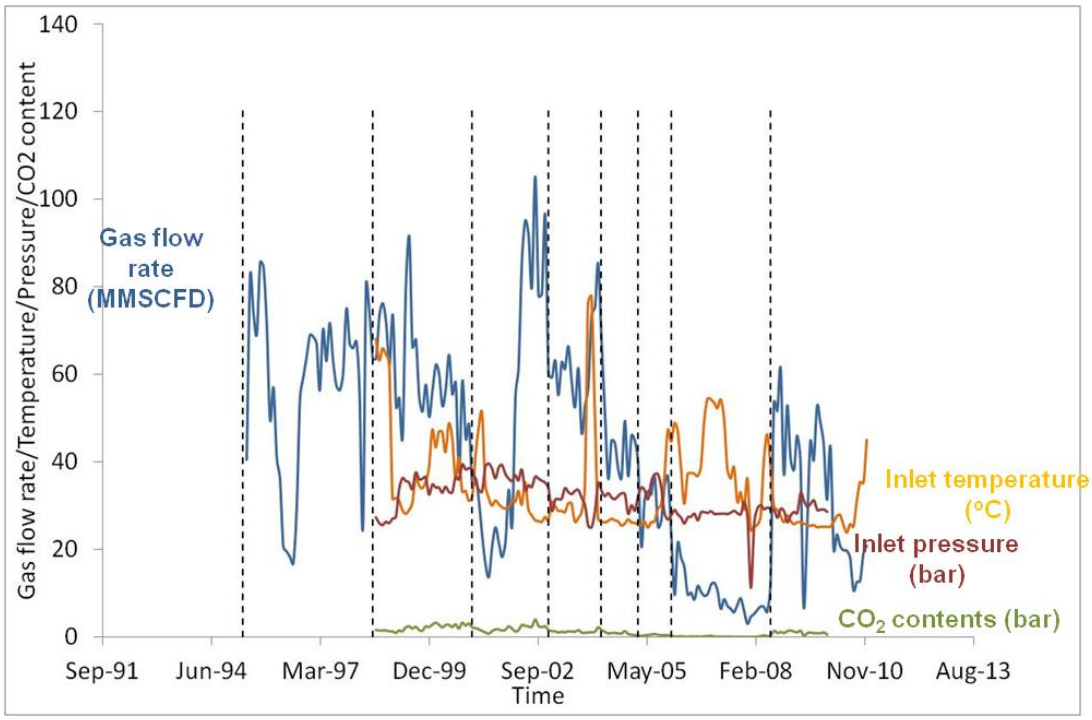

Figure 11: Input parameter variation over time for Line A.

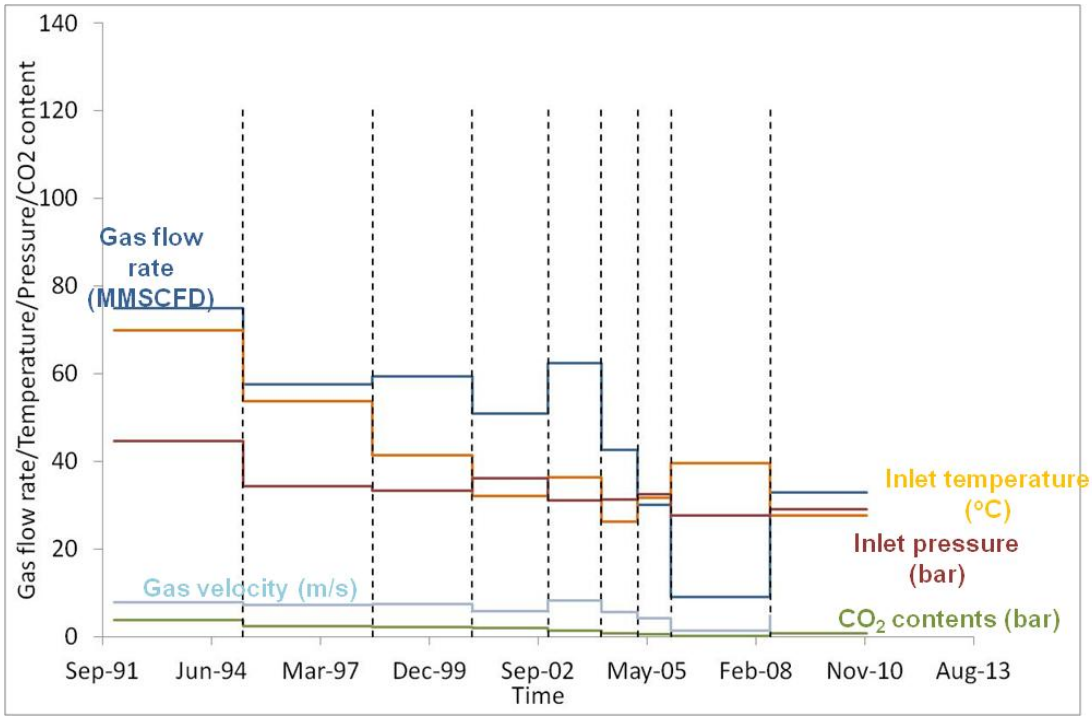

Figure 12: Averaged input parameters for Line A using nine time intervals.

4.2.2.2 Line B

Table 2 shows pipe characteristics of Line B and Figure 13 presents production and TLC parameters profiles. The available information was not complete from the start-up year 1993. Therefore, the weight-averaged input values in the first and second time intervals were assumed. This was calculated by using 70% of the values in the third time interval as illustrated in Figure 14. Even though Line B was laid down in the first development phase of the Field X and had been in operation since the production startup, the MFL data shows little metal loss. Consequently, this proves to be an interesting candidate due to the low severity of TLC.

Table 2: Pipe characteristics of Line B

Pipe characteristics	Line B
Steel type	Seamless (API 5LX52)
Pipe length (km)	2.7
Internal diameter (m)	0.34
Steel thickness (mm)	15.9
Insulation type	3LPP
Insulation Conductivity (W/mK)	0.22
Insulation thickness (mm)	2

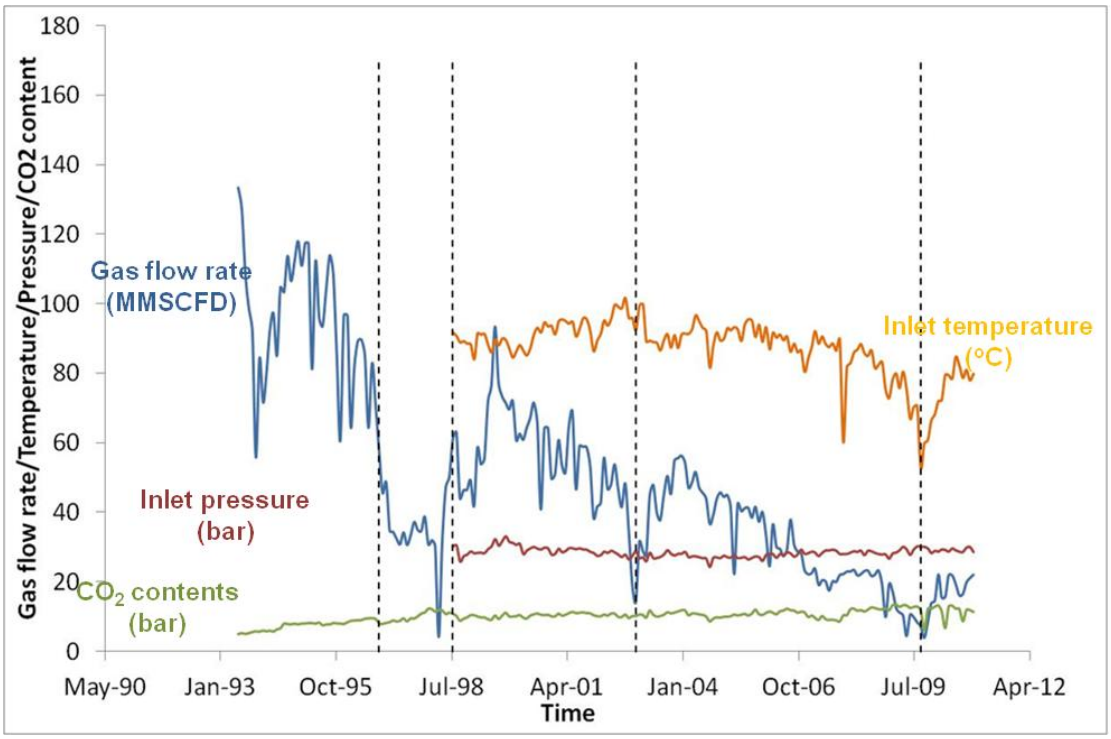

Figure 13: Input parameter variation over time for Line B.

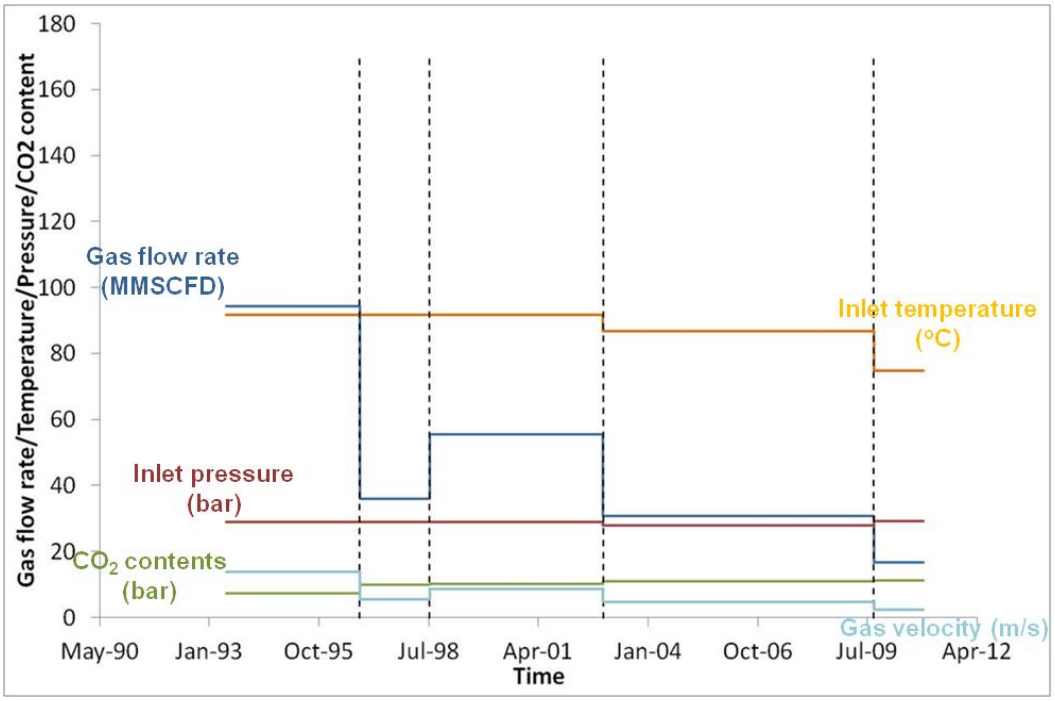

Figure 14: Averaged input parameters for Line B using five time intervals.

4.2.2.3 Line C

The complete production data of Line C from the start-up year to 2010 was available as presented in Figure 15. In addition, the MFL report showed low wall thickness loss along the length of the pipeline. Therefore, Line C was determined to be another good representative for a non-severe TLC pipeline.

Table 3: Pipe characteristic of Line C

Pipe characteristic	Line C
Steel type	Seamless (API 5LX52)
Pipe length (km)	7.2
Internal diameter (m)	0.44
Steel thickness (mm)	20.6
Insulation type	3LPP
Insulation Conductivity (W/mK)	0.22
Insulation thickness (mm)	2

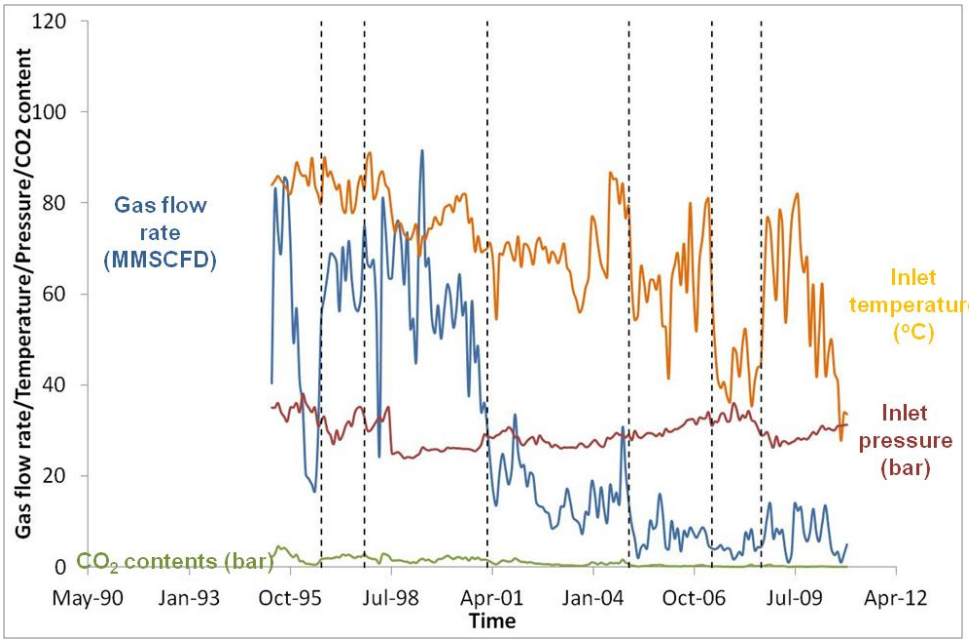

Figure 15: Input parameter variation over time for Line C.

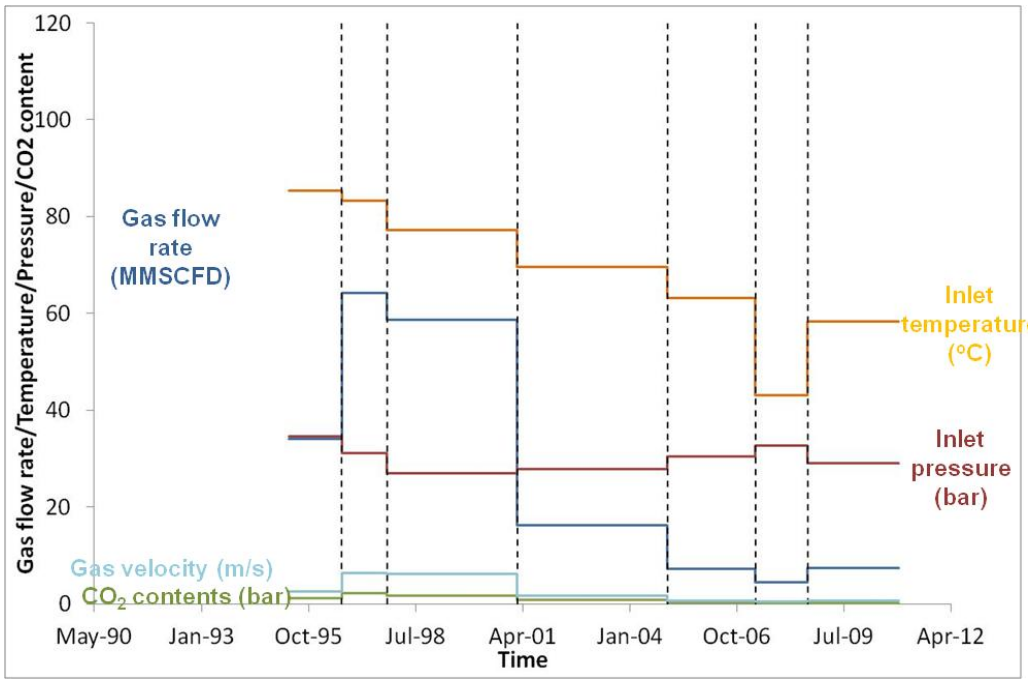

Figure 16: Averaged input parameters for Line C using seven time intervals.

4.2.2.4 Line D

An available-complete production history of Line D is presented in Figure 17. The production and input profiles were separated into seven time intervals as shown in Figure 18. High production was acheived in the first four time intervals. Then, it decreased after 7 years of operation. High TLC severity was expected at the beginning of the operation.

Table 4: Pipe characteristics of Line D

Pipe characteristic	Line D
Steel type	Seamless (API 5LX52)
Pipe length (km)	11.9
Internal diameter (m)	0.44
Steel thickness (mm)	20.6
Insulation type	3LPP
Insulation Conductivity (W/mK)	0.22
Insulation thickness (mm)	2

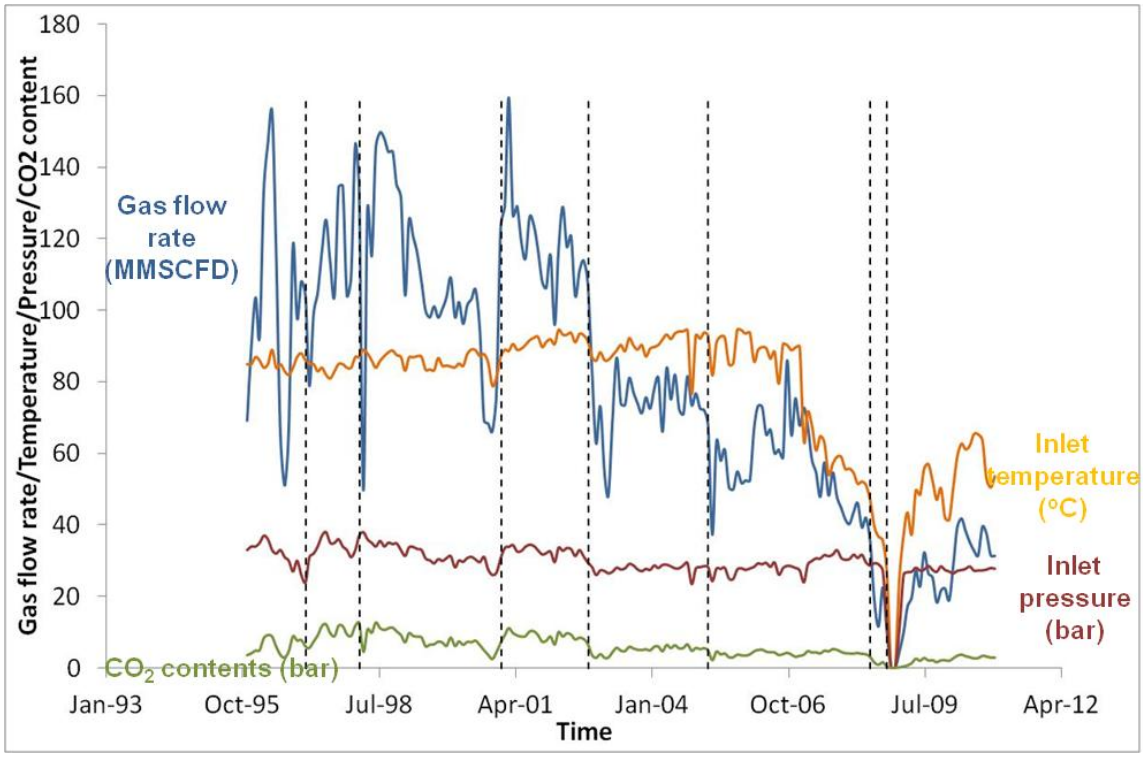

Figure 17: Input parameter variation over time for Line D.

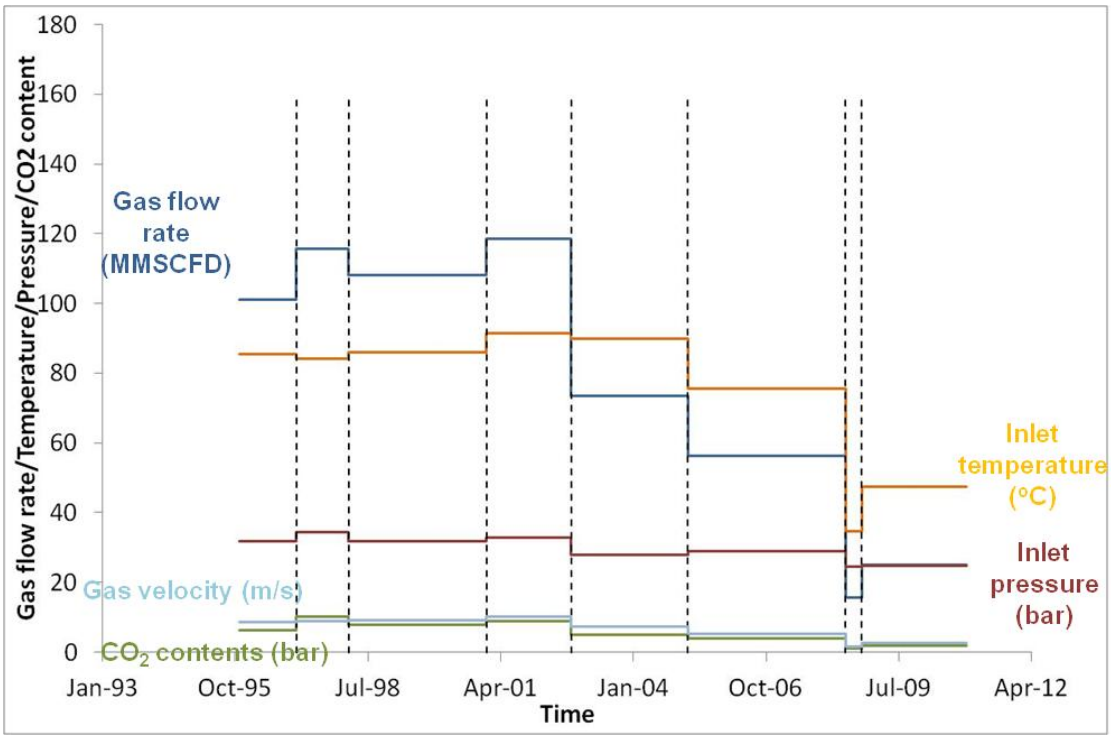

Figure 18: Averaged input parameters for Line D using eight time intervals.

4.2.2.5 Line E

Figure 19 shows the production profile of Line E from the start-up year to 2010. The MFL tool was used to inspect the severity of internal corrosion in 2005. Highly severe TLC was seen. In 2008, two leaks were detected at the 2nd and the 3rd anodes and cold spot TLC was identified as the cause of the failure as presented in Figure 7 [18]. With this kind of clear evidence, Line E was selected for the present study. As mentioned above, the MFL tool was run in 2005, the TLC occurrences during the start-up year to 2005 were simulated in this work.

Table 5: Pipe characteristic of Line E

Pipe characteristic	Line E
Steel type	Seamless (API 5LX52)
Pipe length (km)	7.1
Internal diameter (m)	0.34
Steel thickness (mm)	15.9
Insulation type	3LPP
Insulation Conductivity (W/mK)	0.22
Insulation thickness (mm)	2

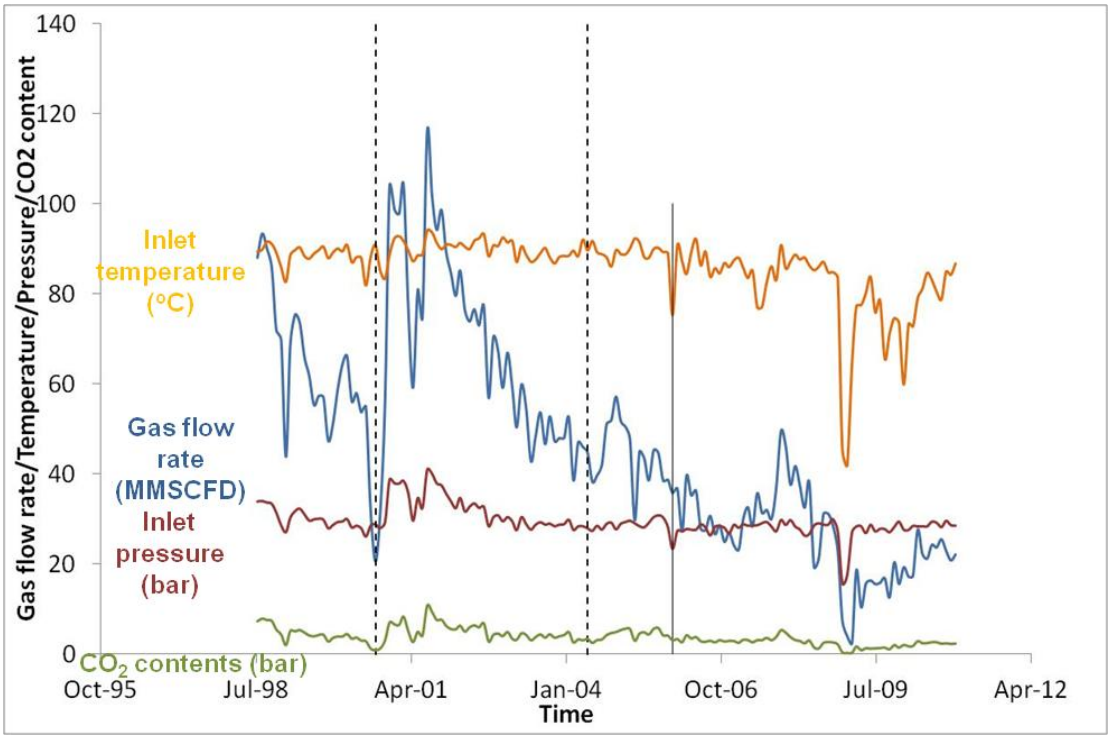

Figure 19: Input parameter variation over time for Line E.

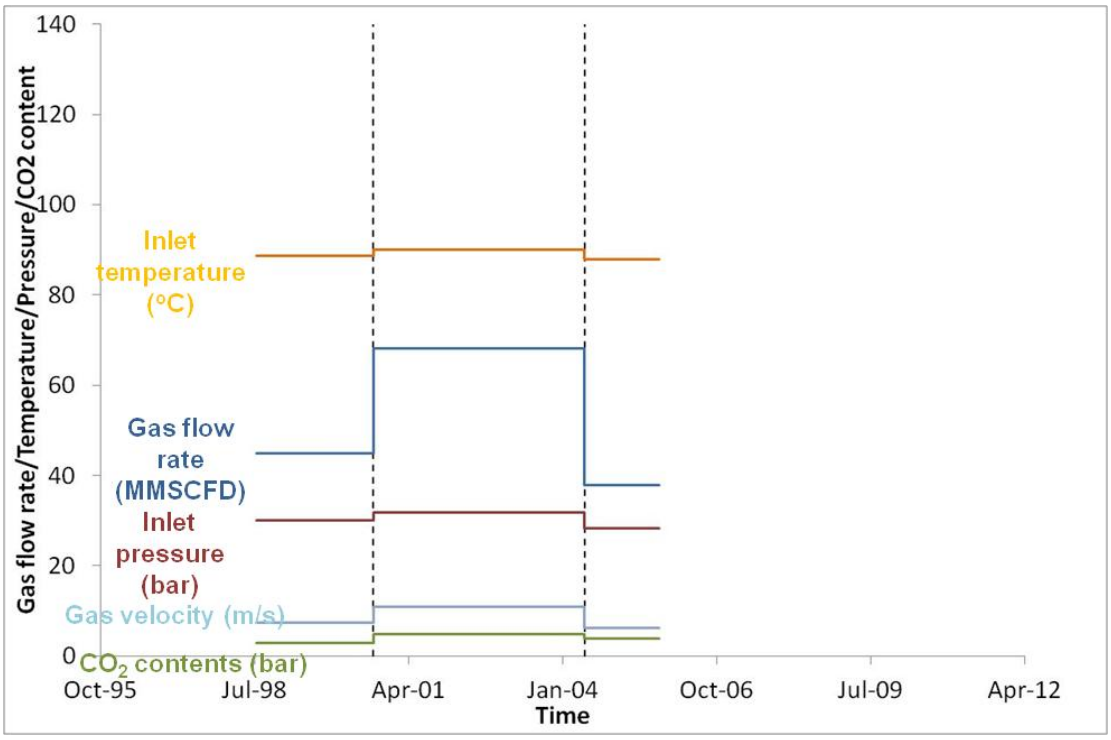

Figure 20: Averaged input parameters for Line E using three time intervals.

4.2.2.6 Line F

Line F also presented serious evidence of a TLC occurrence in the field. In 2008, a leak was visually detected. As a result, a short section of the pipeline, between the first and second flanges, was replaced. Figure 21 and Figure 22 present a production history and weight-averaged values, respectively.

Table 6: Pipe characteristic of Line F

Pipe characteristic	Line F
Steel type	Seamless (API 5LX52)
Pipe length (km)	26.9
Internal diameter (m)	0.39
Steel thickness (mm)	15.9
Insulation type	3LPP / concrete
Insulation Conductivity (W/mK)	0.22/0.5
Insulation thickness (mm)	2/25.4

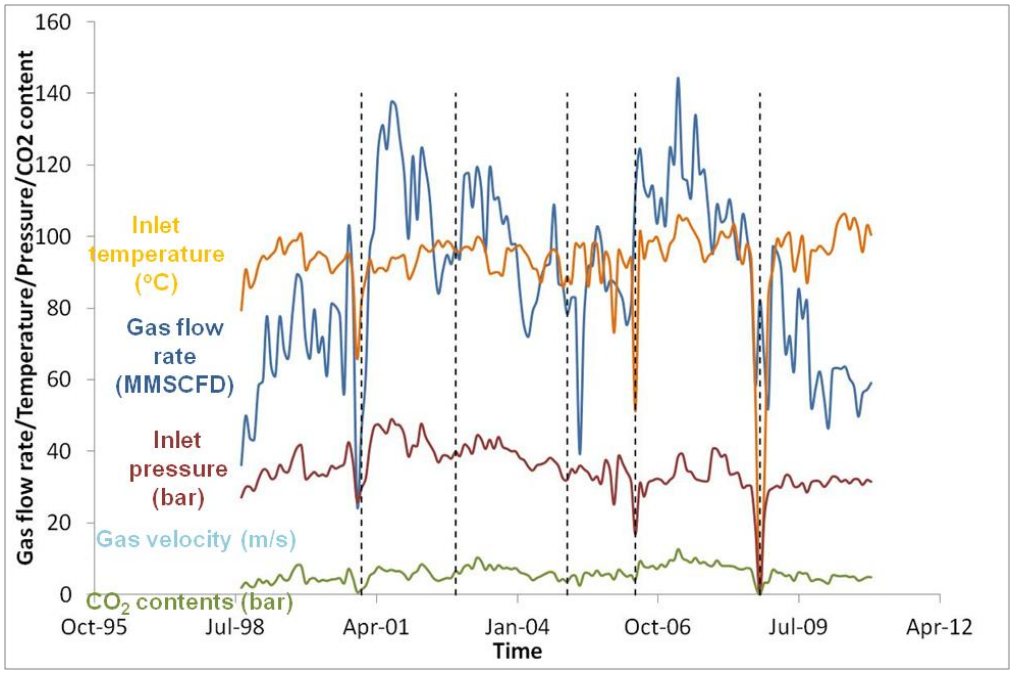

Figure 21: Input parameter variation over time for Line F.

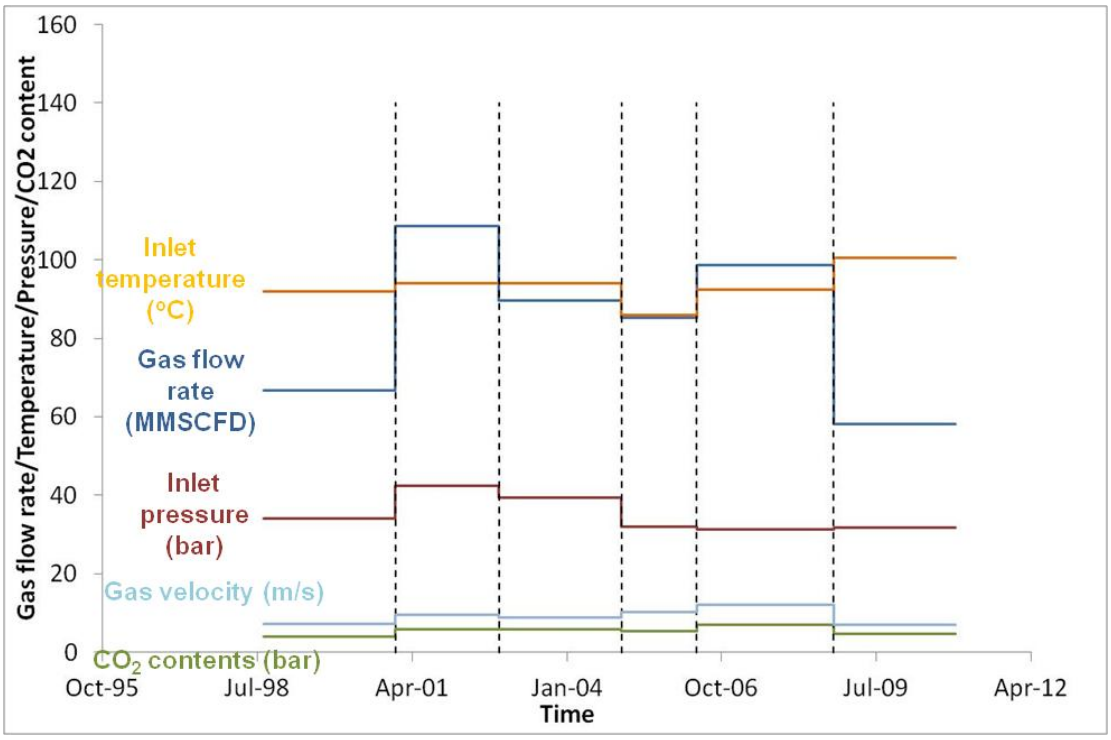

Figure 22: Averaged input parameters for Line F using six time intervals.

4.2.2.7 Line G

Line G is another pipeline that had available and complete production information as presented in Figure 23. The production and input data were analyzed by dividing them into five time intervals and the calculated weight-averaged values are shown in Figure 24.

Table 7: Pipe characteristic of Line G

Pipe characteristic	Line G
Steel type	Seamless (API 5LX52)
Pipe length (km)	19.7
Internal diameter (m)	0.34
Steel thickness (mm)	15.9
Insulation type	3LPP
Insulation Conductivity (W/mK)	0.22
Insulation thickness (mm)	2

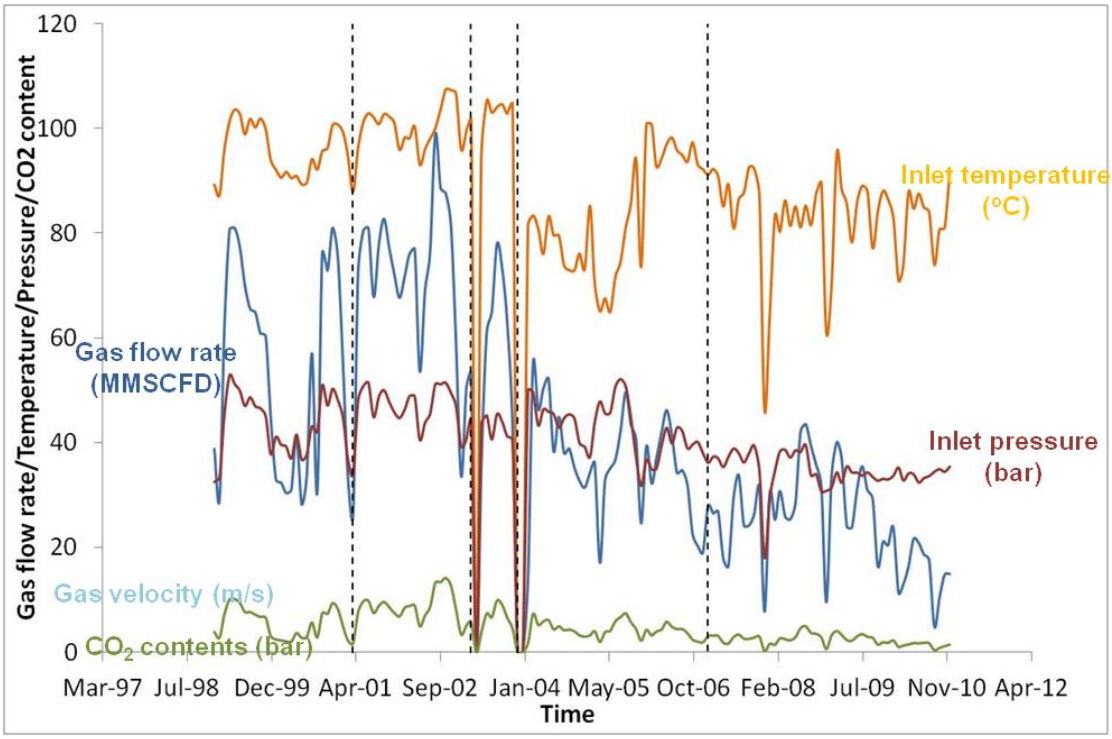

Figure 23: Input parameter variation over time for Line G.

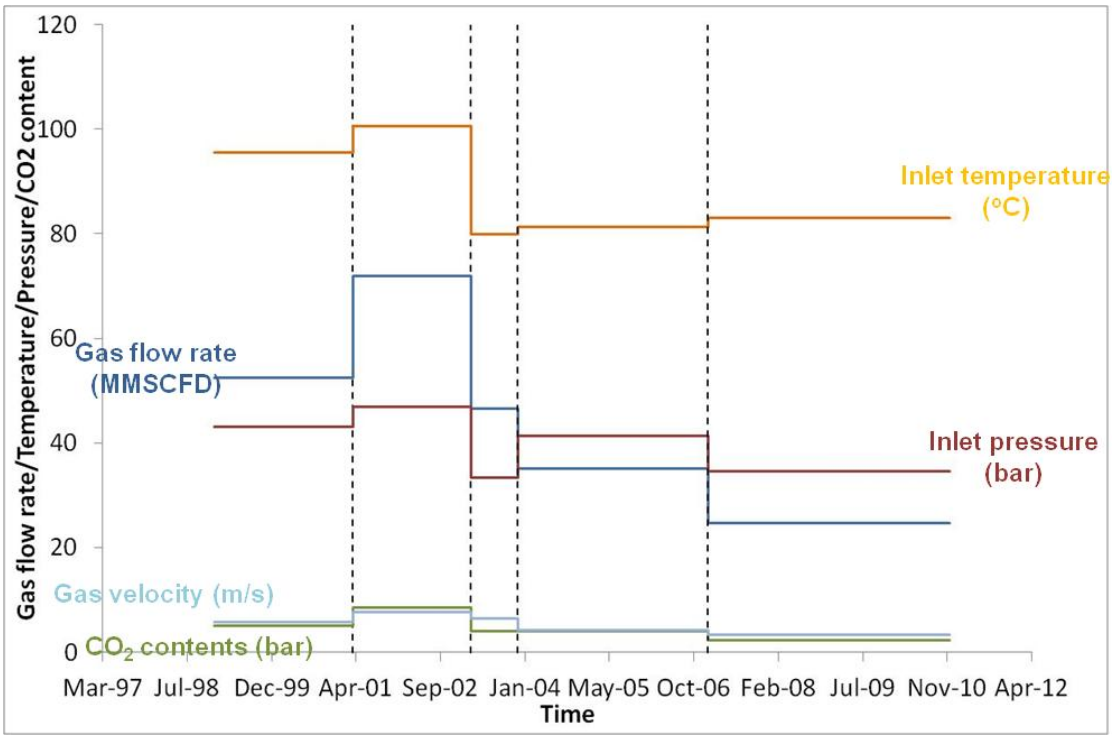

Figure 24: Averaged input parameters for Line G using five time intervals.

4.2.3 In-line inspection analysis

Following the procedure presented in the previous chapter, representative MFL data from the seven pipelines were filtered and are illustrated in Figure 25 to Figure 31. For every pipeline, non-TLC features were eliminated. Subsequently, the maximum penetration envelope capturing the maximum wall thickness loss was identified. Finally, the uniform TLC features identified as clusters were selected. The filtered MFL data were then compared with the model predictions.

4.2.3.1 Line A

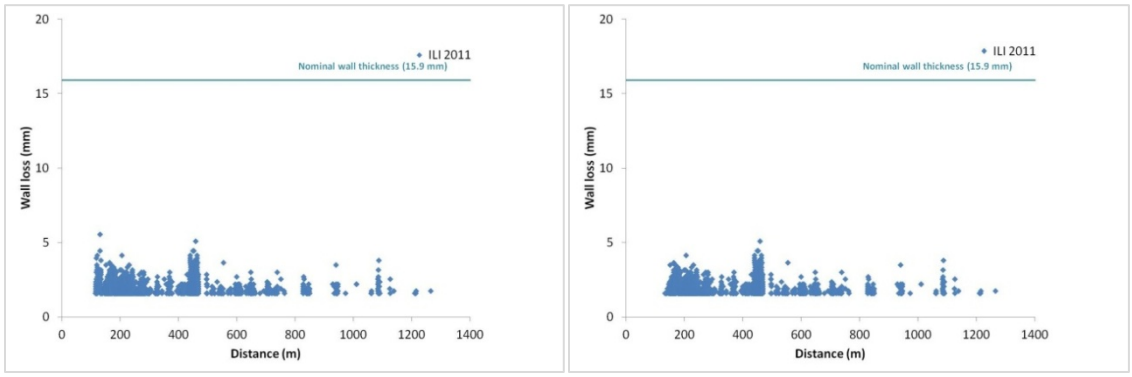

a) all MFL corrosion features

b) a subset containing only TLC features

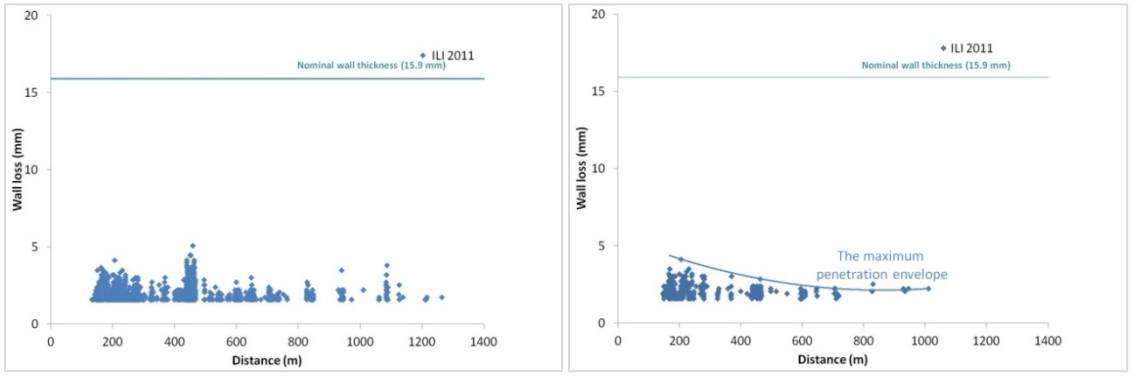

c) a further subset with the noisy measurement close to pipe joints filtered out

d) a final subset showing only TLC clusters along with the maximum penetration envelope

Figure 25: MFL data filtering for Line A.

4.2.3.2 Line B

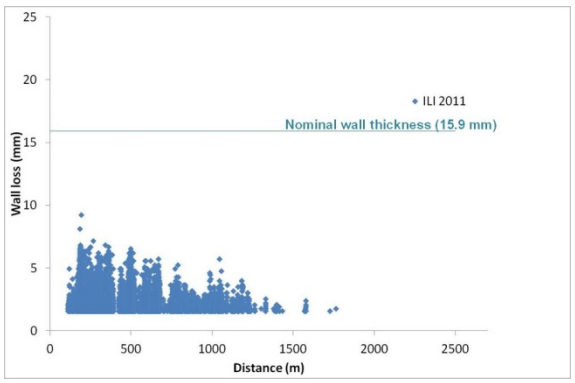

a) all MFL corrosion features

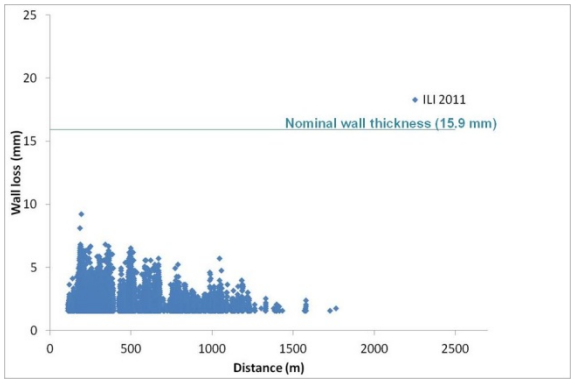

b) a subset containing only TLC features

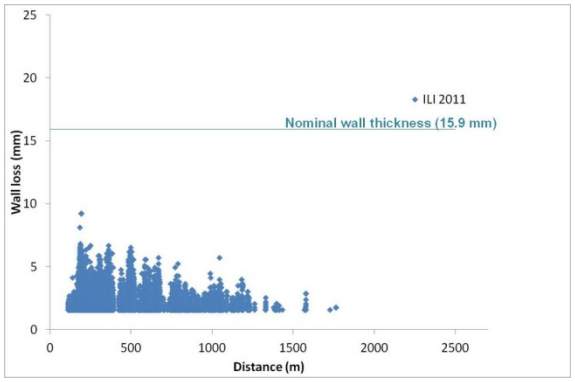

c) a further subset with the noisy measurement close to pipe joints filtered out

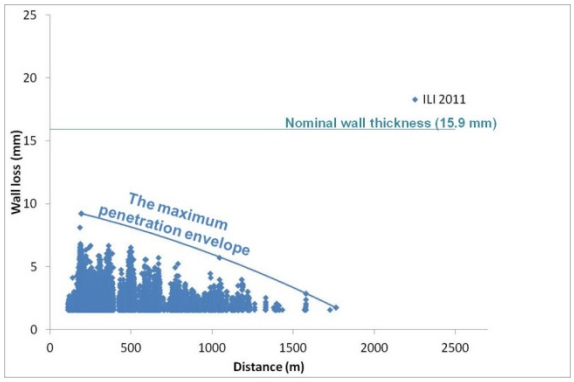

d) a final subset showing only TLC clusters along with the maximum penetration envelope

Figure 26: MFL data filtering for Line B.

4.2.3.3 Line C

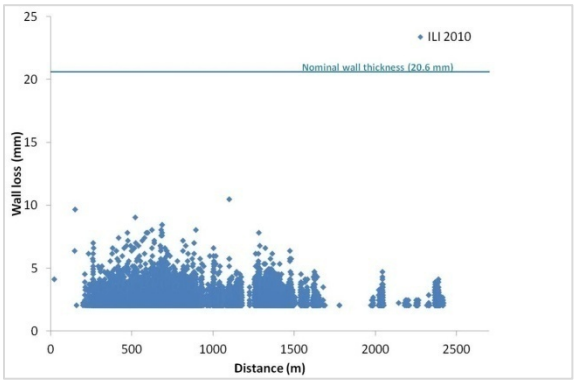

a) all MFL corrosion features

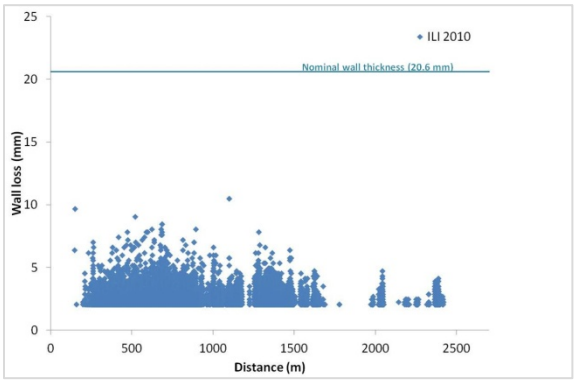

b) a subset containing only TLC features

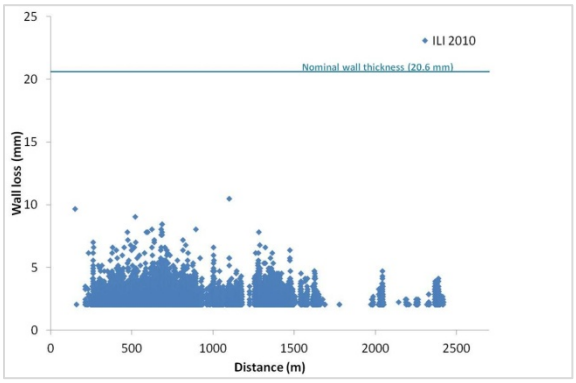

c) a further subset with the noisy measurement close to pipe joints filtered out

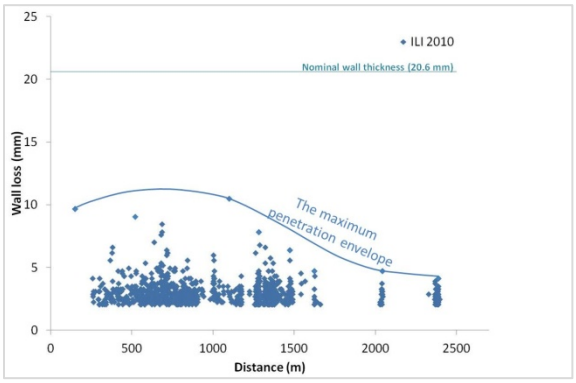

d) a final subset showing only TLC clusters along with the maximum penetration envelope

Figure 27: MFL data filtering for Line C.

4.2.3.4 Line D

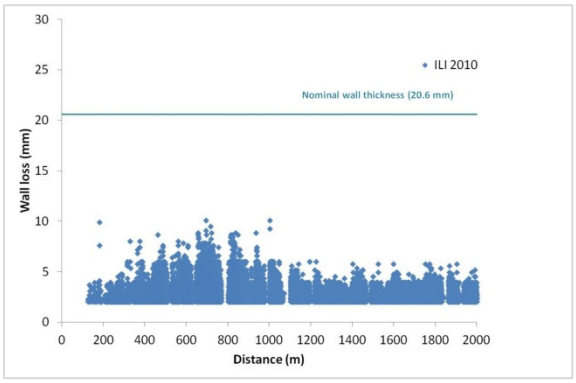

a) all MFL corrosion features

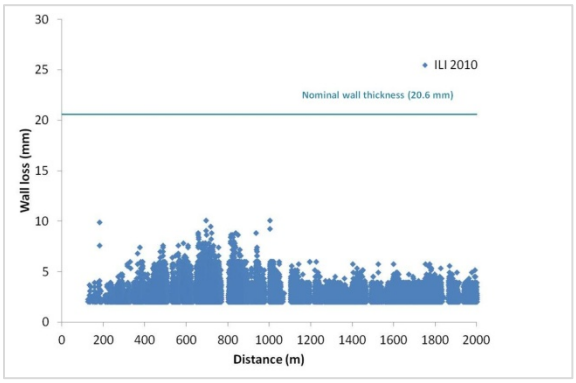

b) a subset containing only TLC features

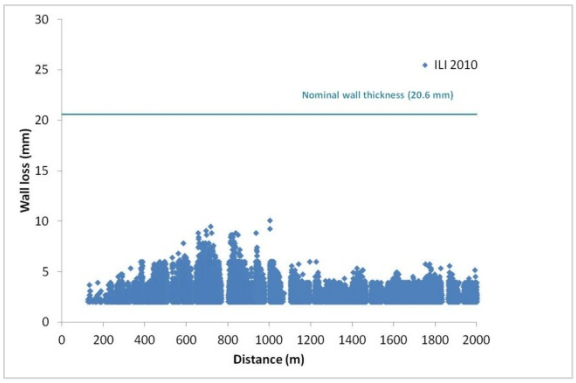

c) a further subset with the noisy measurement close to pipe joints filtered out

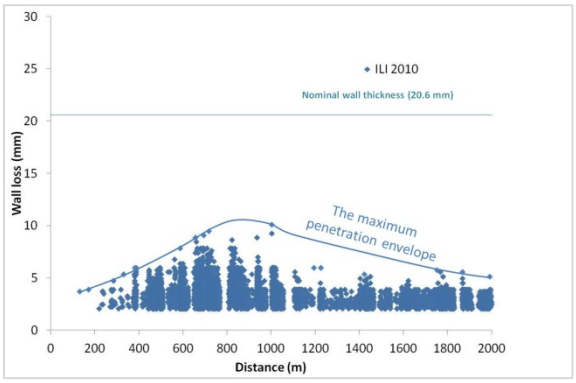

d) a final subset showing only TLC clusters along with the maximum penetration envelope

Figure 28: MFL data filtering for Line D.

4.2.3.5 Line E

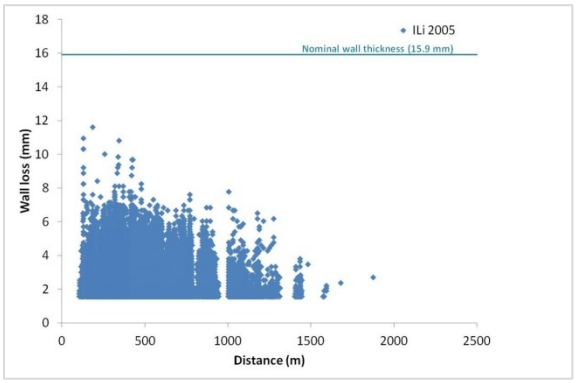

a) all MFL corrosion features

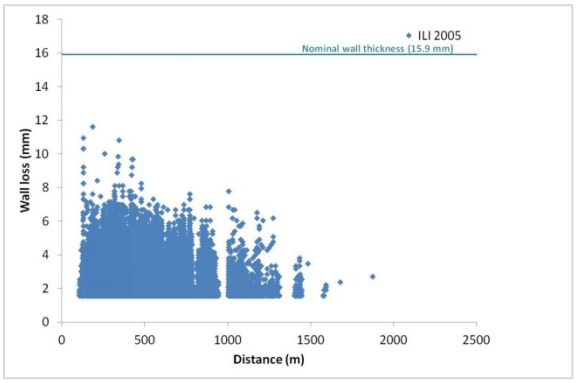

b) a subset containing only TLC features

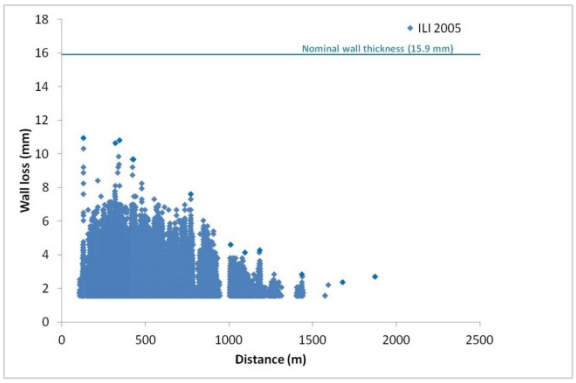

c) a further subset with the noisy measurement close to pipe joints filtered out

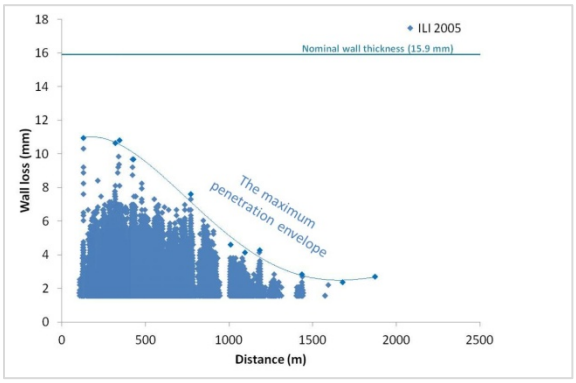

d) a final subset showing only TLC clusters along with the maximum penetration envelope

Figure 29: MFL data filtering for Line E.

4.2.3.6 Line F

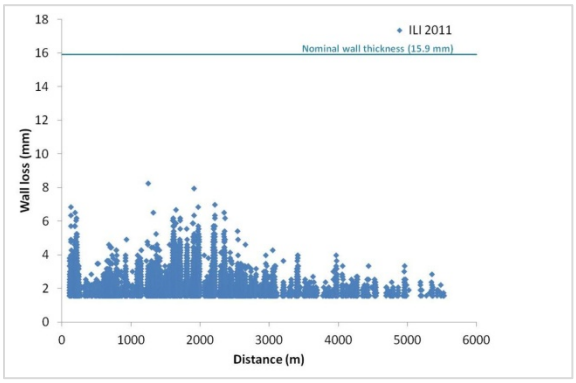

a) all MFL corrosion features

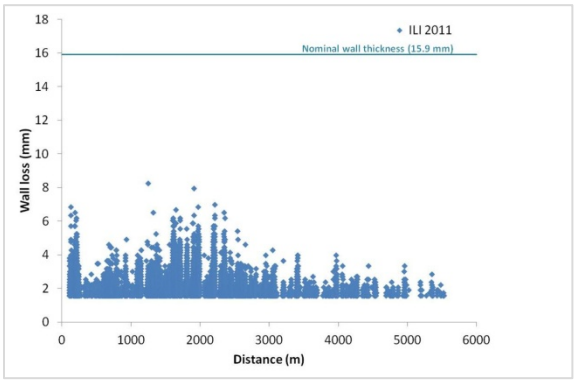

b) a subset containing only TLC features

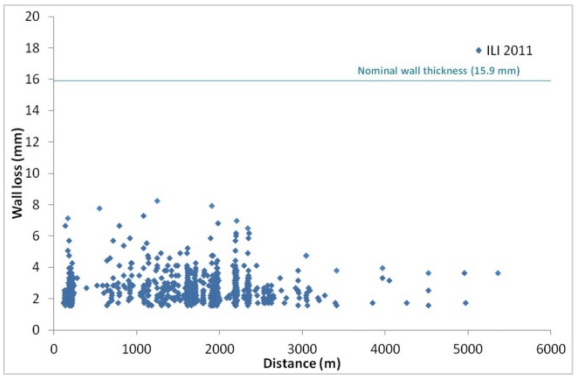

c) a further subset with the noisy measurement close to pipe joints filtered out

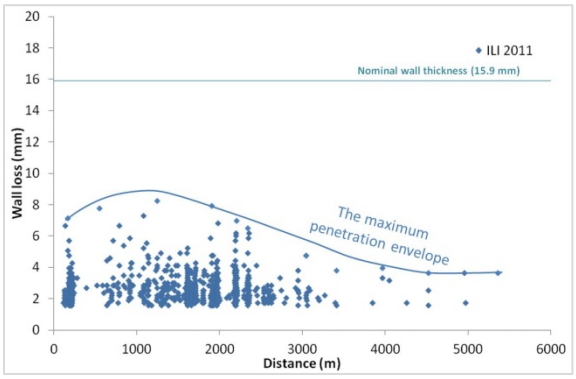

d) a final subset showing only TLC clusters along with the maximum penetration envelope

Figure 30: MFL data filtering for Line F.

4.2.3.7 Line G

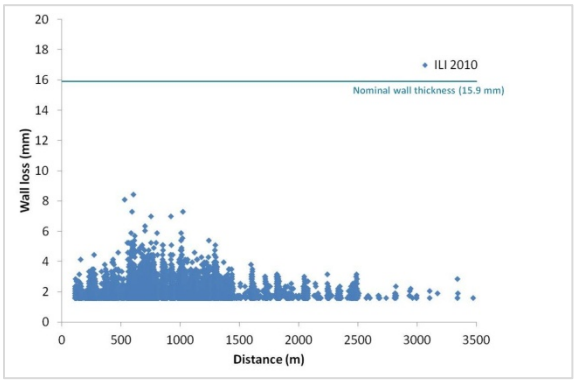

a) all MFL corrosion features

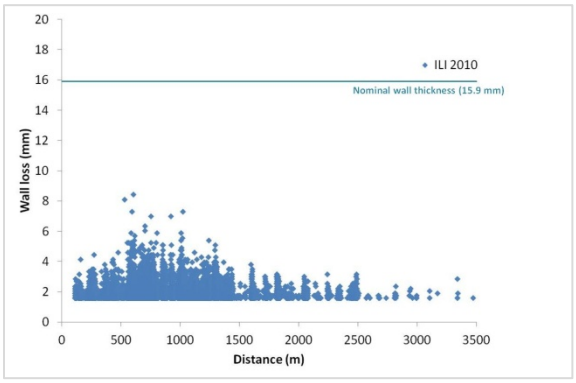

b) a subset containing only TLC features

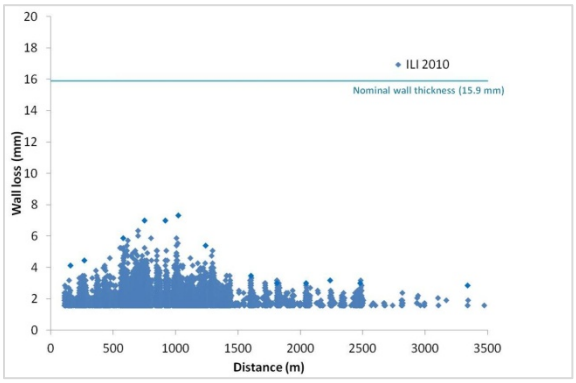

c) a further subset with the noisy measurement close to pipe joints filtered out

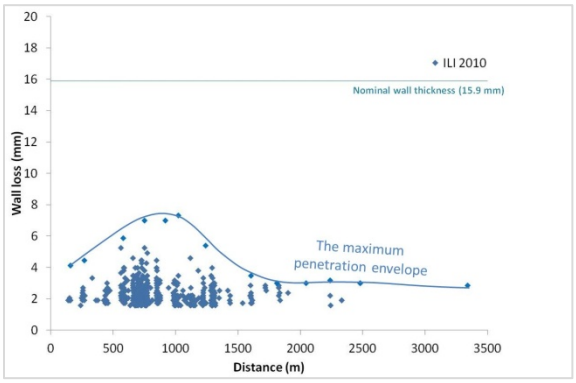

d) a final subset showing only TLC clusters along with the maximum penetration envelope

Figure 31: MFL data filtering for Line G.

4.2.4 Simulation results

4.2.4.1 Line A

The water condensation rate (WCR) and temperature profile of each time interval were simulated by using an in-house line model, as presented in Figure 32 a) to i). The simulated WCRs were low (lower than 0.25 ml/m^2/s) due to the low inlet temperature (lower than 60 ^{o}C) and low CO_2 contents. As a result, predicted TLC rates and wall thickness losses from several selected points were determined to be low as illustrated in Figure 33 and Figure 34.

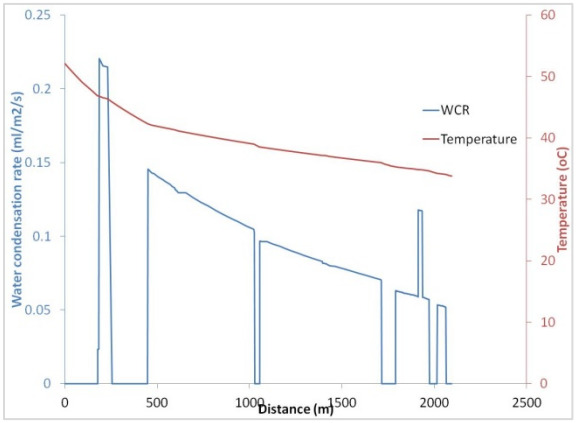

a) Time interval#1

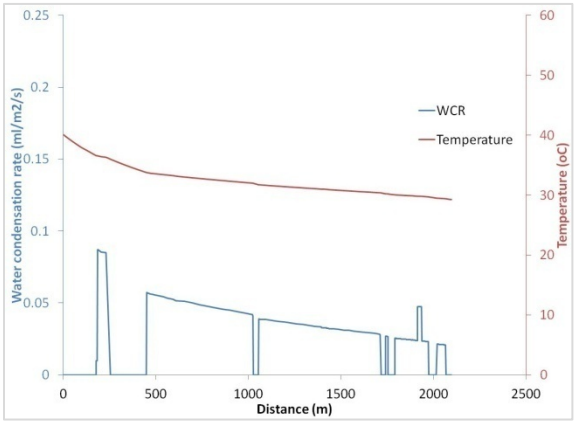

b) Time interval#2

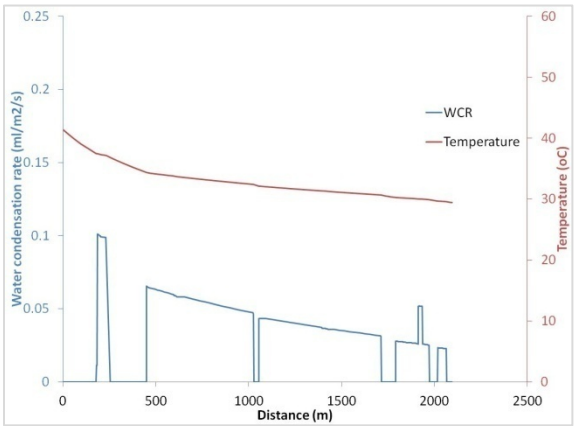

c) Time interval#3

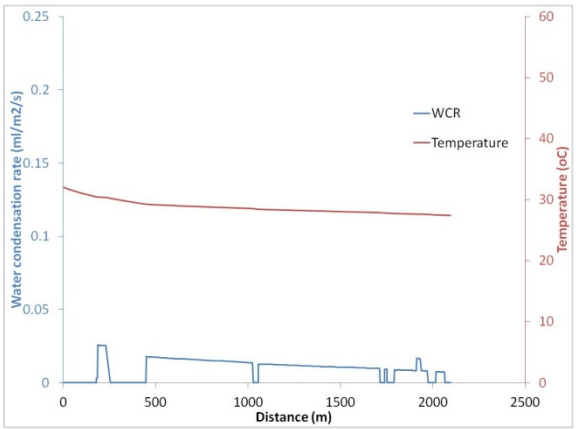

d) Time interval#4

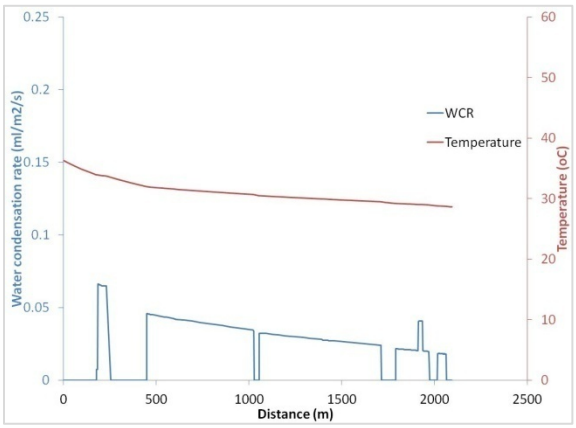

e) Time interval#5

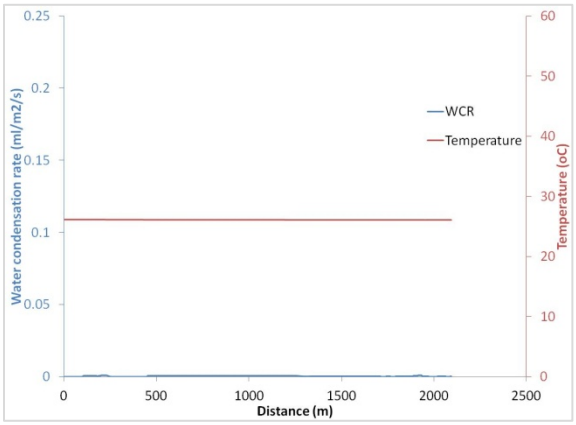

f) Time interval#6

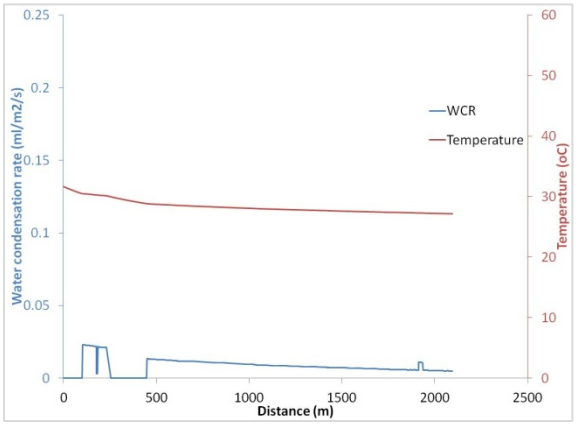

g) Time interval#7

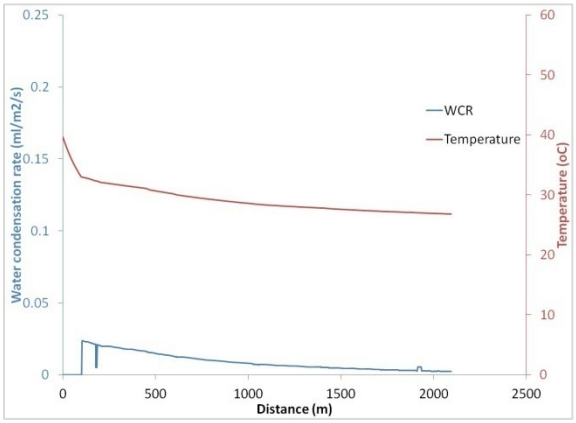

h) Time interval#8

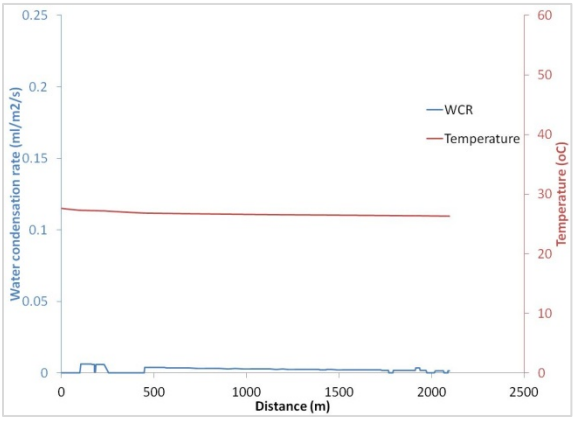

i) Time interval#9

Figure 32: WCR and temperature profile along the length of the Line A predicted from heat and mass transfer line model simulation.

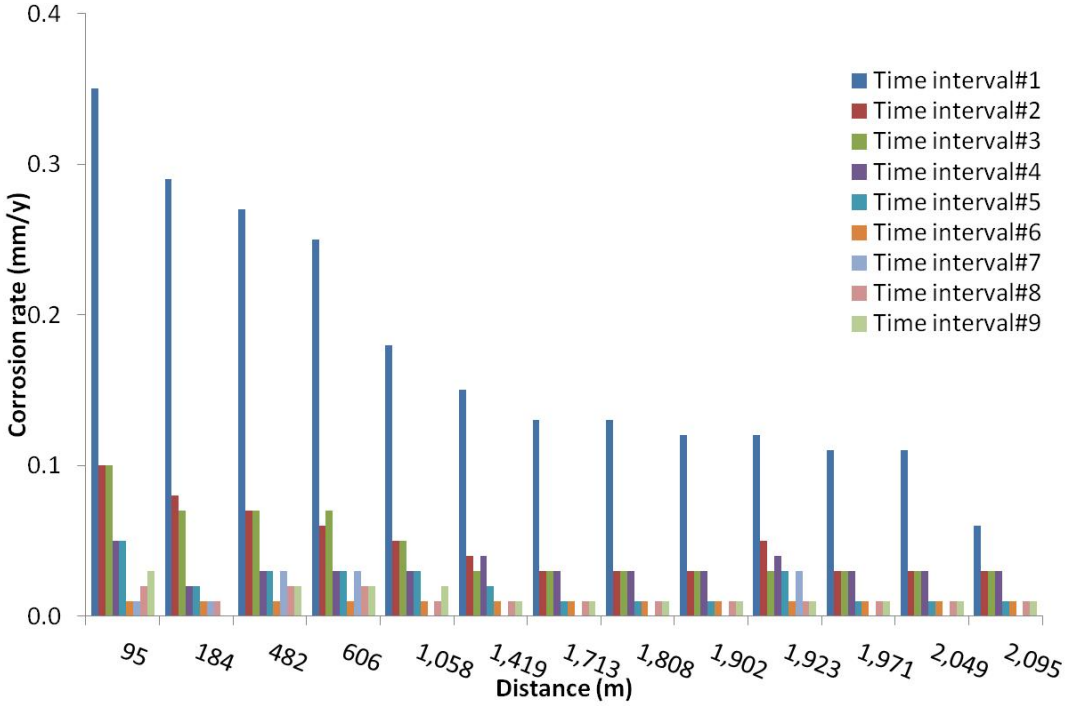

Figure 33: Predicted TLC rate for Line A.

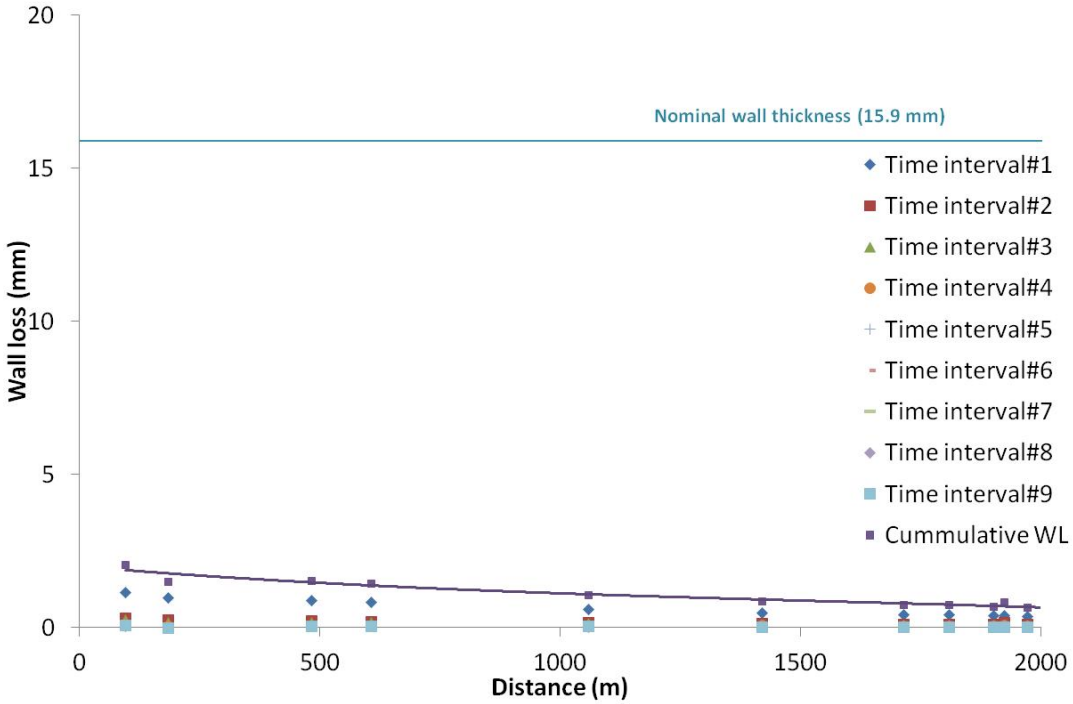

Figure 34: Calculated wall thickness loss values for the nine time intervals and the total cumulative wall thickness loss value for Line A.

4.2.4.2 Line B

Predicted WCR and temperature profiles for each time interval are illustrated in Figure 35 a) to e). In the first time interval, the non-stratified flow regime was predicted because of high gas velocity. Thus, there was no concern about TLC at the beginning of the operation. For other time intervals, values of WCR were calculated due to the predicted stratified flow regime. In the third time interval, high gas velocity was calculated and led to the highest calculated values. As a result, presented in Figure 36, the maximum TLC rate was predicted from the input condition in the third time interval. Calculated wall thickness losses of this line were significantly high. The cumulative value in Figure 37 shows higher than the nominal pipe wall thickness indicating highly severe TLC.

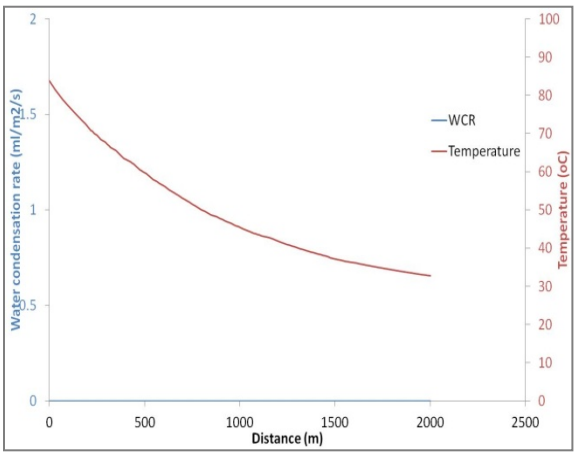

a) Time interval#1

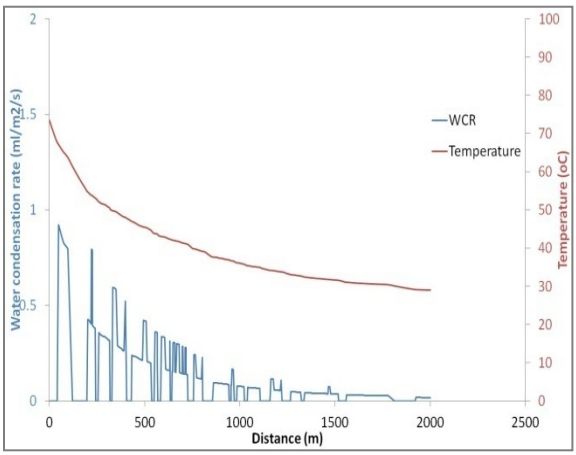

b) Time interval#2

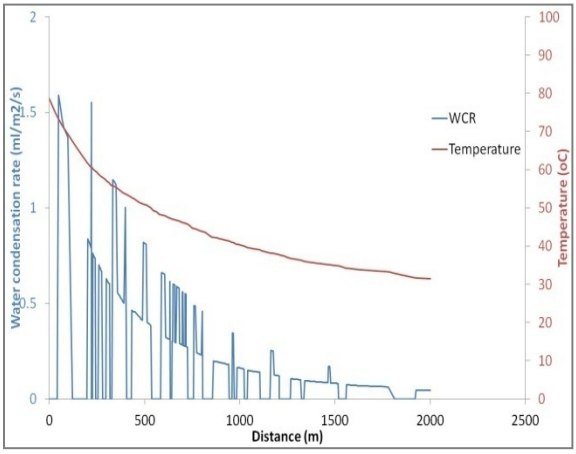

c) Time interval#3

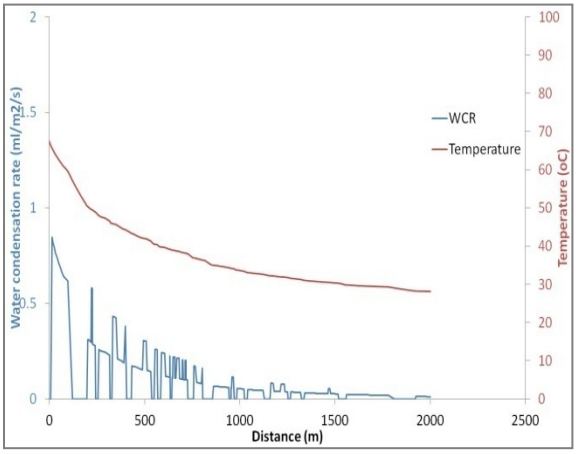

d) Time interval#4

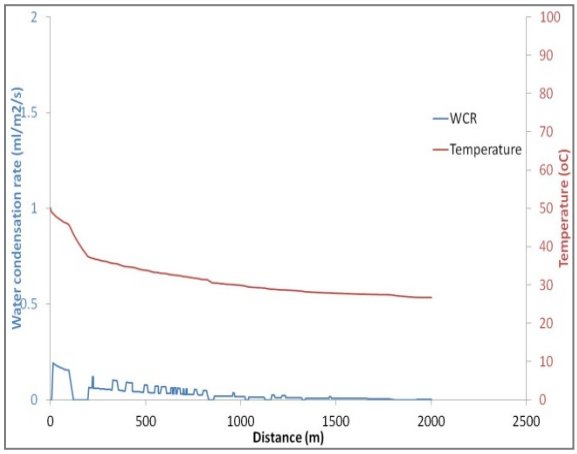

e) Time interval#5

Figure 35: WCR and temperature profile along the length of the Line B predicted from heat and mass transfer line model simulation.

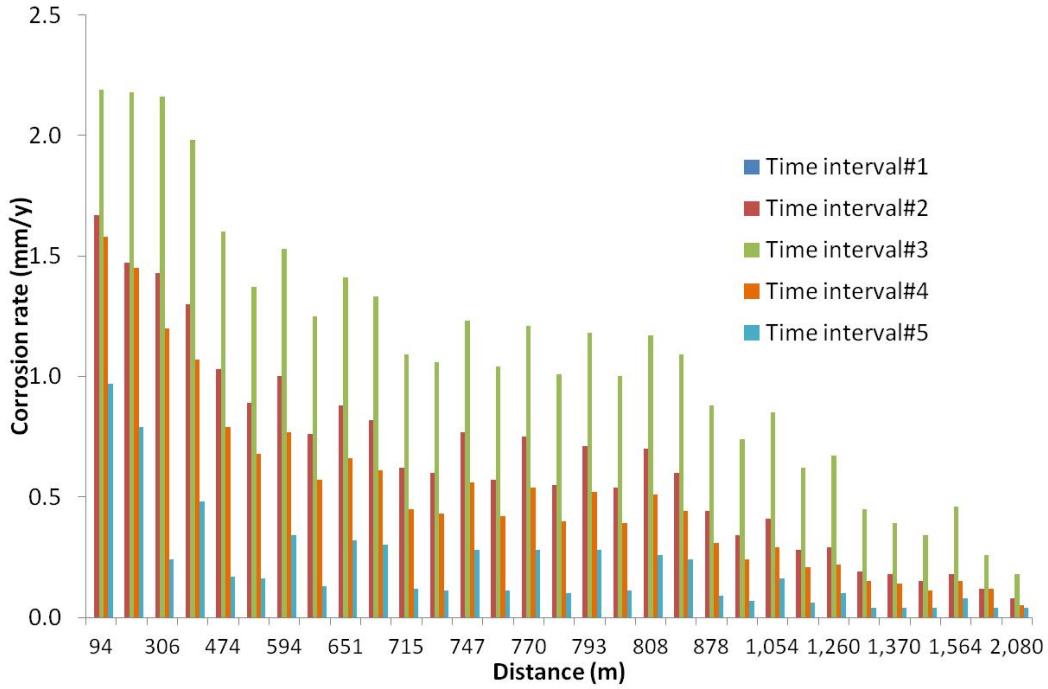

Figure 36: Predicted TLC rate for Line B.

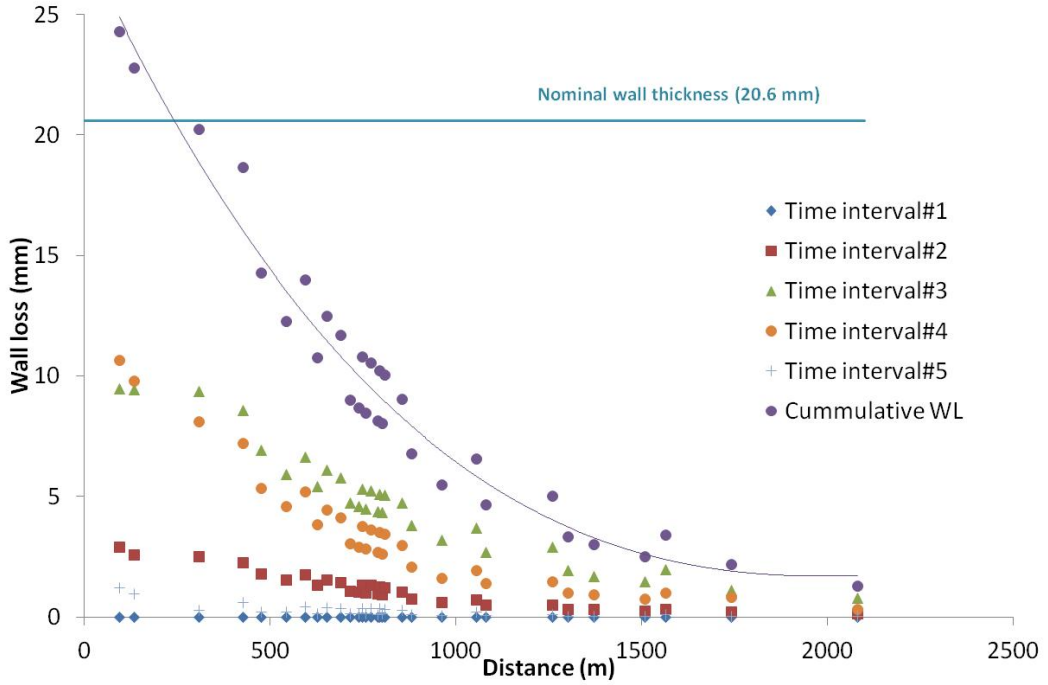

Figure 37: Calculated wall thickness loss values for the five time intervals and the total cumulative wall thickness loss value for Line B.

4.2.4.3 Line C

Figure 38 a) to g) show predicted WCR and temperature profiles for the time intervals #1 to #7, respectively. Even though the high WCR was expected due to a high temperature difference between fluid (40 to 80 ^{o}C) and the surrounding environment (26 ^{o}C), the predicted WCR of Line C is quite low because of a low gas velocity (0.6-6.3 m/s), particularly in the last four time intervals. As a result, simulated TLC rates and wall thickness losses from several selected points in a stratified flow regime were low as illustrated in Figure 39 and Figure 40. In conclusion, the main parameters affecting TLC in this pipeline were gas velocity and low CO_2 content.

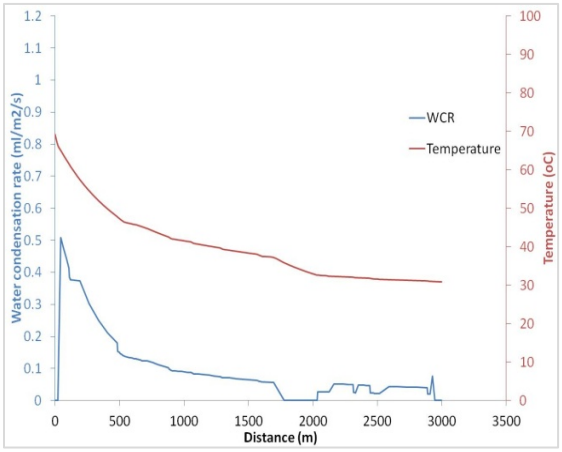

a) Time interval#1

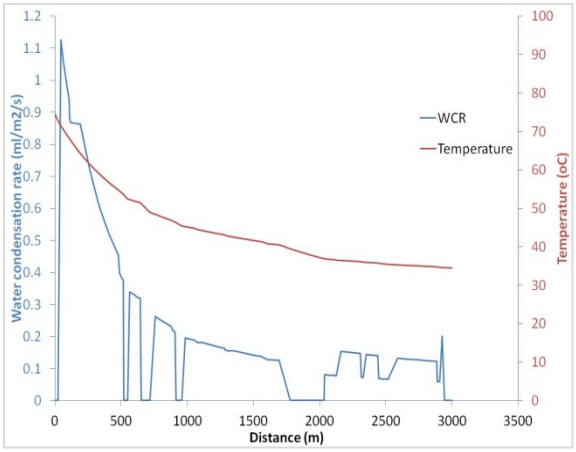

b) Time interval#2

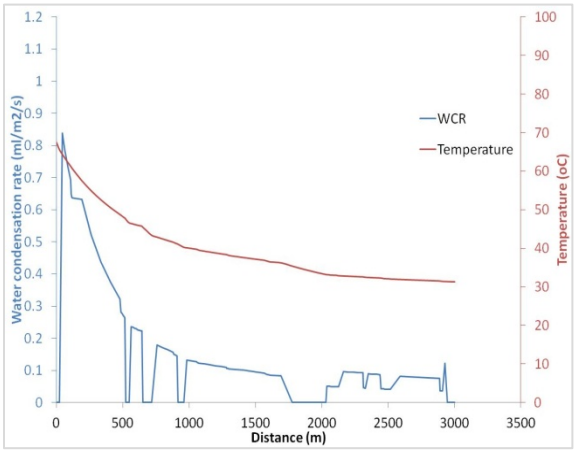

c) Time interval#3

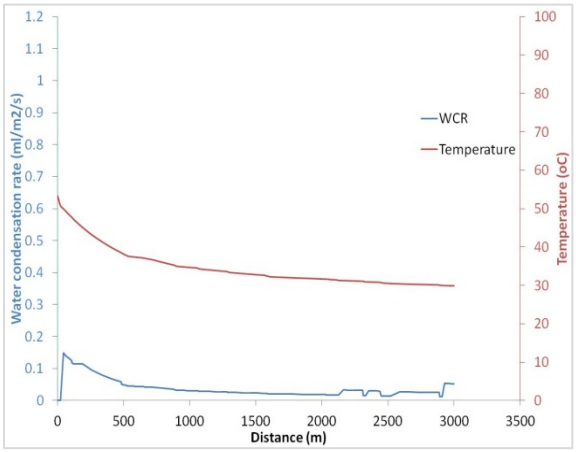

d) Time interval#4

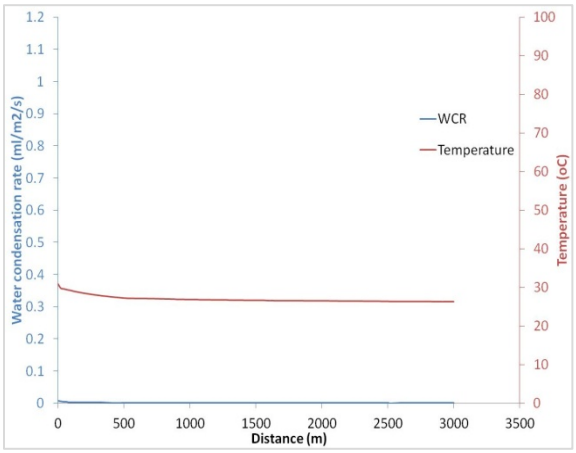

e) Time interval#5

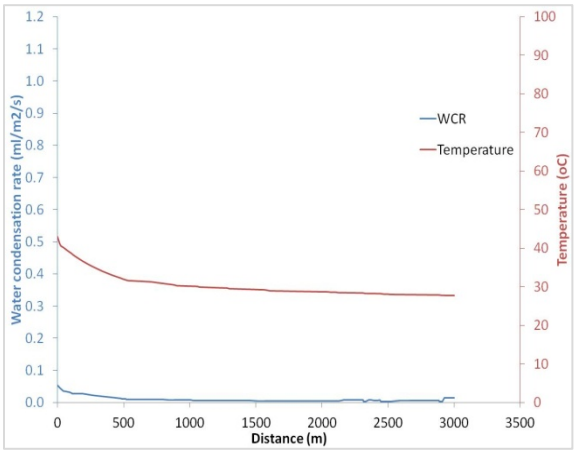

f) Time interval#6

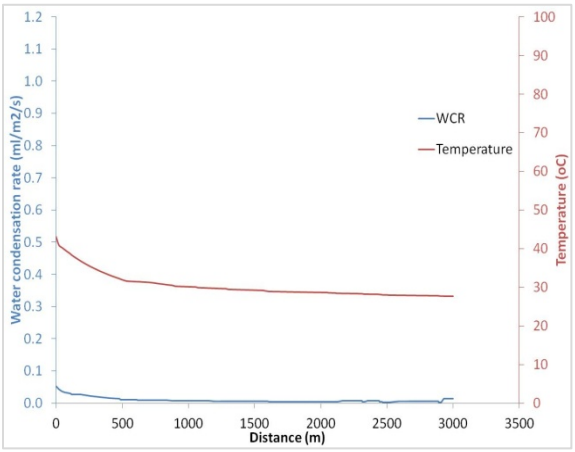

g) Time interval#7

Figure 38: WCR and temperature profile along the length of the Line C predicted from heat and mass transfer line model simulation.

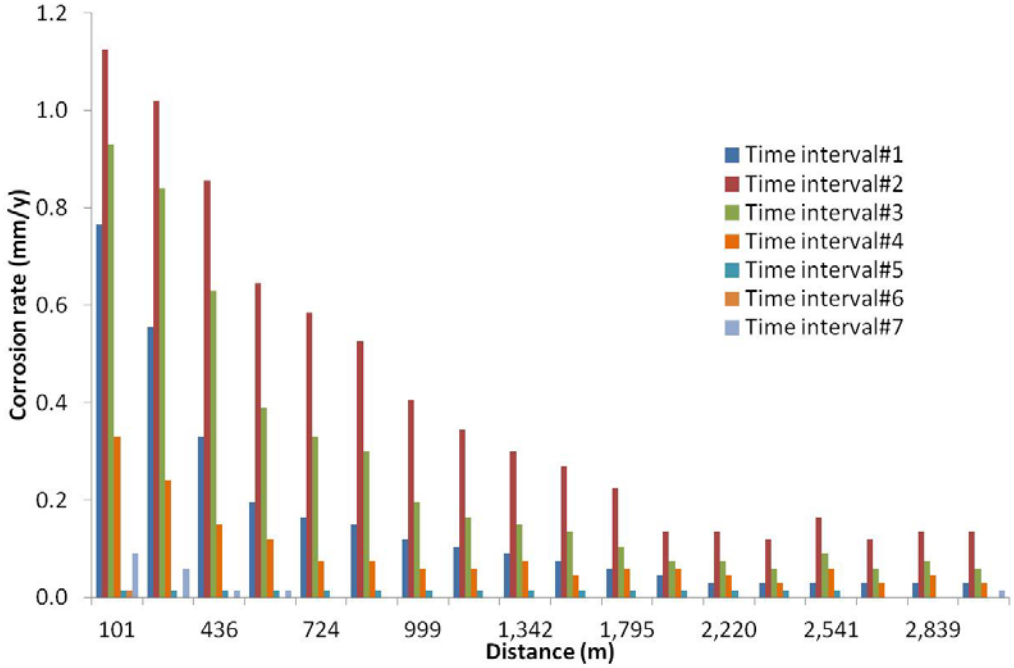

Figure 39: Predicted TLC rate for Line C.

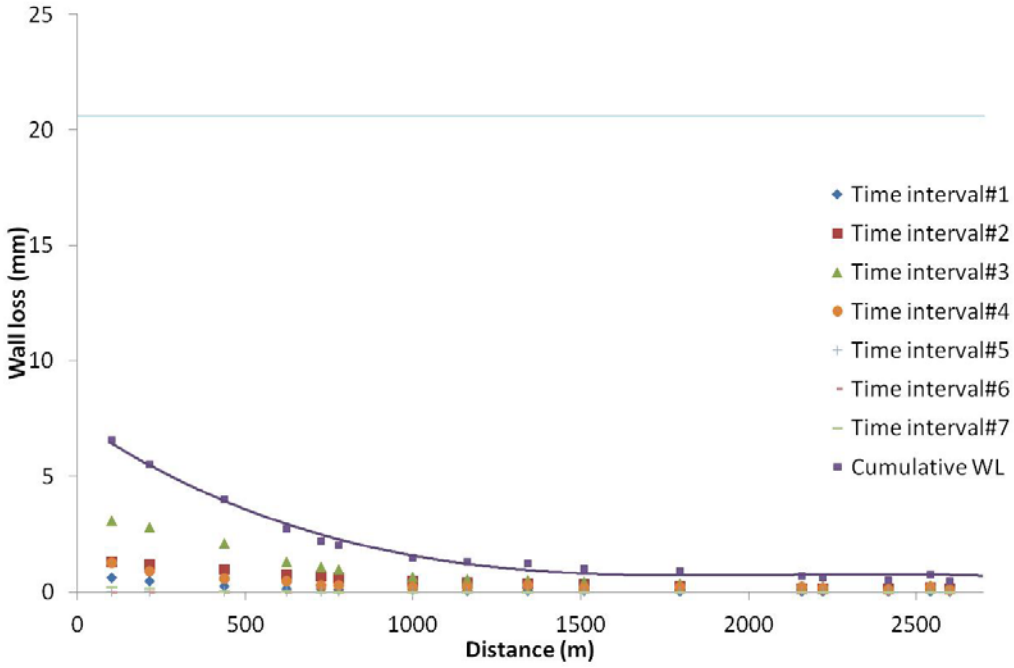

Figure 40: Calculated wall thickness loss values for the seven time intervals and the total cumulative wall thickness loss value for Line C.

4.2.4.4 Line D

The high values of WCR in the first six time intervals, due to high operating temperatures, were calculated and presented in Figure 38 a) thru h). Consequently, a high corrosion rate and wall thickness losses were predicted. However, WCR suddenly decreased due to merging with a cooler pipeline. Predicted WCR was obviously low as illustrated in Figure 38 g) and i). A cumulative wall thickness loss of this line was quite high and indicated likelihood for high TLC.

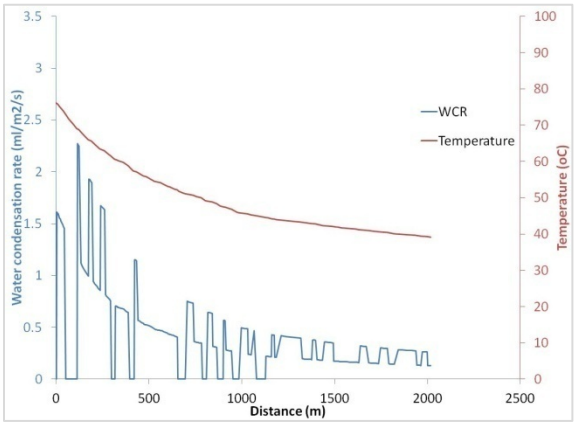

a) Time interval#1

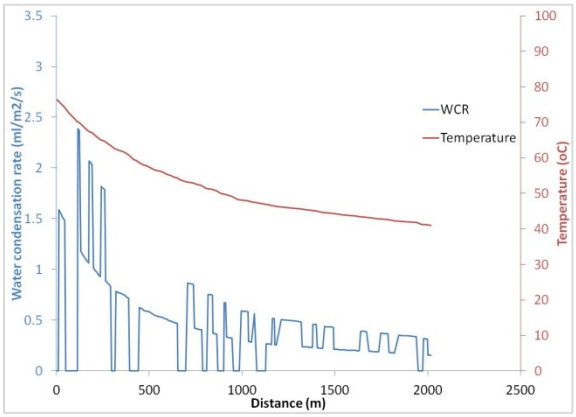

b) Time interval#2

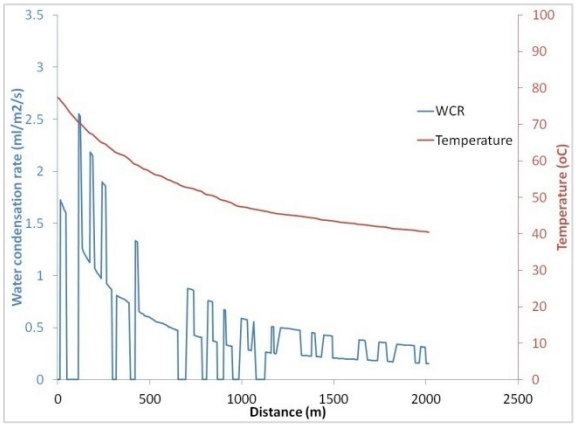

c) Time interval#3

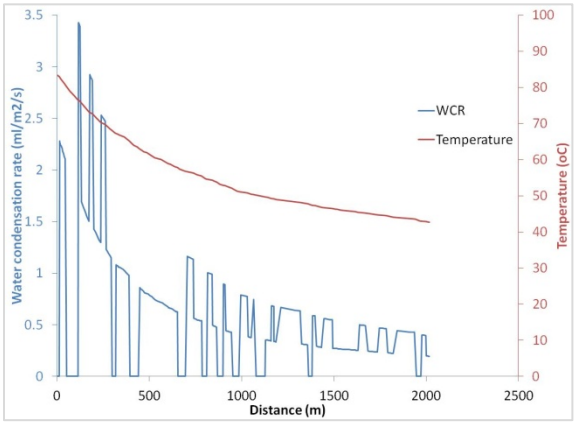

d) Time interval#4

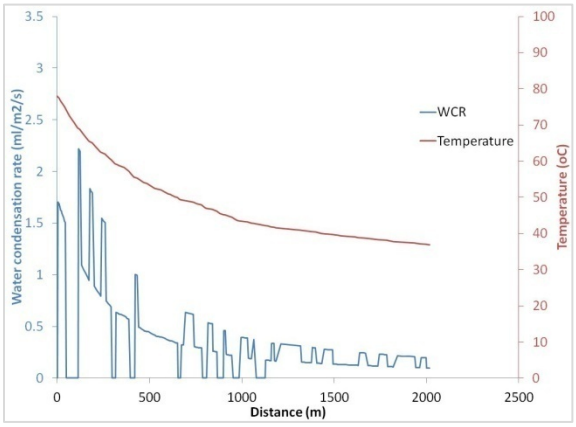

e) Time interval#5

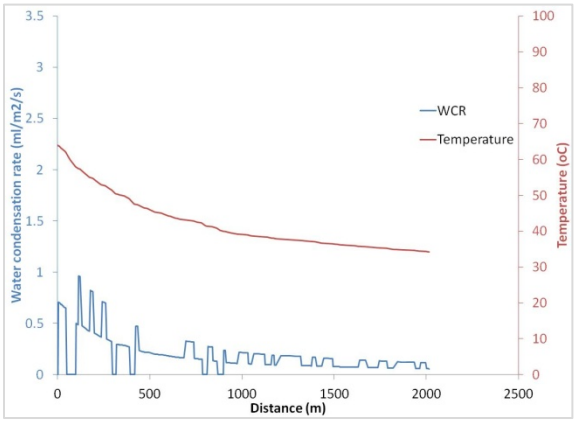

f) Time interval#6

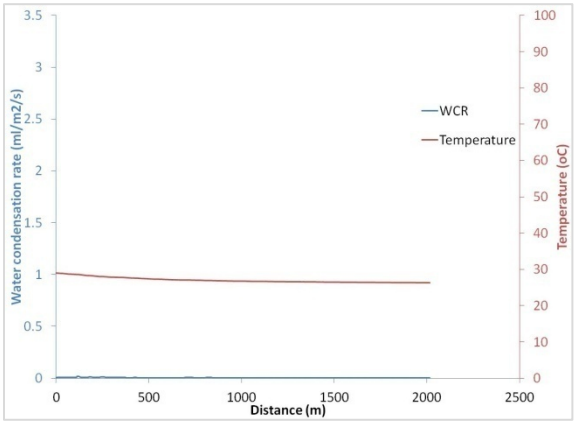

g) Time interval#7

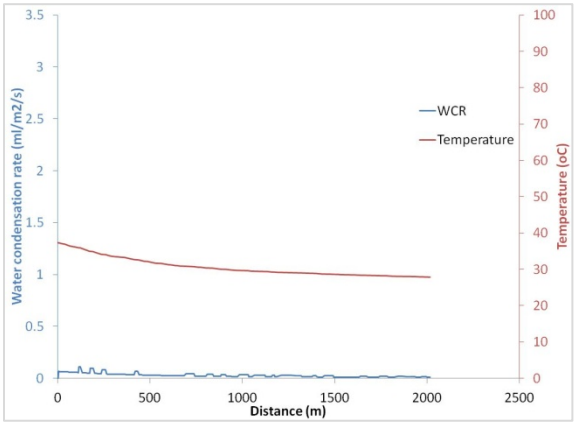

h) Time interval#8

Figure 41: WCR and temperature profile along the length of the Line D predicted from heat and mass transfer line model simulation.

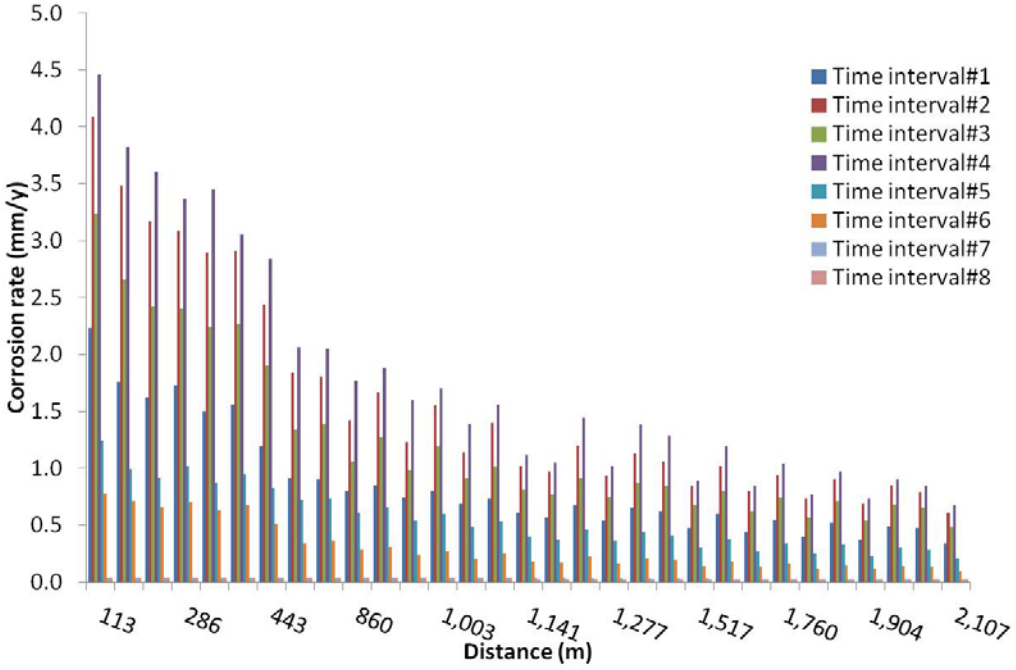

Figure 42: Predicted TLC rate for Line D.

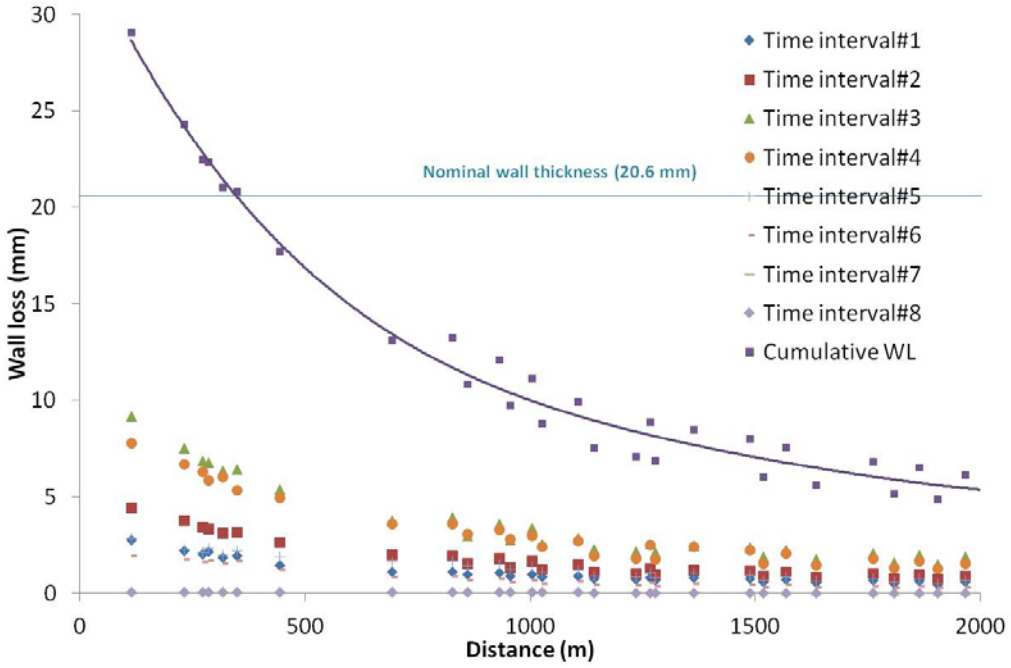

Figure 43: Calculated wall thickness loss values for the eight time intervals and the total cumulative wall thickness loss value for Line D.

4.2.4.5 Line E

Figure 44 shows predicted WCR and temperature profile of time interval #1, time interval #2 and time interval #3, respectively.

During the first time interval, high values of WCR were calculated at the beginning of the pipeline due to a high temperature gradient between the inside and outside of the pipe wall. As expected, the values of WCR decreased along the pipeline because of the decreasing fluid temperature.

For the second time interval, the values for the WCR in the location operating within a stratified flow regime were higher compared to the WCR in the first time interval at the same locations; however, the change in production information (higher gas velocity) obviously affected the change in the flow regime. The non-stratified flow regime was identified in several sections meaning that there was a low TLC risk zone in this time interval.

For the third time interval, predicted WCR is clearly lower than in the first two time intervals because of lower heat exchange between the pipeline and environment.

The operating conditions in the second time interval cause the most severe TLC risk (for specific locations in the line operating in stratified flow regime). As a result, the model predicted a higher risk level for TLC for this line.

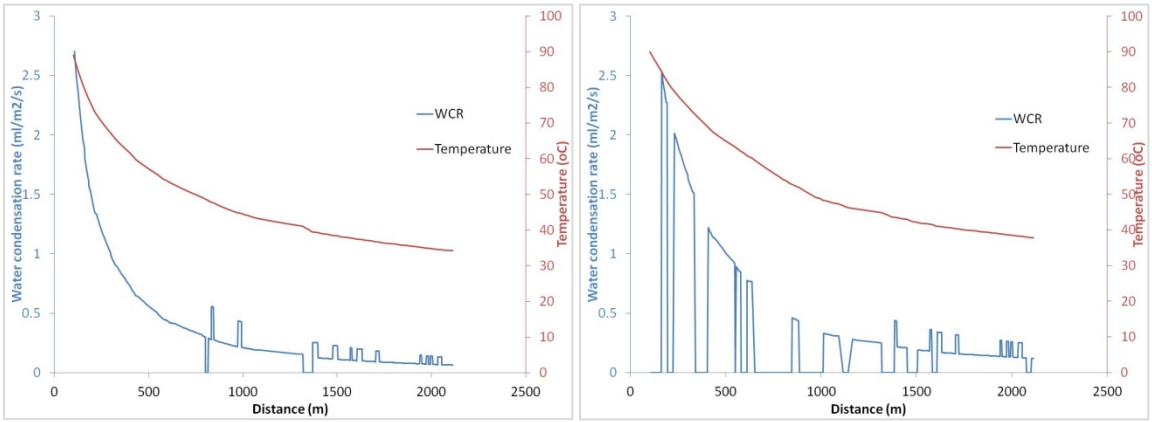

a) Time interval#1 b) Time interval#2

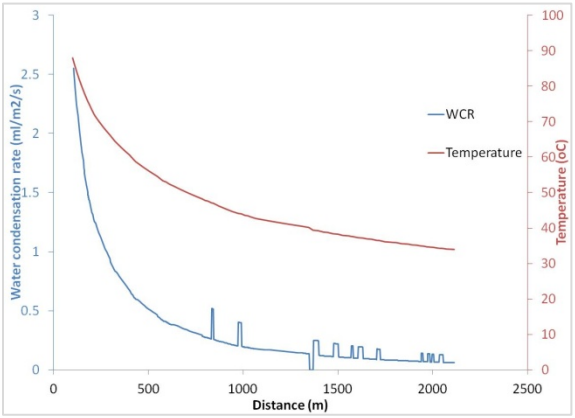

c) Time interval#3

Figure 44: WCR and temperature profile along the length of the Line E predicted from heat and mass transfer line model simulation.

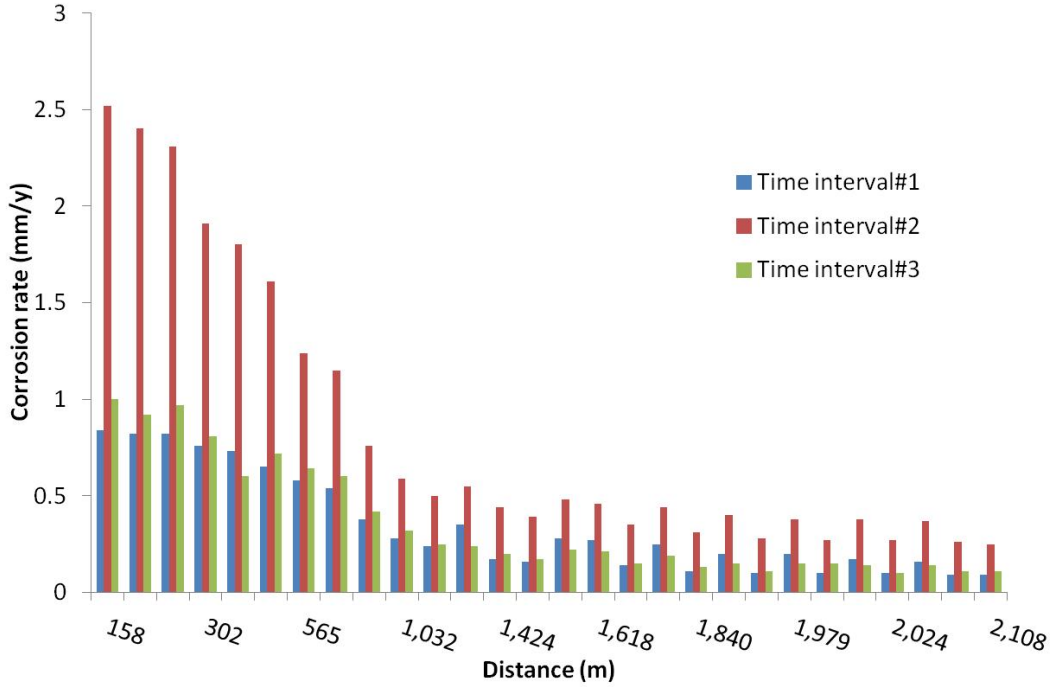

Figure 45: Predicted TLC rate for Line E.

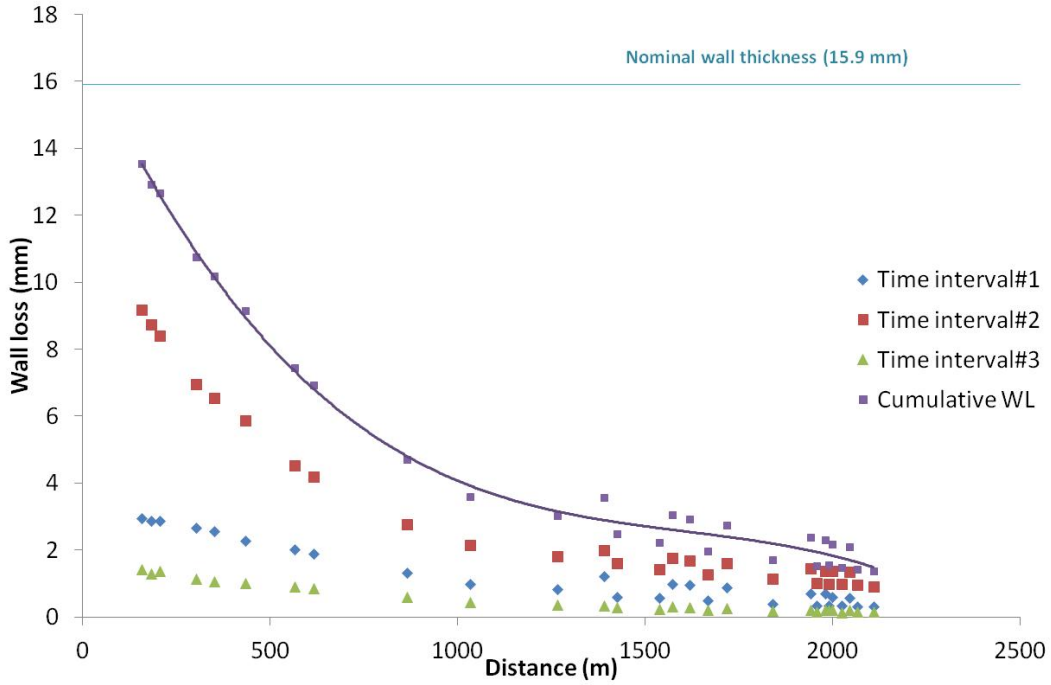

Figure 46: Calculated wall thickness loss values for the three time intervals and the total cumulative wall thickness loss value for Line E.

4.2.4.6 Line F

The in-house line model predicted a stratified flow regime from the data in time interval#1 to time interval#6 as presented in Figure 47 a) to f), respectively. Even though predicted WCR was low, the simulated TLC rates for this line were high due to high inlet temperature and CO_2 contents (93 ^oC and 20 mol% on average). Cumulative wall thickness loss indicates very severe TLC at the beginning of the length confirming the cause of the leak occurrence.

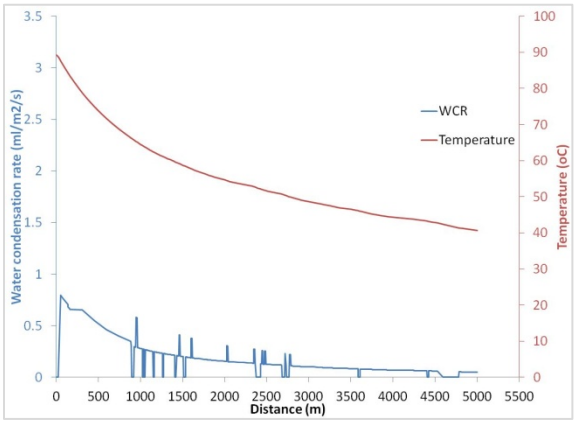

a) Time interval#1

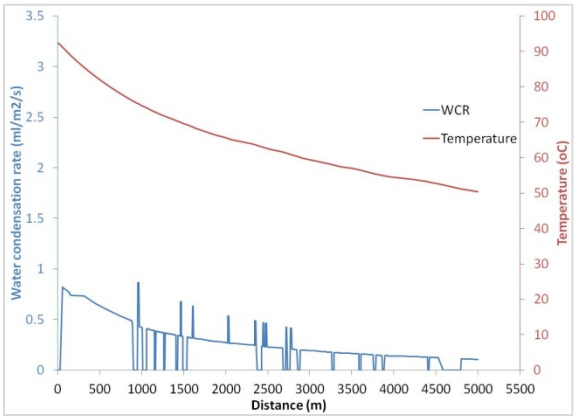

b) Time interval#2

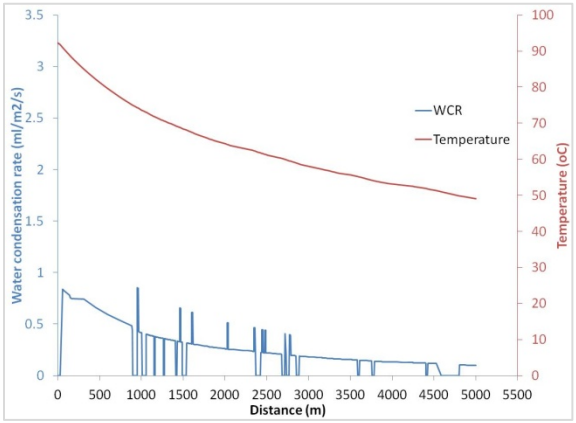

c) Time interval#3

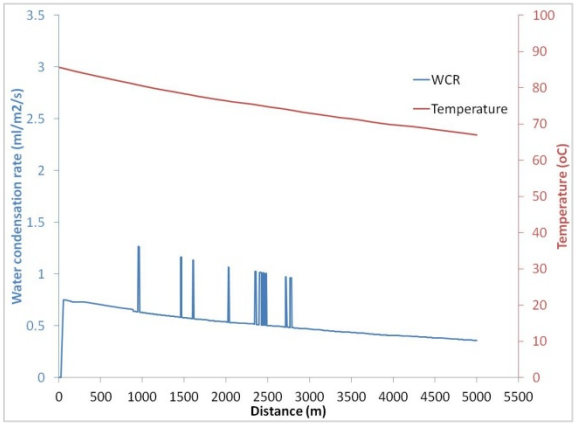

d) Time interval#4

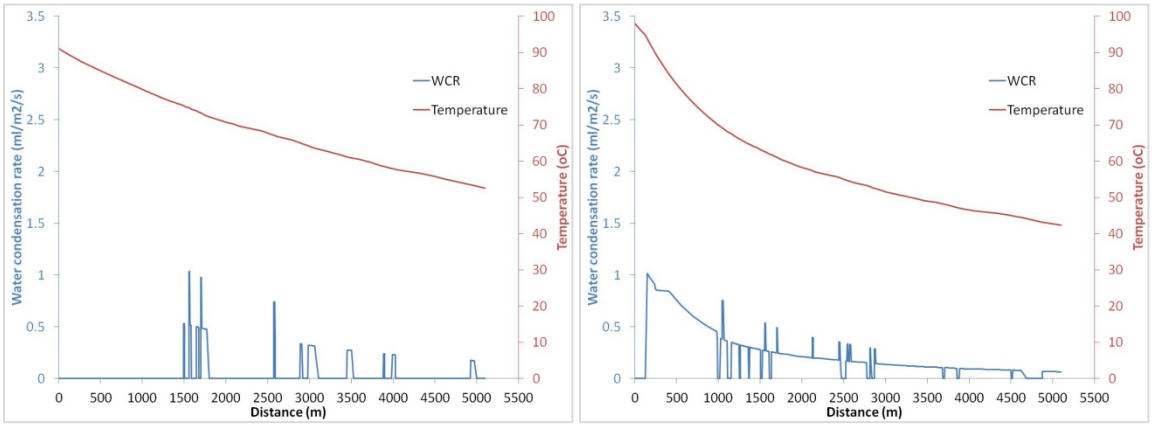

e) Time interval#5 f) Time interval#6

Figure 47: WCR and temperature profile along the length of the Line F predicted from heat and mass transfer line model simulation.

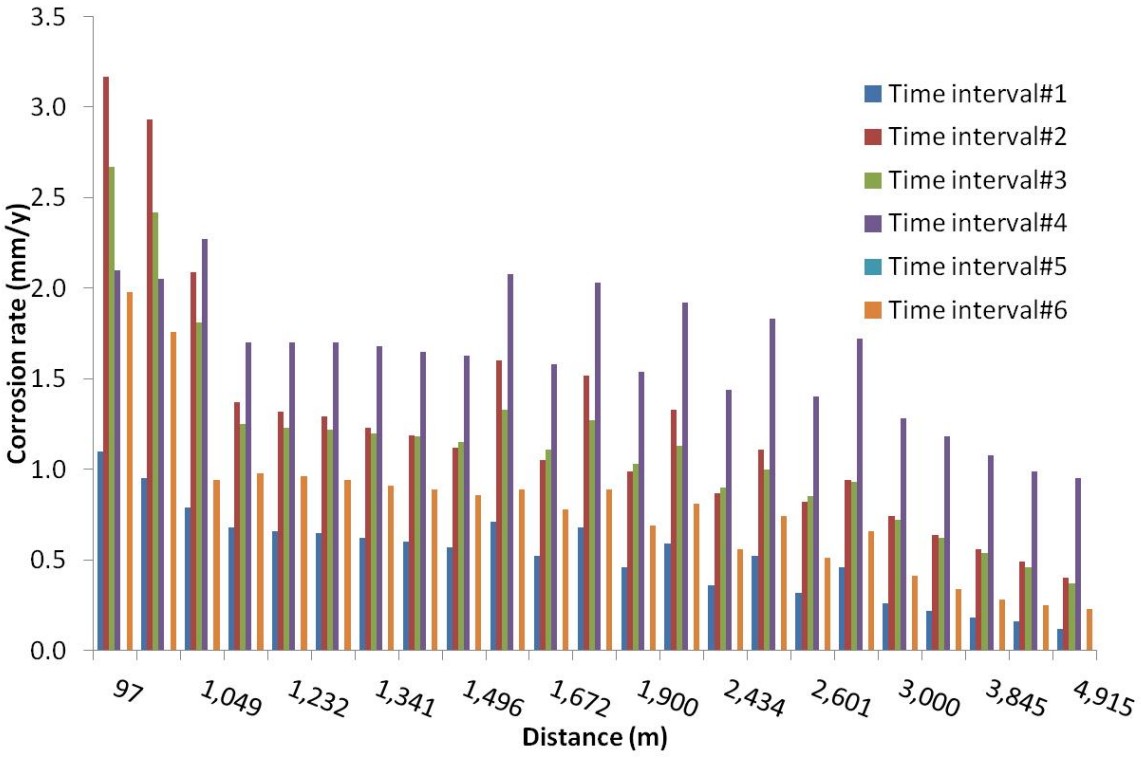

Figure 48: Predicted TLC rate for Line F.

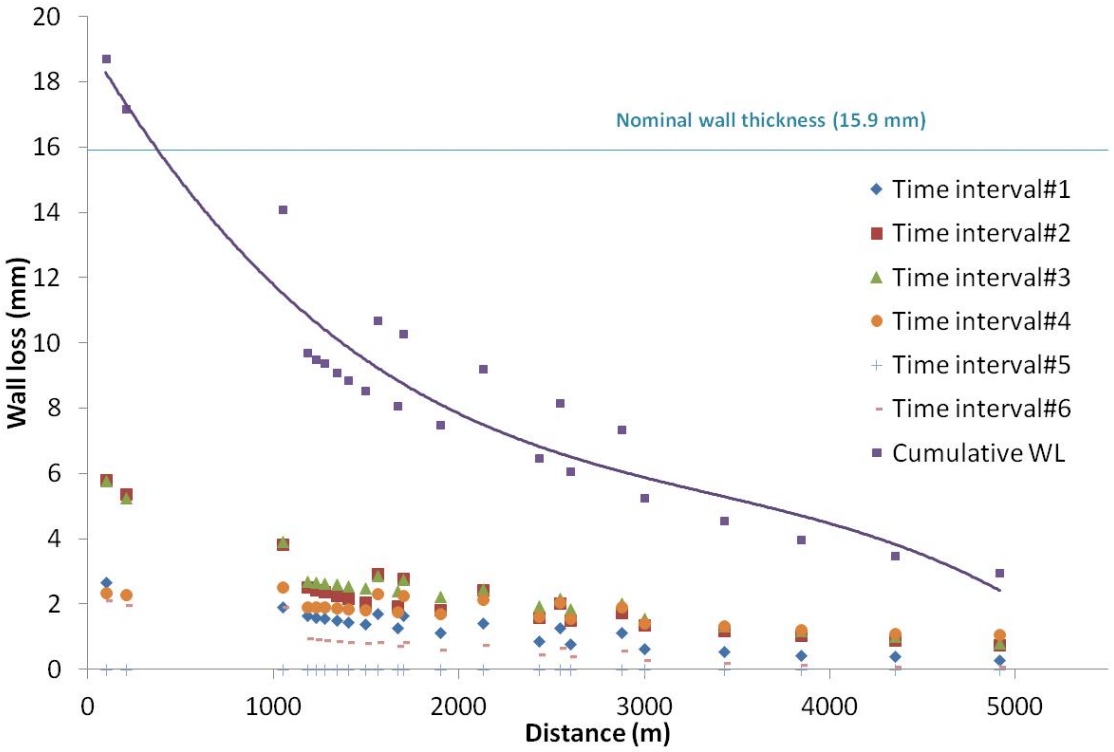

Figure 49: Calculated wall thickness loss values for the six time intervals and the total cumulative wall thickness loss value for Line F.

4.2.4.7 Line G

Line G is another hub line connecting to a cooler sea line. With high severe input conditions in the first two time intervals, a high WCR presented in Figure 50 a) and b) was predicted. As a result, high TLC rates were computed in the first and second time intervals affecting the high wall thickness loss at the beginning of the operation. Low TLC rates from the last three time intervals presented in Figure 51 did not considerably increase the predicted wall loss shown in Figure 52.

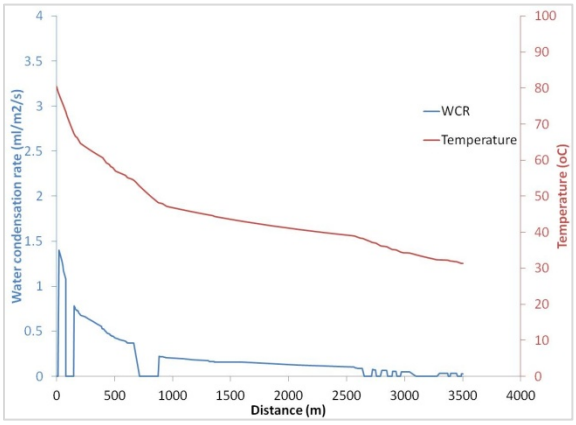

a) Time interval#1

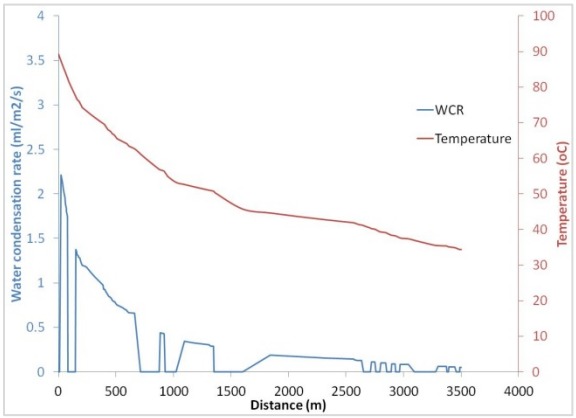

b) Time interval#2

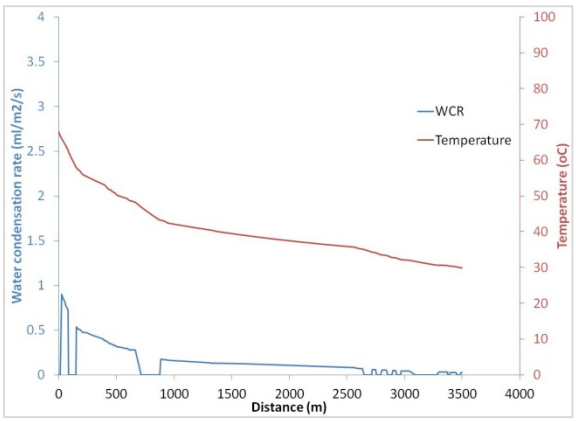

c) Time interval#3

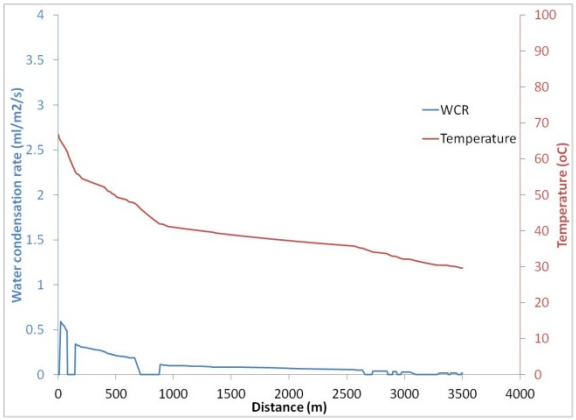

d) Time interval#4

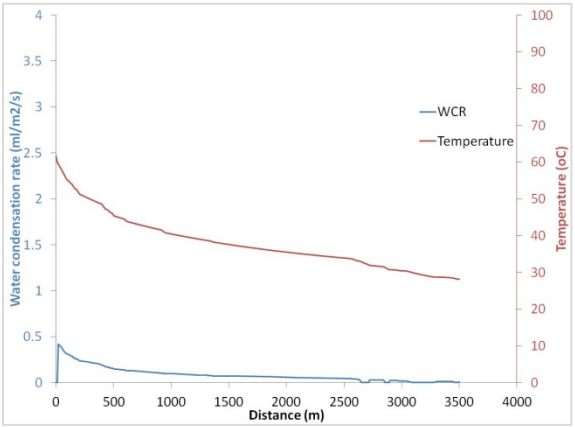

d) Time interval#5

Figure 50: WCR and temperature profile along the length of the Line G predicted from heat and mass transfer line model simulation.

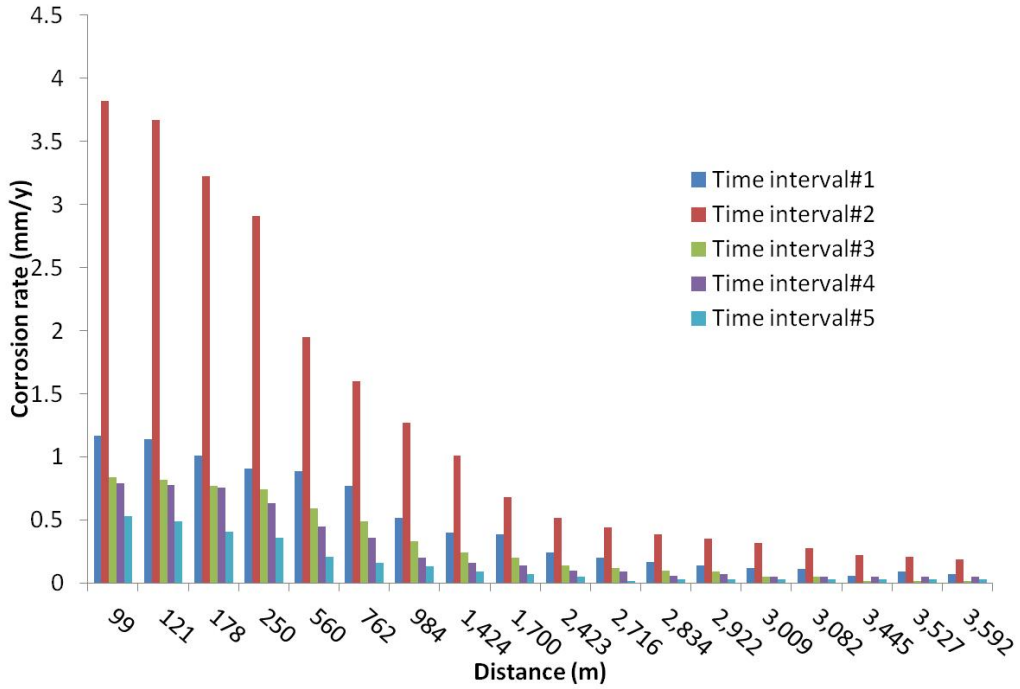

Figure 51: Predicted TLC rate for Line G.

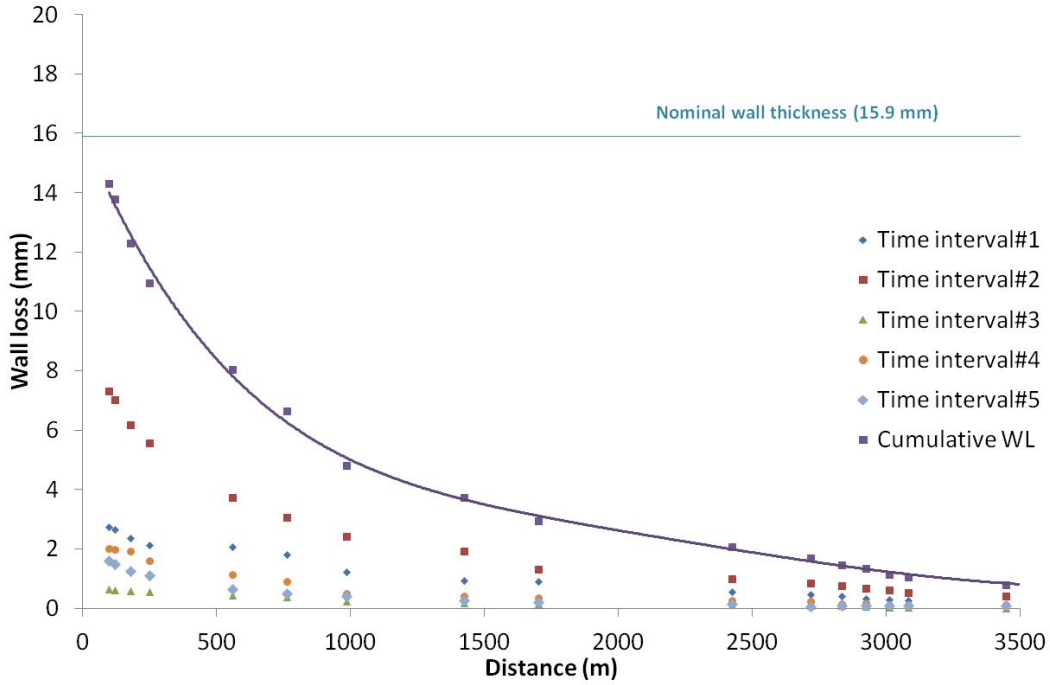

Figure 52: Calculated wall thickness loss values for the five time intervals and the total cumulative wall thickness loss value for Line G.

4.2.5 Comparison between model prediction and field data

4.2.5.1 Line A

For Line A, the simulation result shows wall thickness loss comparable to the average wall loss calculated from MFL data. Operating conditions having low gas velocity and low CO_2 concentration lead to a low risk of TLC in this line. As a result, low-frequency of batch treatment program is suggested for this line.

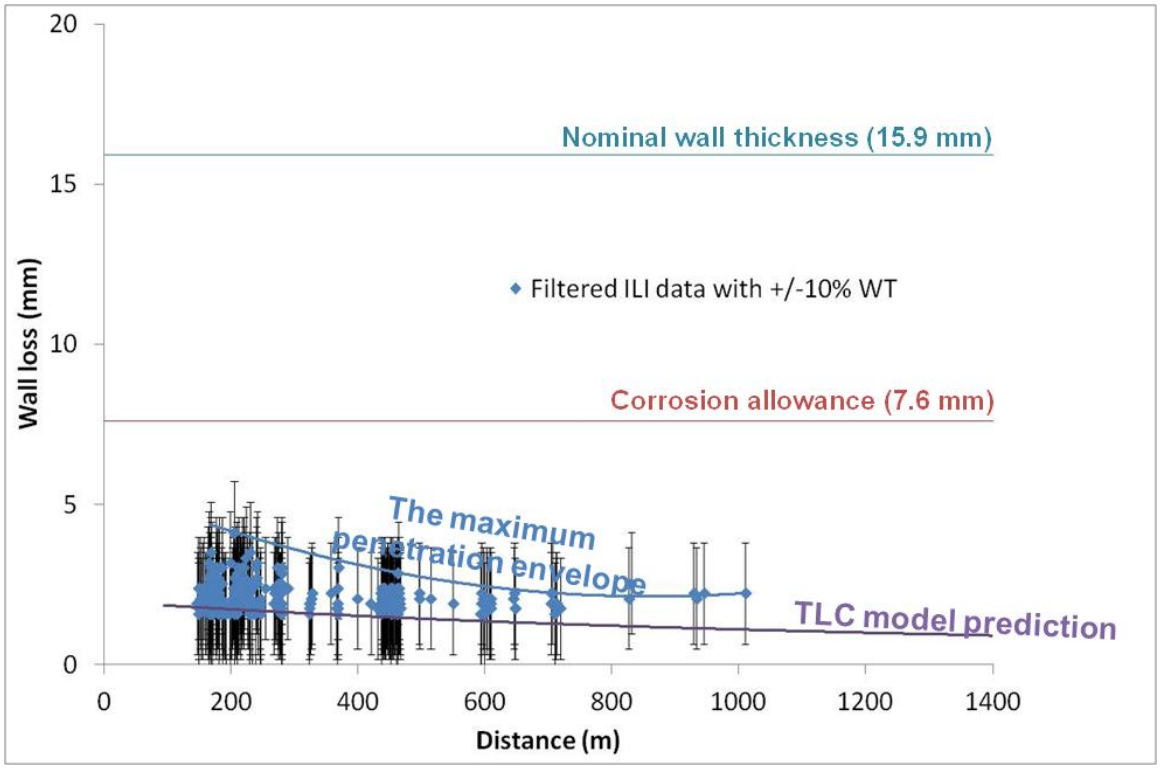

Figure 53: Comparison between filtered MFL data (with error bars equivalent to ±10% wall thickness due to instrument accuracy) and the TLC model predictions for Line A.

4.2.5.2 Line B

For Line B, the simulation shows a significantly higher wall thickness loss indicating a high risk level for TLC. The predictions were more in line with the MFL data defined as the maximum penetration envelope (except for the beginning of the line where a clear over-prediction was obtained). Severe TLC prediction was primary caused by significantly high CO_2 content (35 mol.% average). In order to mitigate TLC and prevent serious future failure, batch treatment program with inhibitor and pipeline corrosion assessment should be considered a top priority.

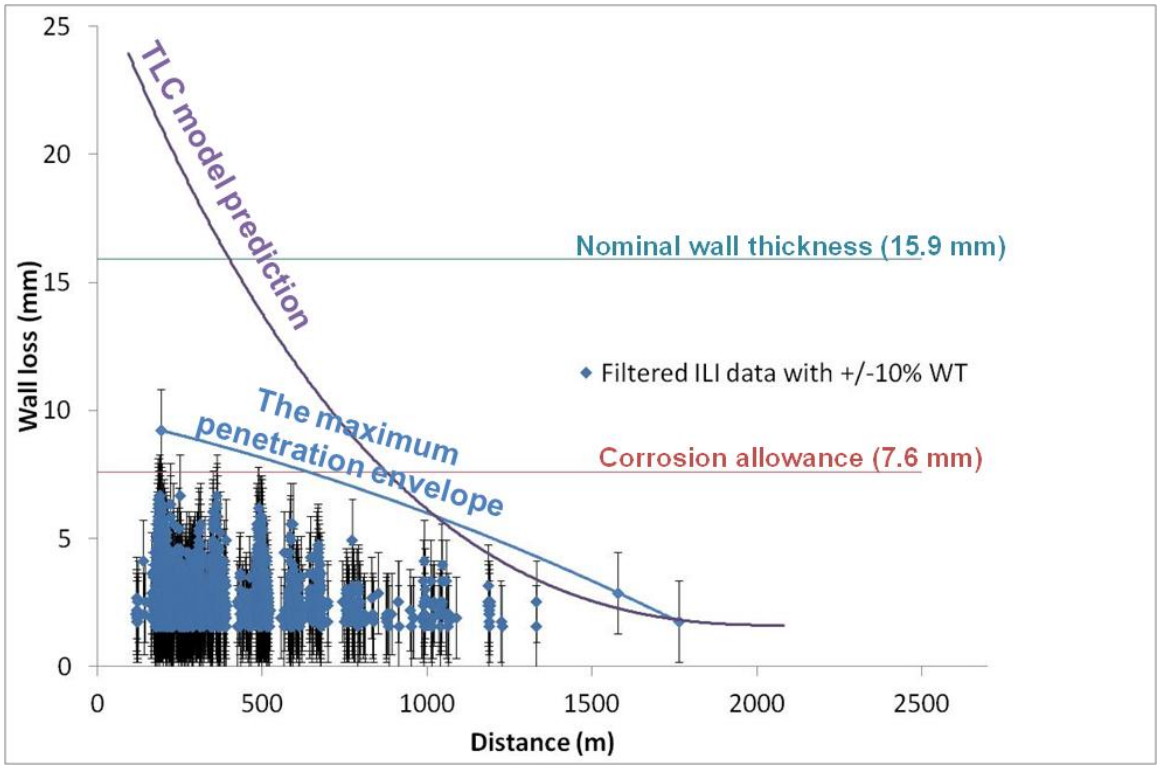

Figure 54: Comparison between filtered MFL data (with error bars equivalent to ±10% wall thickness due to instrument accuracy) and the TLC model predictions for Line B.

4.2.5.3 Line C

For Line C, the model predicted low rate of pipe wall loss and was below the averaged MFL data but still within the accuracy of the method. Low accumulated wall thickness loss confirmed low predicted TLC risk in conditions having small amounts of CO_2.

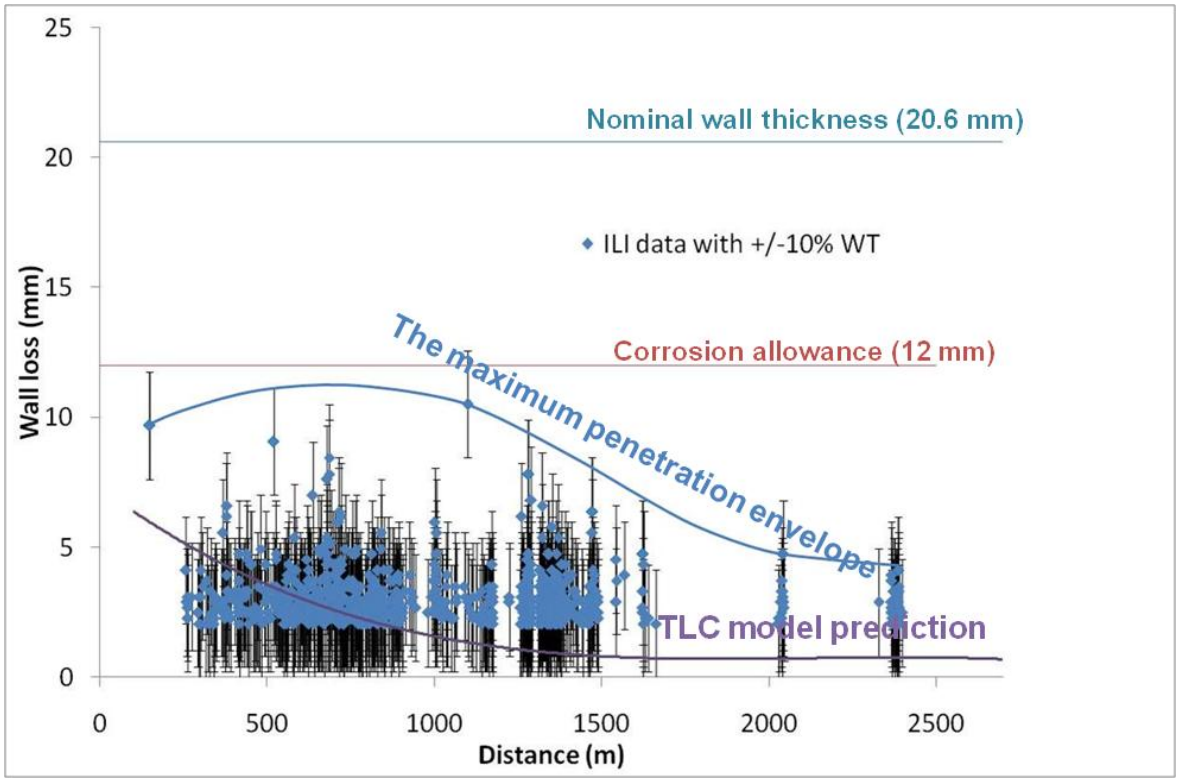

Figure 55: Comparison between filtered MFL data (with error bars equivalent to ±10% wall thickness due to instrument accuracy) and the TLC model predictions for Line C.

4.2.5.4 Line D

For Line D, the line model simulation result shows an overprediction when comparing with the MFL data at the beginning of the line. MFL data show a low and

gradually increasing wall loss from the beginning of the line to approximately 800 m, thereafter, start to decrease after reaching the maximum value. After 800 m, the predicted wall loss has a good agreement with the maximum envelope MFL data.

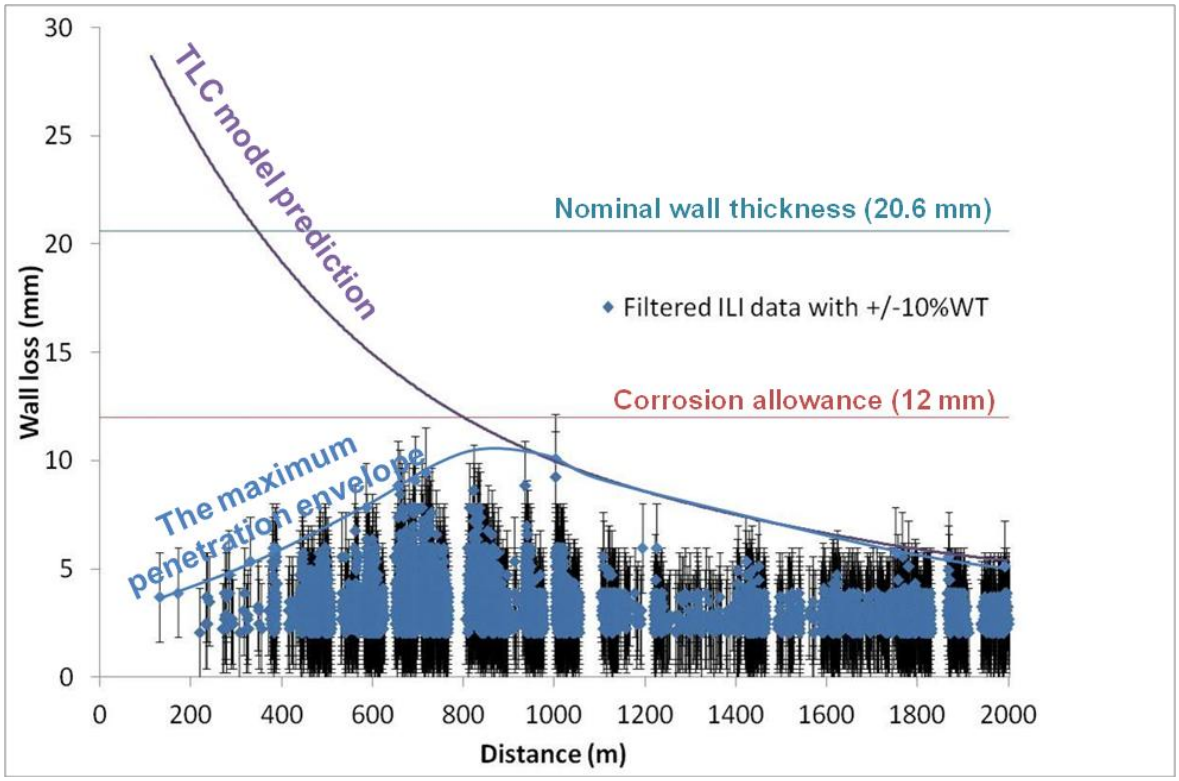

Figure 56: Comparison between filtered MFL data (with error bars equivalent to ±10% wall thickness due to instrument accuracy) and the TLC model predictions for Line D.

4.2.5.5 Line E

For Line E, the model prediction shows significantly high TLC risk, especially at the beginning of the pipeline. The severe operating conditions of this line directly affect the serious concern for TLC. Thus, high-frequency of batch treatment programs and

pipeline corrosion assessment are strongly recommended for mitigation and planning purposes for emergency pipeline repair or replacement, as necessary.

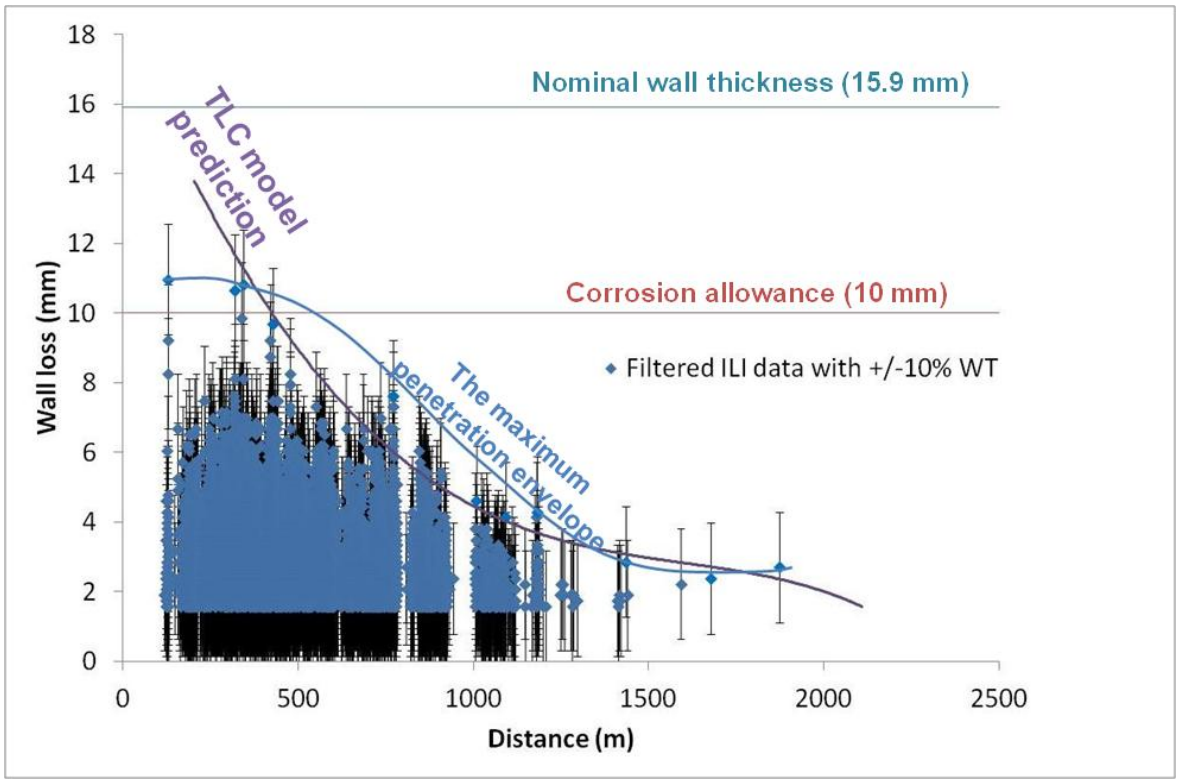

Figure 57: Comparison between filtered MFL data (with error bars equivalent to ±10% wall thickness due to instrument accuracy) and the TLC model predictions for Line E.

4.2.5.6 Line F

For Line F, high TLC was predicted due to the severe TLC conditions due to a high inlet temperature (93 ^{o}C) and high CO_2 content (16.9 mol% in average). Similar to other pipelines, the most severe threat of TLC was predicted in the beginning of the pipeline. Based on MFL data, there seem to be an over-prediction in the initial portion of the line, however a leakage occurred between the first and second flange, and the model

predictions were confirmed. Consequently, the batch treatment process should be applied frequently to this line.

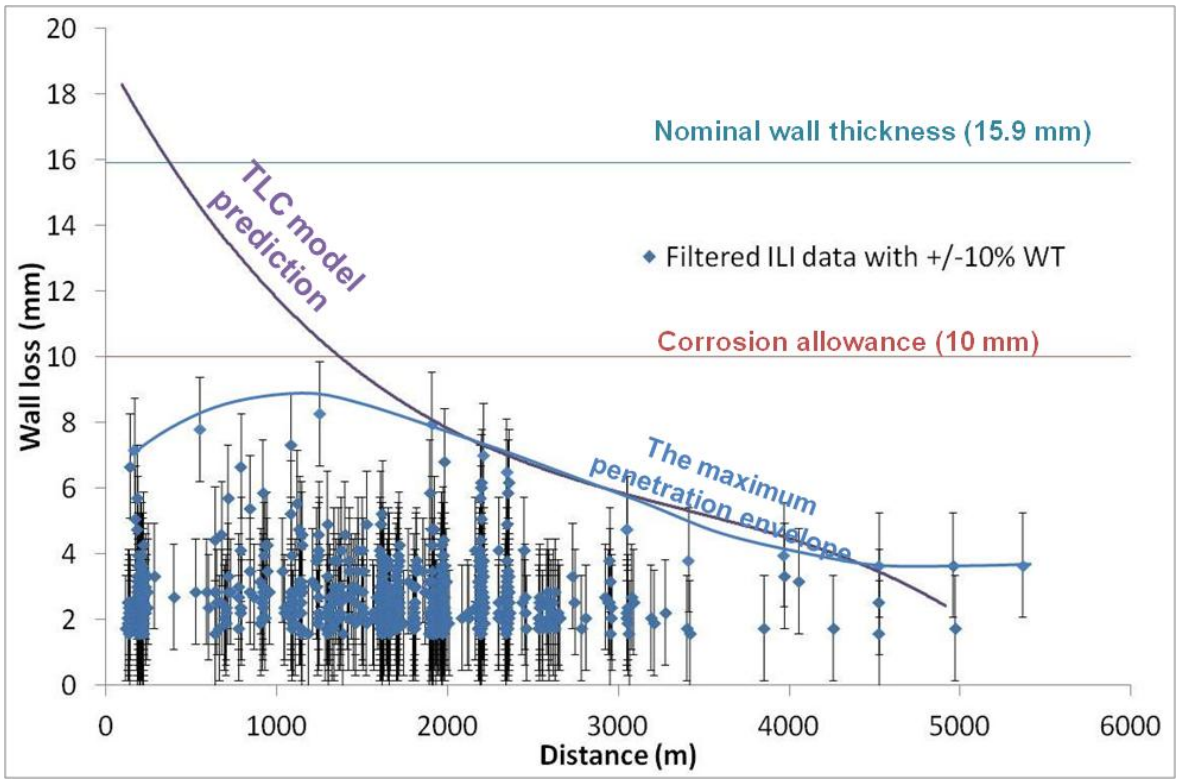

Figure 58: Comparison between filtered MFL data (with error bars equivalent to ±10% wall thickness due to instrument accuracy) and the TLC model predictions for Line F.

4.2.5.7 Line G

For Line G, high cumulative wall loss was predicted given the condition at the beginning of the line at least when compared to the MFL data, which shows quite low TLC at the first 700-800 m.

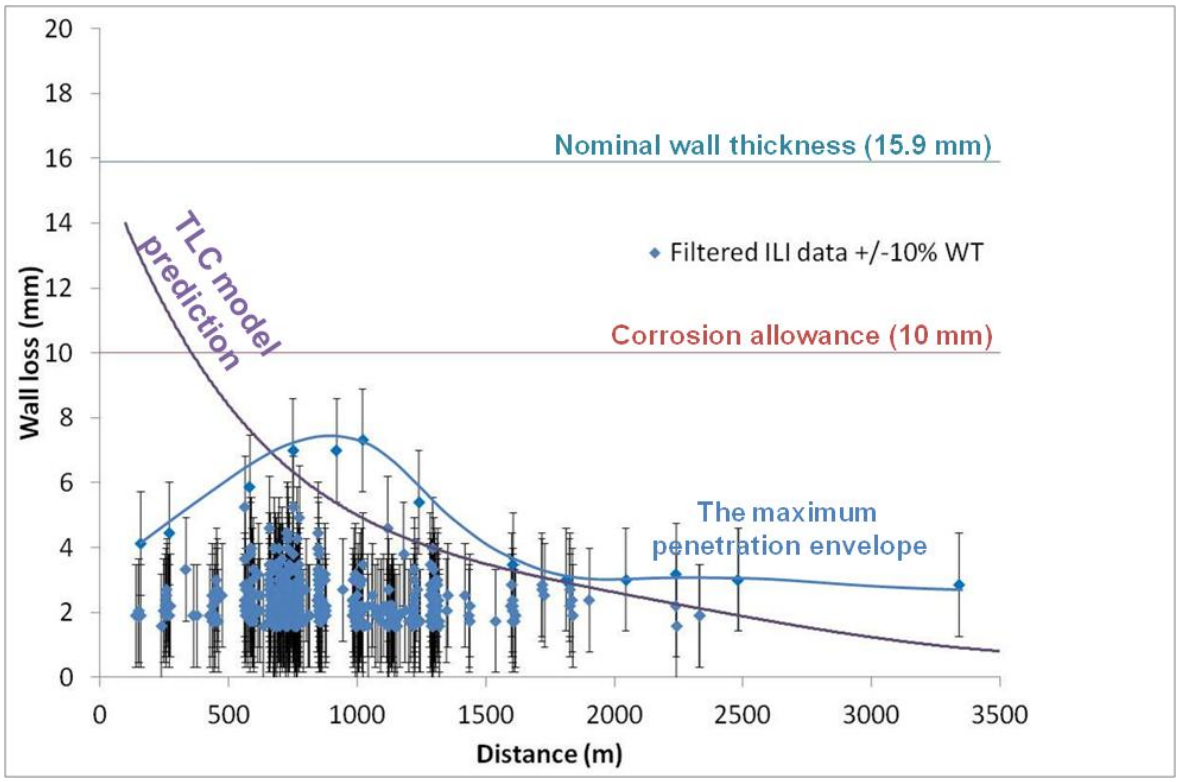

Figure 59: Comparison between filtered MFL data (with error bars equivalent to ±10% wall thickness due to instrument accuracy) and the TLC model predictions for Line G.

4.3 Discussion

As presented in Figure 60, when compared to the MFL data for five out of seven flow lines the predictions are within 10% of the wall thickness (what is the accuracy of this MFL method). This can be considered a reasonably good agreement with the MFL data. However, there are a few consistent outliers in comparison between TLC model predictions and MFL data, which indicate gaps in our understanding. Since the TLC prediction model is only a reflection of the current knowledge, it cannot predict phenomena that are not adequately understood.

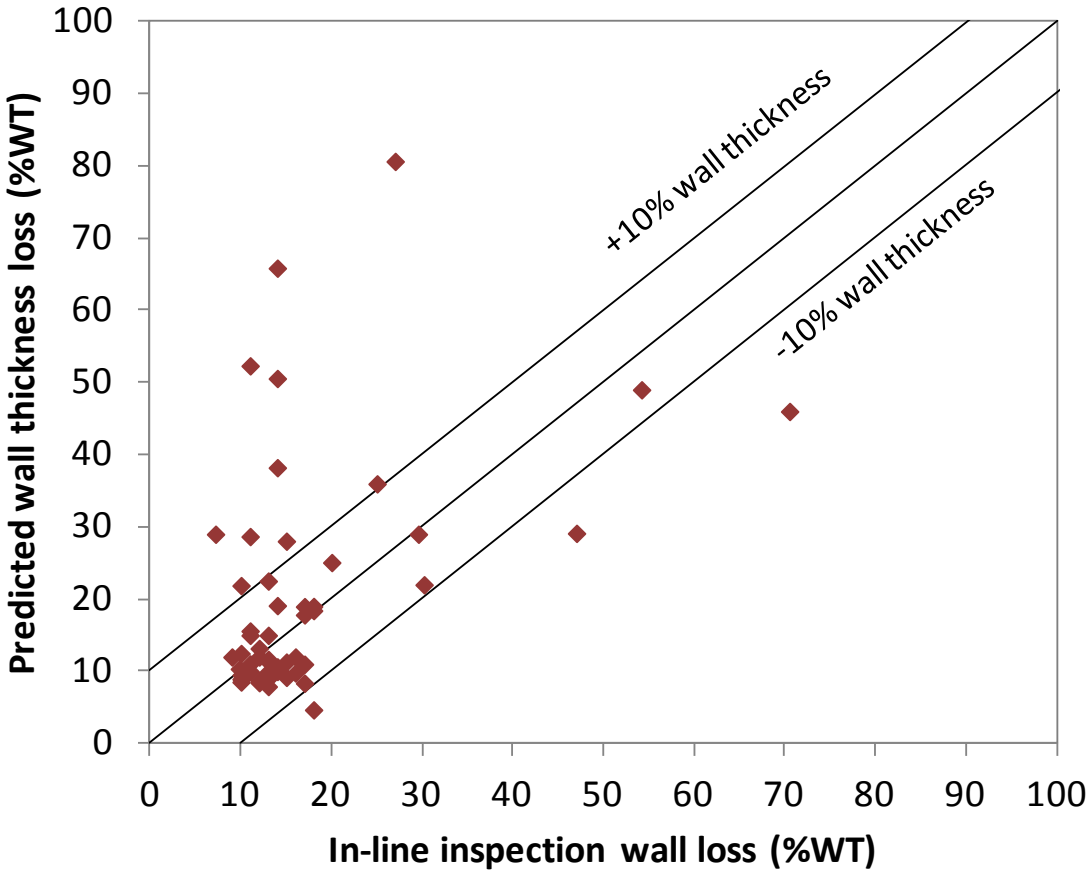

Figure 60: Parity plot between maximum wall thickness loss obtained from the MFL data and the predicted TLC data for eight different lines.

4.4 Limits of the validation

Even though the comparison between the model predictions and the MFL data is generally reasonable, there is still a consistent discrepancy between those data at the beginning of the pipelines. The first few meters of pipelines are where the most severe TLC should be found due to the high operating and corrosive conditions but MFL data shows very low corrosivity. This might lead to a decreased level of confidence in using the selected model.

There are three possible reasons that have been discussed which can explain the discrepancy. First is the effect of co-condensation of hydrocarbons and water. The presence of the heavier hydrocarbons in BLC may act as a barrier against corrosive species. In the condensation process in TLC, water vapor is not the only species condensing in the pipeline, hydrocarbons (natural gas liquids [NGLs]) can condense too. The condensation rate is high at the beginning of the pipeline and decreases along the length of the pipeline. A high hydrocarbon condensation rate at the pipeline entrance might provide some protection from TLC. Nevertheless, when the hydrocarbon condensation rate becomes lower along the pipeline, the water condensation may become a major parameter and lead to severe TLC.

The second possible explanation is related to the effect of turbulent flow at the "dogleg" where there is a bend connecting the vertical riser with the horizontal pipeline. The flow pattern at the dogleg is definitively a non-stratified flow regime, which cannot lead to the TLC phenomena. Moreover, this flow disturbance will carry any corrosion inhibitor to the upper pipe wall. Nevertheless, as the flow settles, a stratified flow regime is expected to reestablish itself after a short distance (10-100m). So it is unclear if this explanation can explain the lack of TLC in the entrance part of the pipe which stretched out for much longer.

The third possible explanation is related to saturation of the vapor/liquid mixture. At the saturation condition, any cooling of the gas will result in condensation, leading to TLC. In principle the gas at the beginning of the pipeline may not be saturated.

Undersaturated conditions cannot lead to the condensation of water at the top of the line and no TLC will occur.

Therefore, the prediction of severe TLC in the first portions of the line can be considered an artifact, until a better understanding of the TLC phenomena and root causes is established, which should help improve the level of confidence in using this predictive tool.

CHAPTER 5: CONCLUSIONS

Any predictive tool needs to be validated with empirical results. The validation of the pipeline corrosion models improves the level of confidence in using the model predictions for pipeline design and/or failure analysis. In this research project, a methodology for comparing the model predictions and field data is developed and tested proving to be a practical and useful procedure.

The complexity and inaccuracy of the field production data, such as accurate production temperature and pressure profiles, are the primary data that needs to be carefully analyzed. In their raw form, these data are incomplete and unreliable. Therefore, analyzing these operating data analysis is developed and verified. The collected field data are divided into several time intervals and the weight-averaged values are calculated. The analyzed data are then used as input for the predictive model to calculate and simulate the severity of corrosion.

The simulation results are compared with the field corrosion, which is provided from collected MFL data. In the methodology developed here, the MFL data is crucial information that needs to be critically analyzed. The analysis of the MFL data filters out noisy data and non-representative data and is a crucial step that should not be overlooked.

A meaningful comparison is performed and the prediction results from the selected model show reasonable general agreement with the MFL data. Consequently, the effective methodology can be confidently applied to evaluate the risk levels of TLC in the pipelines and also to prioritize TLC mitigation programs and pipeline corrosion assessments.

However, there is a discrepancy between the model predictions and MFL data in the first portions of the pipeline. Three possible reasons which can explain the gap are the effect of co-condensation of higher hydrocarbons (C_{3+}) and water, the effect of turbulent flow at the dogleg and the question on saturation of inlet gas.

LIST OF REFERENCES

[1] D.A. Jones, “The technology and evaluation,” in *Principles and Prevention of Corrosion,* 2nd ed. Upper Saddle River, NJ: Prentice-Hall, 1996, pp. 5.

[2] Y. P. Virmani, "Corrosion Costs and Preventive Strategies in the United States," Federal Highway Administration, U.S. Department of Transportation, Tech. Rep. FHWA-RD-01-156, 2002.

[3] C. DeWaard and D.E. Milliams, "Prediction of carbonic acid corrosion in natural gas pipelines," in *proc. 2nd Intl. Conf. on the internal and external protection of pipes,* 1975, pp. 410-417.

[4] L. G. S. Gray, B. G. Anderson, M. J. Danysh and P. R. Tremaine, "Mechanisms of carbon steel corrosion in brines containing dissolved carbon dioxide at pH4," in *Proc. Corrosion*, New Orleans, LA, 1989, paper. 464.

[5] L. G. S. Gray, B. G. Anderson, M. J. Danysh and P. R. Tremaine, "Effect of pH and temperature in the mechanism of carbon steel corroson by aqueous carbon dioxide," in *Proc. Corrosion*, Las Vegas, NV, 1990, paper. 40.

[6] S. Nesic, J. Postlethwaite, and S. Olsen, "An electrochemical model for prediction of CO2 corrosion," in *Proc. Corrosion*, Las Vegas, NV, 1995, paper. 131.

[7] N. Nordsveen, S. Nesic, R. Nyborg and A. Stangeland, “A Mechanistic Model for Carbon Dioxide Corrosion of Mild Steel in the Presence of Protective Iron Carbonate Films - Part 1: Theory and verification,” *Corrosion*, vol. 59, no. 5, pp. 443-456, 2003.

[8] S. Nesic, N. Nordsveen, R. Nyborg and A. Stangeland, “A Mechanistic Model for Carbon Dioxide Corrosion of Mild Steel in the Presence of Protective Iron Carbonate Films - Part 2: A numerical experiment”, *Corrosion*, vol. 59, no. 6, pp. 489-497, 2003.

[9] S. Nesic, N. Nordsveen, R. Nyborg and A. Stangeland, “A Mechanistic Model for Carbon Dioxide Corrosion of Mild Steel in the Presence of Protective Iron Carbonate Films - Part 3: Film growth model”, *Corrosion*, vol. 59, no. 7, pp. 616-628, 2003.

[10] A. Dugstad, "Fundamental Aspects of CO_2 metal loss corrosion-Part 1: Mechanism," in *Proc. Corrosion*, San Diego, CA, 2006, paper. 111.

[11] G. Schmitt and M. Horstemeier, "Fundamental aspects of CO_2 metal loss corrosion-part2: Influence of differenct parameters on CO_2 corrosion mechanisms," in *Proc. Corrosion*, San Diego, CA, 2006, paper. 112.

[12] W. Sun, "Kinetics of Iron Carbonate and Iron Sulfide Scale Formation in CO_2/H_2S Corrosion," Ph.D. dissertation. *Chem. Eng.*, Ohio Univ., OH, 2006.

[13] R. Paillassa, M. Dieumegard and M. Estevoyer, "Corrosion control in the gathering system at Lacq sour gas field", in *proc. 2nd Intl. Congr. of Metallic Corrosion NACE*, New York, 1963, pp. 410-417.

[14] Y. Gunaltun, D. Supriyatman, and J. Achmad, "Top of line corrosion in multiphase gas lines. A case history," in *Proc. Corrosion*, San Antonio, TX, 1999, paper. 36.

[15] Y. Gunaltun and D. Larrey, "Correlation of cases of top of the line corrosion with calculated water condensation rates", in *Proc. Corrosion*, Houston, TX, 2000, paper. 71.

[16] J.R. Piccardino, M. Stuvik, Y. Gunaltun, and T. Pornthep, "Internal inspection of wet gas lines subject to top of line corrosion," in *Proc. Corrosion*, New Orleans, LA, 2004, paper. 345.

[17] M. Thammachart, Y. Gunaltun, and S. Punpruk, "The use of inpection results for the evaluation of batch treatment efficiency and the remaining life of the pipelines subjected to top of line corrosion," in *Proc. Corrosion*, New Orleans, LA, 2008, paper. 471.

[18] Y. Gunaltun, S.Punpruk, M.Thammachart, and P. Tanaprasertsong, "Worst case top of the line corrosion: cold spot corrosion," in *Proc. Corrosion*, San antonio, TX, 2010, paper. 97.

[19] U. Kaewpradap, M. Singer, S. Nesic, and S. Punpruk, "Top of the line corrosion-comparison of model predictions with field data," in *Proc. Corrosion*, Salt lake city, UT, 2012, paper. 1449.

[20] A.K. Dunlop, H.L. Hassell, and P.R. Rhodes, "Fundamental considerations in sweet gas well corrosion", in *Proc. Corrosion*, Anaheim, CA, 1983, paper. 46.

[21] S. Nesic and W. Sun, "Corrosion in acid gas solutions," in *Shreir's Corrosion*, Tony J.A. Richardson, Ed. Oxford: Elsevier, 2010, pp. 1270-1298.

[22] S.N. Smith, "A proposed mechanism for corrosion in slightly sour oil and gas production," in *12th Intl. Corrosion Congr.: Corrosion Control for Low-Cost Reliability Conference*, 1993.

[23] S. Olsen, A. Dugstad, "Corrosion under dewing conditions", in *Proc. Corrosion*, Houston, TX, 1991, paper. 472.

[24] B.F.M. Pots, E.L.J.A. Hendriksen, "CO_2 corrosion under scaling conditions – The special case of top-of-the-line corrosion in wet gas pipelines", in *Proc. Corrosion*, Houston, TX, 2000, paper. 31.

[25] D. Hinkson, M. Singer, Z. Zhang and S. Nesic, "A study of the chemical composition and corrosivity of the condensate in top of the line corrosion", in *Proc. Corrosion*, New Orleans, LA, 2008, paper. 8466.

[26] Y. Chen, L. Zhang, H. Qin, L. Xu and M. Lu, "Top-of-the-line corrosion of pipeline steel", in *Proc. Corrosion*, Houston, TX, 2011, paper. 11327.

[27] H. Qin, L. Xu, W. Chang, M. Lu and L. Zhang, "Top-of-the-line corrosion under low-temperature and high condensation rate conditions", in *Proc. Corrosion*, Houston, TX, 2011, paper. 11328.

[28] T. Pojtanabuntoeng, M. Singer, and S. Nesic, "Water/hydrocarbon co-condensation and the influence on top-of-the-line corrosion", in *Proc. Corrosion*, Houston, TX, 2011, paper. 11330.

[29] M. Singer, S. Nesic and Y. Gunaltun, "Top of the line corrosion in presence of acetic acid and carbon dioxide", in *Proc. Corrosion*, Houston, TX, 2004, paper. 4377.

[30] C. Mendez, M. Singer, A. Camacho, S. Hernandez and S. Nesic, "Effect of acetic acid, pH and MEG on CO_2 top of the line corrosion", in *Proc. Corrosion*, Houston, TX, 2005, paper. 5278.

[31] Z. Zhang, D. Hinkson, M. Singer, H. Wang and S. Nesic, "A mechanistic model for Top of the line corrosion", in *Proc. Corrosion*, Nashville, TN, 2007, paper. 7556.

[32] R. Nyborg, A. Dugstad and T. Martin," Top of line corrosion with high CO_2 and traces of H_2S", in *Proc. Corrosion*, Atlanta, GA, 2009, paper. 9283.

[33] C. DeWaard, U. Lotz and D.E. Milliams, "Predictive model for CO_2 corrosion engineering in wet natural wet gas pipelines", *Corrosion*, vol. 47, no. 12, pp. 976-985, 1991.

[34] F. Vitse, A. Khairul, Y. Gunaltun, D. Larrey de Torreben D. and P. Duchet-Suchaux, “Semi-empirical model for prediction of the top-of-the-line corrosion risk”, in *Proc. Corrosion*, Houston, TX, 2002, paper. 2245.

[35] F. Vitse, Y. Gunaltun, D. Larrey de Torreben and P. Duchet-Suchaux, “Mechanistic model for the prediction of top-of-the-line corrosion risk”, in *Proc. Corrosion*, Houston, TX, 2003, paper. 3633.

[36] Z. Zhang, "A study of top of line corrosion under dropwise condensation," Ph.D. dissertation. *Chem. Eng.*, Ohio Univ., OH, 2008.

[37] *Laboratory corrosion test and standards*, ASTM special technical publication, 2003.

[38] Y.Tan, Y.Fwu, K. Bhardwaj, S. Bailey and R. Gubner, “Review of critical issue in carbon dioxide corrosion testing and monitoring techniques”, in *Proc. Corrosion*, San Antonio, TX, 2010, paper. 10155.

[39] J. Walker, “Non-destructive testing in in-line inspection,” in *In-line inspection of pipelines,* Germany, pp. *24–28.*

[40] Pipeline Operators Forum (POF) document “Specifications and requirements for intelligent pig inspection of pipelines,” 2009, pp. 1-38.

Thesis and Dissertation Services